

HUNTING FOR SUPERMASSIVE BLACK HOLES IN NEARBY GALAXIES WITH THE HOBBY-EBERLY TELESCOPE

REMCO C. E. VAN DEN BOSCH^{1,5}, KARL GEBHARDT²,
KAYHAN GÜLTEKİN³, AKIN YILDIRIM¹ AND JONELLE L. WALSH^{2,4}

Accepted to ApJs.

Abstract

We have conducted an optical long-slit spectroscopic survey of 1022 galaxies using the 10m Hobby-Eberly Telescope (HET) at McDonald Observatory. The main goal of the HET Massive Galaxy Survey (HETMGS) is to find nearby galaxies that are suitable for black hole mass measurements. In order to measure accurately the black hole mass, one should kinematically resolve the region where the black hole dominates the gravitational potential. For most galaxies, this region is much less than an arcsecond. Thus, black hole masses are best measured in nearby galaxies with telescopes that obtain high-spatial resolution. The HETMGS focuses on those galaxies predicted to have the largest sphere-of-influence, based on published stellar velocity dispersions or the galaxy fundamental plane. To ensure coverage over galaxy types, the survey targets those galaxies across a face-on projection of the fundamental plane. We present the sample selection and resulting data products from the long-slit observations, including central stellar kinematics and emission line ratios. The full dataset, including spectra and resolved kinematics, is available online. Additionally, we show that the current crop of black hole masses are highly biased towards dense galaxies and that especially large disks and low dispersion galaxies are under-represented. This survey provides the necessary groundwork for future systematic black hole mass measurement campaigns.

Data, including spectra, are available at <http://www.mpi-a.de/~bosch/hetmgs>.

Subject headings: galaxies: kinematics and dynamics

1. HET MASSIVE GALAXY SURVEY

The masses of black holes, M_{\bullet} , correlate to various properties of their host galaxies. These correlations are the foundation for theories of the (co-)evolution of supermassive black holes and their host galaxies. See Kormendy & Ho (2013) for a recent review. The most commonly used black hole scaling relations are with stellar velocity dispersion ($M_{\bullet}-\sigma$; Gebhardt et al. 2000; Ferrarese & Merritt 2000), bulge mass ($M_{\bullet}-M_{\text{bul}}$; Häring & Rix 2004), bulge luminosity ($M_{\bullet}-L_{\text{bul}}$; Sani et al. 2011), and total luminosity ($M_{\bullet}-L_{\text{tot}}$; Lasker et al. 2014b). Theories on the existence of these scaling relations range from causal links through direct feedback between the black hole and its host (Fabian 1999) to a non-causal origin from random hierarchical galaxy-galaxy merging (Jahnke & Macciò 2011). Another possibility is that the black hole scaling relation only holds for elliptical galaxies and bulges (Kormendy et al. 2011). However not enough black hole masses have been measured to place firm constraints on these hypotheses. Also note that the $M_{\bullet}-L$ and $M_{\bullet}-\sigma$ not mutually consistent for the biggest black holes (Lauer et al. 2007). The main issue, besides small numbers, is that the host galaxy properties only span a small physical range, which is too small to discern between different scenarios, due to measurement uncertainties and the large intrinsic scatter in these relations.

In addition, the black hole masses of nearby galaxies are critically important for black hole mass determinations at higher

redshift. The mass measurements from quasars and active galactic nuclei (AGNs) are measured using reverberation mapping (and its secondary methods), which rely on an empirical calibration that assumes that active black holes follow the local potentially biased $M_{\bullet}-\sigma$ relation (Woo et al. 2010).

Very few galaxies are close enough for direct black hole mass measurements. For a successful measurement, the central region of the galaxy where the potential of the black hole dominates needs to be spatially resolved ($r_i \equiv GM_{\bullet}\sigma^{-2}$, see § 2.2). Even for the closest galaxies, the sphere of influence is typically much smaller than 1''. Hence, black hole masses can only be measured by telescope with the highest spatial resolution, such as the *Hubble Space Telescope (HST)*, large ground-based telescopes assisted by adaptive optics, and radio facilities such as the Very Long Baseline Interferometry Network.

In order to make best use of high spatial resolution facilities, the potential targets for future black hole mass measurements need to be carefully chosen. However, most nearby galaxies (with distances < 140 Mpc) do not have any spectra available, without which it is impossible to ascertain their suitability for expensive high spatial resolution follow-up. Even if spectra are available, the amalgamated literature in the HyperLeda database (Paturel et al. 2003) is often unreliable (see § 4).

The HET Massive Galaxy Survey (HETMGS) aims to find those galaxies that are suitable for a dynamical black hole mass measurement. The survey was a large program on the Hobby-Eberly Telescope (HET; Ramsey et al. 1998) that operated for 10 trimesters and obtained spectra of 1022 galaxies. While the spatial resolution of the HET observations are typically not good enough to measure the black hole masses, this survey lays the necessary groundwork for systematic black hole mass measurement campaigns. As a by-product, the survey also provides a census of the nearest galaxies.

This survey is ideally suited for the unique design of the

¹ Max-Planck Institut für Astronomie, Königstuhl 17, D-69117 Heidelberg, Germany

² Department of Astronomy, The University of Texas at Austin, 2515 Speedway, Stop C1400, Austin, TX 78712, USA

³ Department of Astronomy, University of Michigan, Ann Arbor, Michigan 48109, USA

⁴ George P. and Cynthia Woods Mitchell Institute for Fundamental Physics and Astronomy, and Department of Physics and Astronomy, Texas A&M University, College Station, TX 77843, USA

⁵ email: bosch@mpia.de

Hobby-Eberly Telescope. The 10-meter mirror is spherical and has a fixed elevation angle of 55° . The primary mirror is stationary during observations and objects are tracked by moving the optics and instruments in prime focus. The telescope can only point to a fraction of the sky at any given time. The visible ‘doughnut’ is 8.4° thick. As a target passes through the donut, the telescope can track it for approximately one hour, depending on the declination of the object. The telescope design makes it most suited for programs that have short exposures and have many targets distributed across the sky. All observations are executed by night operators to optimize the science output. The scheduling algorithm is highly flexible and continually ranks all objects in the queue by score from the time allocation committee, visibility, observing conditions, etc. This allows the resident astronomer to adapt to current conditions in real-time. For details see Shetrone et al. (2007).

This paper starts with the description of the survey, sample construction, and completeness metrics in § 2–2.5. Then, the data reduction is described in § 3. The primary data product is the stellar velocity dispersion since this is required to predict the sphere of influence. Subsequently, these dispersion measurements are validated in § 4. When no literature dispersion is available *a priori*, the sphere of influence can be estimated from the photometry using the fundamental plane that relates galaxy size, surface brightness, and velocity dispersion, and a custom fit of this fundamental plane is presented in § 5. The global properties of the HETMGS sample are described in § 6. Then, in § 7, we explore whether the galaxy’s central velocity dispersion or an average velocity dispersion within the galaxy’s half-light radius correlates more strongly with black hole mass. In § 8 we compare the black-hole–host-galaxy demographics with the HETMGS sample and show that the host galaxies currently on the scaling relations are strongly clustered and biased toward the densest galaxies. We also look at the distribution of galaxies with large spheres of influence, and find that there are very few galaxies for which an under-massive black hole could be detected. Finally, we conclude in § 9 with a discussion of future prospects.

2. SURVEY DESIGN

The survey ran from April 2010 to August 2013 (when the telescope was taken down for a major upgrade for HETDEX). The total survey consists of 1022 galaxies, with 1265 long-slit spectra taken over 550 hours. Initially, we focused on galaxies with the largest dispersion. As the survey progressed the criteria on target selection were gradually relaxed and targets with lower dispersions and spheres of influence were added to the queue (§ 2.3). This time dependence is shown in Figure 1. The target selection was continually expanded and improved over the survey life time. Below, we summarize the general overview and strategy, and in the subsections that follow, we describe the target selection in detail. § 2.1 details the parent sample used to select targets. In particular, § 2.2 describes the adopted sphere of influence metric, which defines the suitability for a black hole mass measurement. The main metric of success for the survey is to find the galaxies with the largest predicted spheres of influence, and we quantify this in § 2.3. Subsequently, we detail the success of the secondary goal of sampling all possible host galaxy properties in § 2.4. Lastly, the survey also includes special galaxies, such as those with previously measured black hole masses. These galaxies are described in § 2.5. All observations and the derived galaxy parameters from the survey are presented in Table 1, and are also available from the project website at

<http://www.mpi-a.de/~bosch/hetmgs>.

At the start of each new trimester, we submitted a fresh set of targets. Afterwards the target list was updated about once every 6 weeks in order to account for holes in Local Sidereal Time (LST) in our *and* the overall telescope queue. New observations were processed as the survey progressed, which were then used to optimally select and schedule future targets. During the survey we gradually optimized the target selection and queuing. In the end, the algorithm was very sophisticated: it backfilled the queue with low priority objects in undersubscribed LSTs, while making sure that these new targets did not conflict with our own high priority targets. The algorithm also ensured that both rising and setting targets were available at any time, to work with pointing restrictions (e.g., limitations due to high wind). By always having targets available, our program could capitalize on undersubscribed times in the queue.

We do not select galaxies to observe based on their morphology. The only exception is to exclude strongly interacting galaxies and those that are too large to fit in the $8'$ slit. All HETMGS galaxies are within the telescope’s declination limit of $-11 < \delta < 73^\circ$, and we minimized target overlap with the SAURON (de Zeeuw et al. 2002), ATLAS^{3D} (Cappellari et al. 2011) and CALIFA (Sánchez et al. 2012) surveys, as their integral field unit (IFU) observations are of a higher quality and publicly available. The observed sample is not complete since it was scheduled as a low priority filler program.

2.1. Parent sample

The targets in the survey were selected from a (continually updated) parent sample which was constructed from 2MASS photometry and literature velocity dispersions. We chose the 2MASS Extended Source Catalog (XSC; Jarrett et al. 2000) as it is the best all-sky catalog of extended sources that is currently available. It is deep enough to include all the nearby galaxies for which direct black hole masses can be robustly measured. Additionally, the catalog contains many useful parameters such as half-light radius (R_e), position angle (PA), and flattening.

Note that the 2MASS observations are relatively shallow and the XSC is known to underestimate the total flux of apparently large, faint or low-surface-brightness objects by an appreciable amount (Jarrett et al. 2003; Graham & Scott 2013; Kormendy & Ho 2013; Läsker et al. 2014a). Furthermore, the half-light radii are measured over circular apertures and are not corrected for the effect of beam smearing. As a result many objects with a full width at half maximum (FWHM) smaller than $2.^{\circ}5$ are overestimated in size.

The parent sample needs to include all possible targets, and must therefore be much larger than the survey itself. From the XSC all 23000 objects were selected that have apparent K_s magnitudes (K_M_EXT) within the range $5 < m_{K_s} < 11$. Fainter galaxies are expected to have a sphere of influence that cannot be resolved. For an apparent brightness of $m_{K_s} = 11$ the largest expected θ_i in the parent sample is $0.^{\prime\prime}04$ when adopting the $M_\bullet - \sigma$ relation and the fundamental plane from § 5. Current state-of-the-art adaptive optics reaches $0.^{\prime\prime}1$ FWHM and the $m_{K_s} = 11$ limit of the parent sample is thus sufficient.

The parent sample is further augmented with velocity dispersions from various literature sources. We added the 7800 literature velocity dispersions that were available from the HyperLeda database in early 2011. The two biggest sources in that database are McElroy (1995) and Wegner et al. (1999). Out of the 7800 galaxies, 4600 were not in our parent sample. (Most of these are fainter than $m_{K_s} > 11$.) This increased the

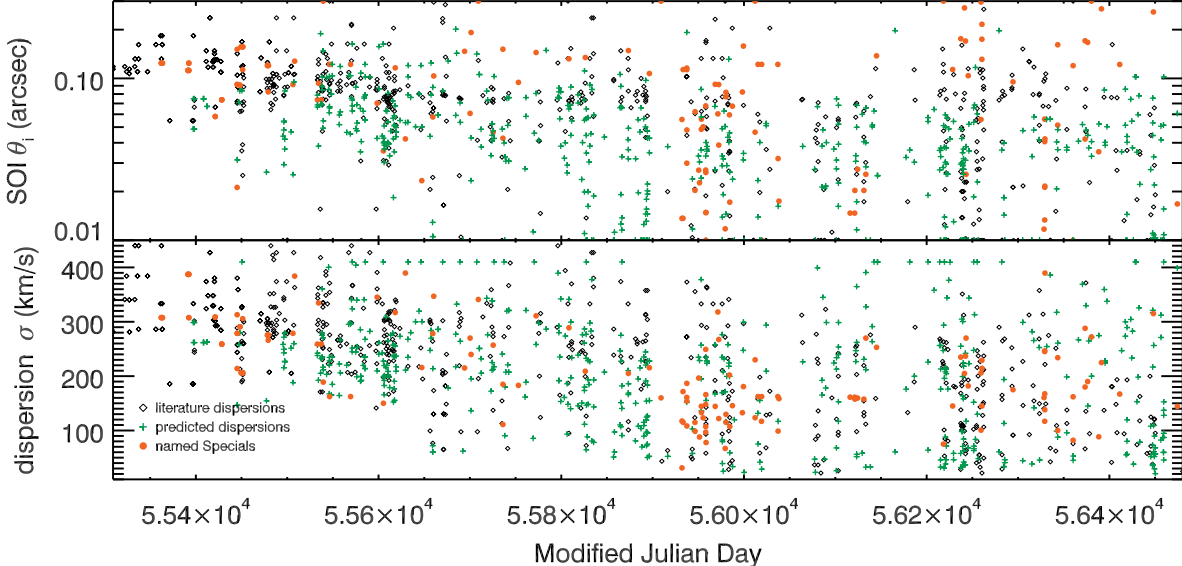


Figure 1. The **top** and **bottom** panels show the sphere of influence and velocity dispersion of the observed targets as a function of Modified Julian Day. The diamonds denote the observed targets with a literature dispersion from the final parent sample. When no literature dispersion is available a predicted velocity dispersion is indicated by a cross (Capped at 410 km s^{-1} . See §5.). Special galaxies (see § 2.5) are shown as filled circles. As the survey progressed, galaxies were targeted with smaller dispersions and spheres of influence.

total size of the parent sample to 29000 objects. We cross-matched the resulting catalog with SDSS NYU Value Added Catalog (Blanton et al. 2005; Adelman-McCarthy et al. 2008) which added another 4500 stellar velocity dispersions to the parent sample.

We added redshift distances from the NASA Extragalactic Database (NED) and the 2MASS redshift survey (Huchra et al. 2012) and redshift-independent distances from NED-1D. For the redshift distances we use $H_0 = 70.5 \text{ km s}^{-1}$ from Komatsu et al. (2009) and the reference frame from Mould et al. (2000), which corrects for Virgo infall, the Great Attractor, and the Shapley supercluster. Almost all galaxies in the parent sample have estimated distances. Out of the parent sample 12% of the objects have no associated redshift, but this reduces to 0.7% when objects near the galactic plane ($|b| < 5^\circ$), large extinction ($A_b > 2$) and non-galaxy-like colors ($0.75 > J - K > 1.25$) are removed (see also Huchra et al. 2012). For each object, the amount of Galactic foreground extinction was determined using the $100 \mu\text{m}$ dust maps from Schlegel et al. (1998).

2.2. The Sphere of Influence

For survey target selection, we need to adopt a criteria for determining the suitability of a galaxy for a black hole mass measurement. The mass of the black hole at the center of galaxies can best be determined by spatially resolving the kinematics near the black hole, using tracers like rotating gas or stars. The closer the tracer is to the black hole, the more accurate the measurement. Ideally, the region where the gravitational forces of the black hole dominates over the rest of the galaxy should be probed. The size of this sphere of influence is usually⁶ defined

⁶ An alternative to this dynamical definition is to use photometry. By deprojecting the photometry, the total amount of enclosed stellar mass as function of distance from the black hole can be estimated. The light can be converted into mass with a mass-to-light ratio (from either dynamics or a stellar population analysis), and the mass can then be compared to the mass of a putative black hole. However, the photometry needs to have sufficient spatial resolution to resolve the region of interest. Typical ground-based imaging is not good enough for this, and thus, for this survey, we adopt the the dynamical θ_i estimator.

as $r_i \equiv GM_\bullet\sigma^{-2}$. Given distance D , the apparent size of the sphere of influence is then $\theta_i = r_i D^{-1}$. This definition is derived from the virial theorem by assuming a spherical geometry and isotropy near the black hole (Peebles 1972). Sometimes a less conservative definition is adopted that uses the diameter instead of the radius (e.g., Valluri et al. 2004).

The definition of θ_i is very convenient, especially when planning observations where the black hole mass is not yet known a priori. By adopting a black hole scaling relation, the sphere of influence can be estimated and the feasibility of proposed observations can be evaluated. The most practical scaling relation for this purpose is $M_\bullet - \sigma$, which yields a prediction for the sphere of influence $\theta_i = G\sigma^{2.5}D^{-1}$, when adopting a slope of 4.5 in $M_\bullet - \sigma$ from Gultekin et al. (2009). As a result, the sphere of influence can be predicted with just a distance and a velocity dispersion as input. Note that θ_i is just a prediction; it depends on the adopted scaling relations and the true sphere of influence can only be known once the black hole mass has been measured. Throughout this paper θ_i is repeatedly used, and it always refers to the *predicted* θ_i , unless the black hole mass has been measured.

The $M_\bullet - \sigma$ relation is the only practical black hole mass proxy available. Other scaling relations have larger intrinsic scatter or require a more detailed analysis of the host galaxy. For example, the $M_\bullet - L_{\text{bul}}$ relation relies on bulge–disc decompositions. As such the resulting measurement of bulge luminosity is often very degenerate (Läsker et al. 2014a) and cannot be robustly determined with an simple algorithm that can be applied to a large data set. Hence it is impractical to use the bulge luminosity to select targets. On the other hand, the velocity dispersion σ can be measured cleanly. Furthermore, the $M_\bullet - \sigma$ relation also yields a smaller—more conservative—estimate of θ_i than expected from the $M_\bullet - L_{\text{tot}}$ relation (See § 8). Many other scaling relations exist, (e.g., Aller & Richstone 2007; Graham 2012; Hopkins et al. 2007; Graham 2012), but those are not a significant improvement of $M_\bullet - \sigma$. In practice, such alternative predictors would have targeted much the same galaxies. See § 8 for a direct comparison with $M_\bullet - L_{\text{tot}}$.

2.3. Sphere of influence completeness

The survey originally started by targeting the 65 galaxies with highest literature dispersions $\sigma > 270 \text{ km s}^{-1}$ and spheres of influence $\theta_i > 0.^{\circ}1$ solely based on the HyperLeda database. We adopt the $M_{\bullet}-\sigma$ parameters from Gultekin et al. (2009) to estimate the sphere of influence. As the survey progressed and transitioned into a large program, these hard limits on σ and θ_i were gradually relaxed and additional sources were added (Figure 1).

The sphere of influence of the 546 targeted galaxies with literature dispersions are shown in left panel of Figure 2. Many of these literature dispersions turn out to be overestimated compared to the HETMGS measurements. Of the 100 observed galaxies with a predicted $\theta_i > 0.^{\circ}1$ a significant percentage (17%) turned out to have $\theta_i < 0.^{\circ}08$. This is largely caused by the large uncertainties and systematics of the HyperLeda velocity dispersions, which is also apparent in Figure 6.

The middle panel of Figure 2 shows the sphere of influence of all the 471 observed targets without literature dispersions. For the galaxies that did not have a literature velocity dispersion, the sphere of influence was predicated by combining the $M_{\bullet}-\sigma$ relation and a dispersion estimate from the fundamental plane from § 5. These dispersion estimates are good enough to yield adequate predictions for θ_i . When selecting targets this way, we omitted probable quasars that have both small sizes ($r_e < 2''$) and AGN-like colors ($0.75 < J-K < 1.25$). In total, we found 31 objects with spheres of influence bigger than $0.^{\circ}1$ that also did not have a velocity dispersion measurement in the literature.

The final survey include 95% and 50% of all galaxies with a sphere of influence above $0.065''$ and $0.045''$, respectively (from the subset of galaxies in the parent sample, visible from the HET, and excluding galaxies with a known black hole mass and ATLAS^{3D} data). The right panel of Figure 2 shows the predicted spheres of influence of all the HETMGS observed galaxies based on our dispersions. The final sample contains 114 galaxies with a sphere of influence greater than $0.^{\circ}1$. Under the assumption that $M_{\bullet}-\sigma$ is a reasonable predictor for black hole mass, the survey has satisfied its goal of finding almost all galaxies with a large sphere of influence in the parent sample.

The θ_i is strongly coupled to galaxy dispersion ($\theta_i \propto \sigma^{2.5}$) and galaxies with large dispersions have the largest sphere of influence. Selecting galaxies based on largest θ_i , as is done here, is strongly biased towards galaxies with the largest densities. This is apparent as the strong clustering in Figure 3. Many object in the survey are denser still than average early-type galaxies.

2.4. Sampling all sizes and surface brightnesses

If targets were selected merely on the largest possible θ_i using the $M_{\bullet}-\sigma$ relation, the survey would contain mostly dense (early-type) galaxies with dispersions over 200 km s^{-1} , as these galaxies have the largest spheres of influence. This bias occurs because the most important term in θ_i is $\sigma^{2.5}$. This is directly visible in figure 2, as the highest dispersion galaxies have the largest θ_i . The early-type galaxies are already overrepresented in black hole studies and hence diversifying the parameter space to other types of galaxies would create leverage on the scaling relations. Especially to test the universality (e.g., spiral galaxies appear to have low black hole masses for their dispersions; Greene et al. 2010; Kuo et al. 2011).

To ensure that the survey is in not solely restricted to high dispersion galaxies, we need to employ an alternative way

of selecting targets, independent from velocity dispersion. A good alternative would be to use bulge luminosities, as that correlates very well with black hole mass also. However, the bulge luminosity is impractical; they require a photometric decomposition, to separate the disk and the bulge. Those decompositions are often very degenerate and require a lot of fine-tuning. Other desirable galaxy parameters, like optical ($g-r$) colours, are not available over the whole sky and can thus not be used when the distance (in Mpc) of the targets is key priority.

We chose to select additional targets by sampling in galaxy size and average surface brightness ($\langle \mu_e \rangle$). These two properties make up a near face-on projection of the fundamental plane ($R_e \propto \sigma_e^\alpha \langle \mu_e \rangle^\beta$, see §5) and is also independent of the (often unknown) velocity dispersion. For our purposes, surface brightness is a better choice than absolute luminosity, as the latter has a much tighter relation with galaxy size. This selection automatically ensures sampling across galaxy types, because Spiral galaxies occupy a different region on fundamental plane than early-type galaxies.

For a given set of galaxies with the same properties, the ones with the largest θ_i will have the lowest distances (in Mpc). To diversify the sample in size R_e and surface brightness $\langle \mu_e \rangle$, we only have to do a sampling in these two parameters and select the closest ones (in Mpc) at every given value-pair of R_e and $\langle \mu_e \rangle$. We define a euclidian distance norm of $\|x\| := \sqrt{\Delta(\langle \mu_e \rangle)^2 + \Delta \log(R_e)^2}$, with $\langle \mu_e \rangle$ in units of mag/arcsec² and R_e in kpc. This allows us to quantify our sampling in the $R_e-\langle \mu_e \rangle$ plane. In theory the strategy would be straightforward: Just select the nearest galaxies, until sufficient coverage is created. In practice, the targeting is dependent of what galaxies can be observed at the telescope in the remainder of the trimester. Hence we created an algorithm that would add the nearest (in Mpc) galaxies to our sample to would best enhance our coverage w.r.t the norm. This used an iterative method; Every time new targets were scheduled, we sorted the subsample of visible targets in order of increasing distance in Mpc. Then, we started with the nearest galaxy and checked if it had any nearer (in Mpc) neighbors with norm $\|x\| < \varepsilon$ among the previously observed and queued objects still visible in the remainder of the trimester. If not, then the galaxy is added to queue. As more galaxies were observed, we decreased ε in order to find enough observable targets. At the end of the survey ε was reduced to 0.07. The method was also the primary method for backfilling the undersubscribed LST slots in the telescope queue, by iterative shrinking ε until targets where found with the required LST.

This method is completely independent of the adopted black hole mass scaling relation, and it produces a survey sample that has the same extent in galaxy size and surface brightness as the parent sample (see Figure 3). Furthermore, the selection method picks out the closest galaxies with the largest sphere of influence for a set of galaxy properties. In the final survey, 90% of the galaxies have a neighbor within a norm of $\|x\| < 0.10$. Our procedure selected many nearby spirals galaxies that otherwise would not be included in the survey at all, including the most extreme galaxies such as the biggest and smallest spiral galaxies. Many of the galaxies selected this way are the low sphere of influence objects seen in Figure 2.

2.5. Special targets

The survey also contains ~ 150 special galaxies, which were targeted to create overlap with other black hole studies and

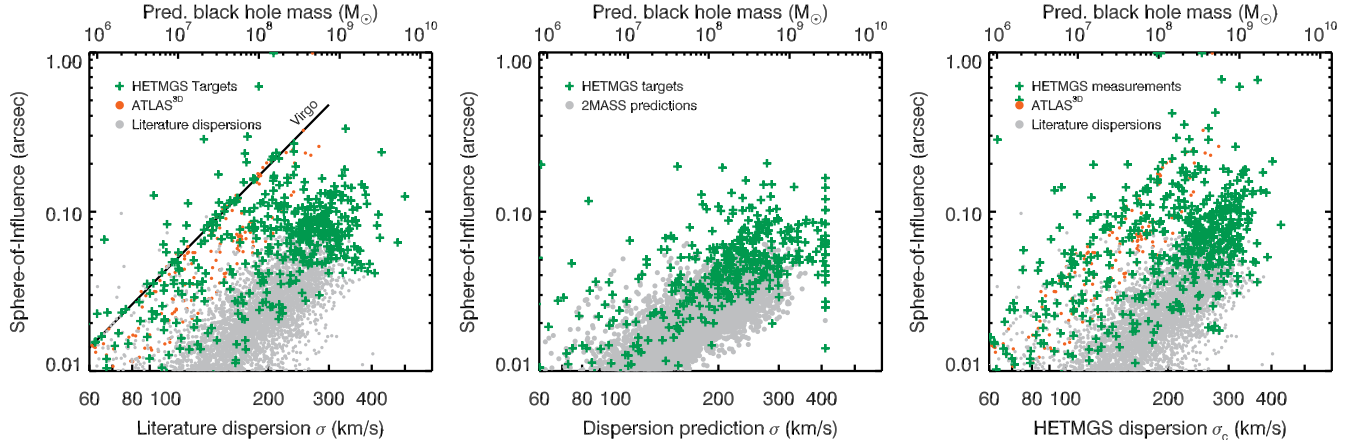


Figure 2. The HETMGS targets are shown as function of velocity dispersion, estimated black hole mass from $M_{\bullet} - \sigma$, and estimated sphere of influence. The primary objective of the HETMGS is to observe galaxies with the highest predicted spheres of influence. The survey succeeded in observing 95% of all galaxies with θ_i greater than $0.065''$. **Left panel:** galaxies from the parent sample with literature dispersions and their spheres of influence predicted using $M_{\bullet} - \sigma$ are shown as grey circles and the HETMGS targets that were observed from this subset are plotted as green crosses. The black line indicates where galaxies at the distance of the Virgo cluster lie. **Middle panel:** the predicted velocity dispersions from the galaxy fundamental plane and the estimated θ_i of all 2MASS galaxies in the parent sample without literature dispersions are given by the grey circles, while the HETMGS targets selected from this subset are shown as green crosses. **Right panel:** all 1022 galaxies in the HETMGS sample are displayed with the green crosses. The velocity dispersion values shown are the measurements made from the HET data. The grey circles are the remaining parent sample galaxies with a literature dispersion. The red points are galaxies in the ATLAS3D survey, but not in HETMGS. For reference the *HST* resolution is $0.1''$ FWHM. Galaxies with a known black hole masses or not visible from the HET are not shown.

allow for cross-calibration checks. These galaxies were drawn from a dedicated list, and were queued at an elevated priority. The red dots in the timeline in Figure 1 represent the special galaxies, as reconstructed from the final list. Once observed, these objects were not treated differently in terms of data reduction or kinematic analysis, and are considered part of the total sample. All special galaxies are included in Table 1 and the figures.

More specifically, the special targets include galaxies with direct black hole mass measurements from literature compilations (McConnell & Ma 2013; Graham & Scott 2013; Kormendy & Ho 2013, and references therein) and black hole estimates from Beifiori et al. (2009). We observed 53 of the 63 Northern galaxies, with a known black hole mass. We also targeted galaxies for which black hole mass efforts are currently under way, but are yet unpublished (Greene, priv. comm., Kravović, priv. comm., McConnell, priv. comm.). Most of those galaxies were already in the sample, and were previously selected, following the procedure outlined in § 2.2. The primary reason to observe these objects is to create a homogeneous data set among the galaxies with known black hole masses. In § 7, we use this homogeneity to show that the central dispersion, σ_c , can be used in $M_{\bullet} - \sigma$.

One of the first results from the HETMGS is the discovery of compact galaxies that may host black holes weighing $\sim 10\%$ of their host galaxy mass (van den Bosch et al. 2012; Läsker et al. 2013; Walsh et al. 2015 subm.; Yıldırım et al. 2015 subm.). These über-massive black hole candidates appear to be significantly more massive than expected based on their host galaxy's luminosity. The host galaxies are relatively small and have high velocity dispersions for their (stellar) mass. In our survey, such objects are selected because they have large spheres of influence due to their high dispersions and because of the diversity sampling from § 2.4 that targets extreme galaxies. Nevertheless, we specifically targeted compact galaxies using a mass-size cut: $-6.91 - 0.29M_{Ks} > \log(0.75R_e)$. We further required that the galaxy have no previous velocity dispersion measurement, or a literature velocity dispersion value that was 20% higher than predicted from our fundamental plane calibration (see § 5). This selection criteria produced about 30 targets.

Overall, there are 200 galaxies below this mass-size cut in the survey. A full analysis and discussion of these compact galaxy systems is outside of the scope of this paper.

3. MARCARIO LOW RESOLUTION SPECTROGRAPH DATA REDUCTION

All the observations were taken with the Marcario Low Resolution Spectrograph (LRS; Hill et al. 1998), which is an optical long-slit spectrograph with a slit length of $4'$ and a $3k \times 1k$ CCD. We used the g2 grating, which covers $4200 - 7400 \text{ \AA}$, and the default 2×2 binning. This setup provides an instrumental resolution of 4.8 \AA (7.5 \AA) FWHM, or a dispersion of 108 km s^{-1} (180 km s^{-1}) for the $1''$ -wide ($2''$ -wide) slit, as measured from the 5577 \AA night sky line. When practical, we aligned the slit on the major axis and centered it on the galaxy. During each visit, we obtained a single 15 minute exposure. The typical spatial resolution of the observations is $2.5''$ FWHM.

The observations and calibration data were retrieved and processed using a dedicated pipeline written in IDL⁷. The pipeline is fully automated and executes a series of basic steps. First, the spurious pixels in each exposure are masked using a bad pixel map, and cosmic rays are masked using PyCosmic (Husemann et al. 2012). The frames are overscan and bias subtracted, and then flat fielded. The next step is a direct interpolation onto a frame that is linear in the spatial dimension and logarithmic in the wavelength dimension, using a spatial distortion map from a pinhole exposure and the wavelength solution from nightly arc lamp exposures. A variance (error) frame is propagated in the same way. During each exposure, the effective aperture of the HET continually changes because the prime-focus optics move to track an object, thereby affecting the throughput along the spatial direction. These throughput changes are measured in each science exposure using the apparent brightness of the sky lines along the slit. For this reason, we do not attempt to perform absolute or relative flux calibration⁸, and no attempt

⁷ We gratefully acknowledge the use of the IDL astrolib (Landsman 1993) and MPFit (Markwardt 2009)

⁸ The LRS calibration program does provide flux and radial velocities

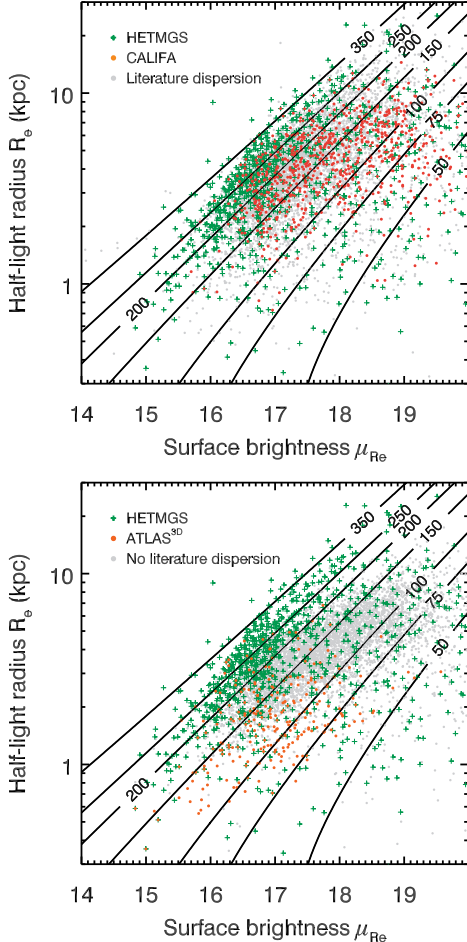


Figure 3. The distribution of average surface brightness $\langle \mu_e \rangle$ and half light radius R_e of surveyed galaxies. The **left** panel shows the HETMGS, CALIFA mother sample and literature dispersions. The **right** panel shows the HETMGS, ATLAS^{3D} and un-surveyed galaxies in the parent sample. The HETMGS samples different types of galaxies than both ATLAS^{3D} and CALIFA. Faint galaxies in the CALIFA mother sample are not shown as they are too faint to be in the 2MASS XSC. The over-plotted lines indicate the velocity dispersion predictions in km s^{-1} using our calibration of the fundamental plane (§5).

was made to measure the absolute emission-line fluxes.

The data products, presented in Table 1, include the following quantities: heliocentric velocity, stellar absorption line velocity dispersions, the emission line ratios $[\text{N II}]/\text{H}\alpha$ and $[\text{O III}]/\text{H}\beta$, and their uncertainties. These quantities are all measured within a $3.^{\prime\prime}5$ aperture centered on the brightest pixel in the slit. For the stellar kinematics, the pipeline fits the stellar continuum with the pixel-fitting code (pPXF; Cappellari & Emsellem 2004) using template stars from MILES (Sánchez-Blázquez et al. 2006; Falcón-Barroso et al. 2011a). Inside the central aperture the Signal-to-Noise ratio (S/N) is typically over 100, resulting in robust stellar kinematic measurements, as shown in § 4. The fit to each (central) galaxy spectrum is manually inspected to find systematics and errors. An example spectrum is shown in figure 4.

The stellar kinematic extraction is obtained from the stellar continuum in an observed window of $5000 - 6100 \text{ \AA}$, selected to minimise instrumental resolution changes across the slit. Additionally all regions with possible contamination from

standards stars on a regular cadence.

emission lines were masked. For the both the stellar kinematics and emission-line extraction, we apply multiplicative (M DEGREE) and additive polynomials (DEGREE) of degree 25 and 5, respectively, to the template stars to match the continuum and account for dust, AGN light and the (absence of) flux calibration. The number of polynomials is chosen to be large enough to be able to compensate for (uncommon) issues with the uneven flat fields. In the next section, we show that our kinematics are robust.

The sky is measured in two large bins on each end of the slit, and were added as a sky-template to pPXF to do the sky subtraction. For the emission-line fit we use all the 1000 template stars in the MILES library and the full wavelength range available. For the stellar kinematics, we construct a single composite template by first fitting the full wavelength range using a subset of 90 stars that get used most frequently in all the aforementioned emission line extractions. Adding more stars increases the computational time and does not change the derived values. Typically 20 stars get a non-zero weight in the initial pPXF fit. The uncertainties on the stellar kinematics were computed by running a 100-iteration Monte-Carlo in which the flux is randomly perturbed and with a single composite template. During the Monte-Carlo the instrumental dispersion of the composite template is also perturbed, which insures realistic uncertainties when the galaxy dispersion is unresolved. The mean and standard deviation of the Monte-Carlo run are adopted as the measured value and the formal 1σ uncertainty.

When present, emission lines are obtained using GANDALF (Sarzi et al. 2006). An example GANDALF fit is shown in figure 4. We consider an emission as detected when the residuals underneath the line are 4 times lower than the amplitude of the line (Amplitude-over-Noise AoN>4; see Sarzi et al. 2006). The errors on the emission lines are directly computed by GANDALF. The [S II] emission lines often overlap with a broad telluric feature, and therefor are not included in Table 1.

The survey contains 50 galaxies with broad emission lines, which are presumably AGN. The dispersion for these objects could not be reliably measured in the central aperture, as the stellar continuum is washed out. Instead, an attempt was made to measure the dispersion using a larger aperture and masking the nucleus. Such objects are flagged in Table 1 as AGN.

Most observations were deep enough that spatially resolved kinematics could be extracted as well, allowing us to measure rotation curves and velocity dispersion profiles. To ensure adequate signal for the stellar kinematics extraction, we combine spatial rows into bins with a minimum S/N of 25. An example is shown in figure 5. The kinematics are available from the project website at survey website <http://www.mpi-a.de/~bosch/hetmgs>.

4. KINEMATICS COMPARISON

There is a large overlap between the HETMGS and other spectroscopic surveys, which we use to validate our heliocentric velocities and stellar velocity dispersions. The SDSS survey provides a good comparison, as these homogeneous measurements all come from the same instrument and its $3.^{\prime\prime}$ fibers are approximately the same size as our pseudo-apertures from the HET long slit. There are 148 galaxies in common with SDSS and there is excellent agreement with their dispersion measurements, as shown in Figure 6. The standard deviation of the relative difference between the two dataset is only 11%. Which is smaller than the 35% relative uncertainty of the HETMGS errors of the same subset. Such small dif-

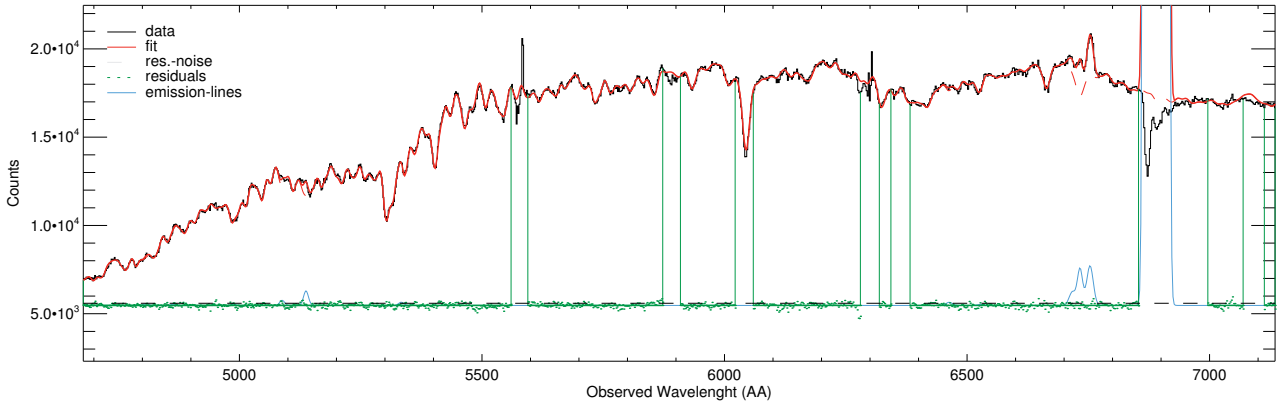


Figure 4. Reduced data and best-fit model of the central spectrum of NGC 5228 using pPXF and GANDALF. The observed heliocentric velocity and dispersion of this galaxy is 7500 and 215 km s⁻¹, respectively. Strong sky lines (i.e. 5577 and 6300 Å) and telluric features (6900 Å) are masked from the fit. Emission from [OIII], [NII] and H_B is detected in this spectrum.

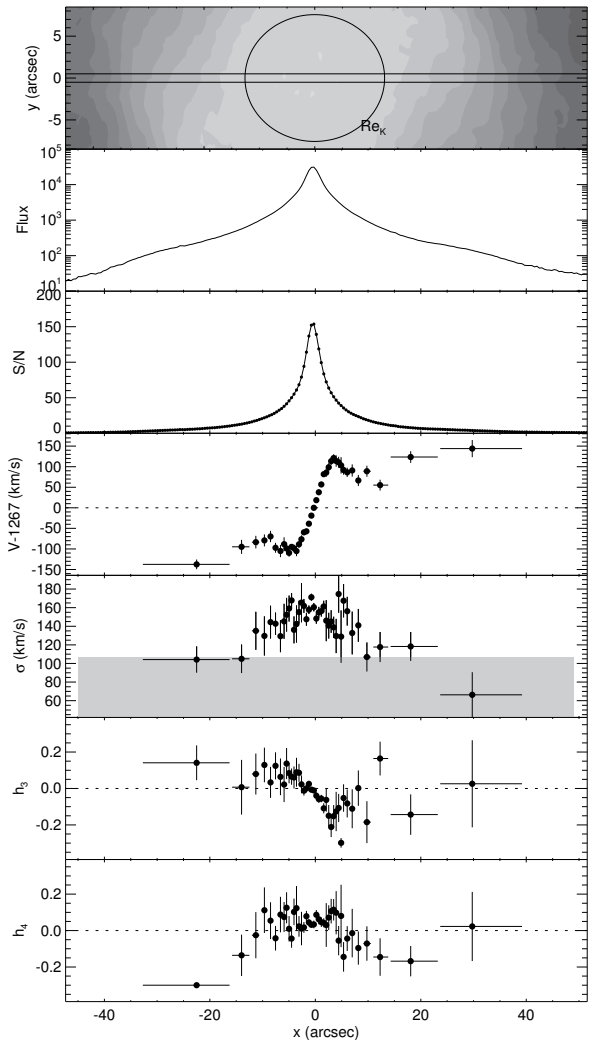


Figure 5. Example of the resolved stellar kinematics using exposure 262031 of NGC2950. The kinematics are measured in bins that are combined to reach Signal-to-Noise of 35. Top to bottom panels show: Finder chart and approximate slit alignment based on the DSS image. (Unitless) Flux. S/N. Stellar velocity, dispersion, and Gauss-Hermite moment h_3 and h_4 . The grey shaded region indicates where the instrumental dispersion is larger than the stellar velocity dispersion.

ferences are consistent with the expected systematics due to the changes in seeing and positioning of the apertures of the different telescopes.

The velocity dispersions from HyperLeda are much less reliable, as this database consists of amalgamated literature. The 471 galaxies in common have a standard deviation in the difference of 16% or 30 km s⁻¹. It is noteworthy that HyperLeda values over 300 km s⁻¹ are commonly too large by a significant amount, as seen in Figure 6. There is an overlap of 1677 galaxies between SDSS and HyperLeda, and the comparison between the two data sets shows the same trend. These biases and large uncertainties need to be taken into account when preparing observations with HyperLeda.

The Palomar survey by Ho et al. (2009) published velocity dispersions for the 428 galaxies with the largest apparent brightnesses. These values were not yet included in the HyperLeda database when the parent sample was constructed. There are 188 galaxies that overlap for which there is agreement that is similar to that of the HyperLeda sample: the standard deviation of the difference is 17%.

The SDSS redshifts are very precise with a formal uncertainty of 3 km s⁻¹. In the cross-matched sample between HETMGS and SDSS the mean difference between the heliocentric velocities is 23 km s⁻¹ with a standard deviation of 20 km s⁻¹. The redshift comparison with the rest of the parent sample shows a larger offset: their mean and standard deviation are -38 and 43 km s⁻¹, respectively. In rotating galaxies the mean velocity changes rapidly near the center, and thus these kinematic offsets are expected just based on small positional offsets.

5. THE FUNDAMENTAL PLANE AS DISPERSION PREDICTOR

For the target selection we need an estimate of θ_i . However most of the galaxies in the parent sample do not have a literature stellar velocity dispersion measurement, which is required to compute their θ_i . In those cases the fundamental plane $R_e \propto \sigma^\alpha \langle \mu_e \rangle^\beta$ —the relation between galaxy size, surface brightness and dispersion—can be employed to estimate their dispersion. To get dispersion estimates, we fitted a fundamental plane to the combination of XSC photometry and the SDSS and HETMGS dispersions. After some experimentation, the best results were achieved with the 2MASS catalog values for the half light radius R_e (K_R_{EFF}) and effective surface brightness ($\langle \mu_e \rangle = K_M_{EXT} + A_K + 2.5 \log(2\pi R_e) + 0.394$)

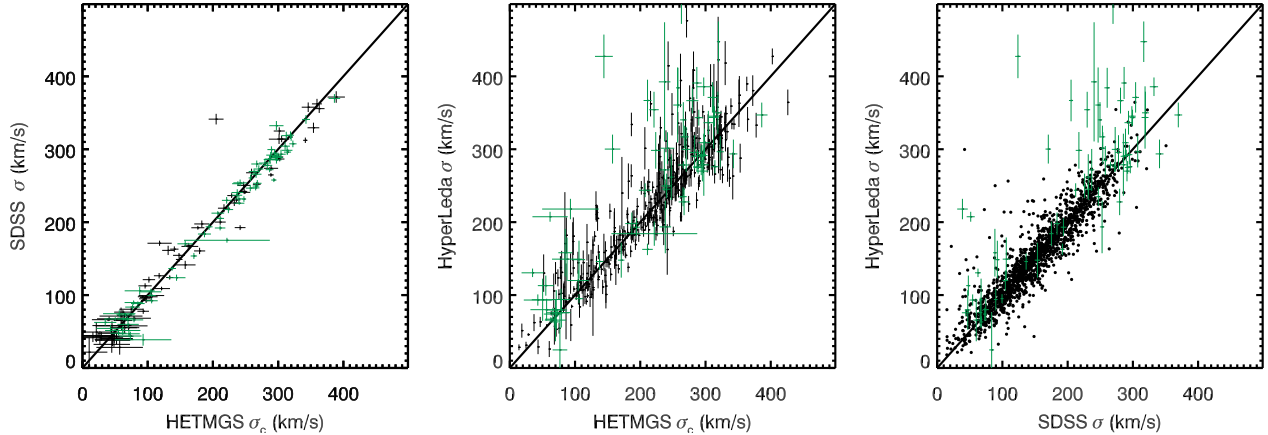


Figure 6. A comparison of the HETMGS central velocity dispersion measurements to literature values from the SDSS and the HyperLeda database. The HETMGS values are measured in the central $3.5 \times 2''$ or $3.5 \times 1''$. The SDSS measurements are from $3''$ fibers, while the HyperLeda database draws from the amalgamated literature. The 73 green objects represent the galaxies present in all three samples. The HETMGS dispersions agree well with SDSS. The HyperLeda dispersion are very unreliable, especially for values above 300 km s^{-1} . In the middle and right panel, the error bars on the x-axis and both axis are suppressed for clarity, resp.

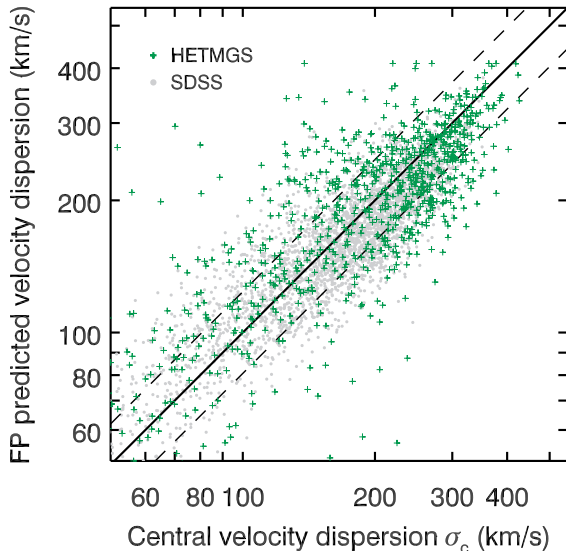


Figure 7. Velocity dispersion predictions from the Fundamental Plane. The figure shows measured stellar velocity dispersion versus predicted velocity dispersion from the fundamental plane (§5). The comparison is done with galaxies that have a HETMGS dispersion (green crosses) and the grey dots are SDSS galaxies. The thick and dashed lines show equality and the 0.09 dex RMS scatter, respectively.

combined with the dispersion from the HETMGS and the SDSS galaxies within 140 Mpc. With this dataset, a robust quartic fit from ROBLIB yields a fundamental surface that predict the velocity dispersion of all the galaxies in our parent sample with an RMS error of 0.09 dex. The residuals, shown in figure 7, do not show systematic biases, which is remarkable as the sample contains both early and Late type galaxies. And the fundamental plane is normally only used for early types. Our fundamental plane parameters are a significant improvement over the parameters from Pahre et al. (1998), which has an RMS error of 0.2 dex on this data set, and only includes ETGs.

A flat plane fit resulted in larger residuals and a systematic bias for the largest dispersion galaxies, which is unfortunate as they are the highest priority targets of the HETMGS. The curvature in our quartic surface is not very strong, as seen in figure 3. The coefficients of the surface fit are $\log \sigma = 6.39 - 0.32\langle\mu_e\rangle + 0.004\langle\mu_e\rangle^2 - 0.10\log R_e + 2.14(\log R_e)^2 + 0.27\langle\mu_e\rangle\log R_e$.

For the survey, only the predictive power of the fundamental plane is important. The functional form is irrelevant, as long as the dispersion is predicted reliably. Nonetheless, it is remarkable the fundamental plane derived from photometry of the 2MASS XSC catalog has so little scatter. A full treatment of a 2MASS fundamental plane is outside of the scope of this paper, but see Magoulas et al. (2012) for a near-infrared study based on 10^4 early types from 6dFGS, and also see Falcón-Barroso et al. (2011b) for a near-IR fundamental plane that includes both early- and late type galaxies from the SAURON survey.

During the target selection process, the dispersion estimated from the fundamental plane is used when no literature dispersion measurement is available. Velocity dispersion predictions over 410 km s^{-1} were truncated, as such galaxies are not expected to exist, nor found in our survey. In practice most of these objects turn out to be quasars.

6. THE HETMGS GALAXIES

With 1022 galaxies, the HETMGS survey is the largest galaxy survey with spatially resolved spectroscopy to date. The final sample has a median distance of 65 Mpc and all available combinations of galaxy size, luminosity, and dispersions, as shown in figure 8. The survey is representative of the local volume above a $M_k < -21$, and sizes of 0.5 kpc. The survey is strongly weighted towards the densest galaxies. This is apparent in the mass-size panel. Those objects have the highest dispersions, which is the most important factor for the sphere of influence ($\theta_i \propto \sigma^{2.5}/D$). The sample contains about 30% late type galaxies, based on the galaxy morphology identifiers from HyperLeda.

There is a significant amount of overlap between the HETMGS and other surveys. Between ATLAS^{3D}, CALIFA mother-sample, SDSS and the Palomar survey, there is 56, 83, 148 and 188 galaxies overlap. However all these samples are very different. For example, the Palomar spectroscopic survey (Ho et al. 2009) contains 426 velocity dispersions for the brightest galaxies with apparent magnitudes of $B < 12.5$. The SDSS only includes a (small) fraction of the nearby galaxies (Adelman-McCarthy et al. 2008). And the 600 CALIFA galaxies are selected within $0.005 < z < 0.03$ and are typically too far away for a black hole mass measurement (Sánchez et al. 2012; Walcher et al. 2014). The 260 ATLAS^{3D} (Cappellari et al. 2011) galaxies includes all the massive early-type galaxies inside 24 Mpc, but misses large luminosity galaxies due to

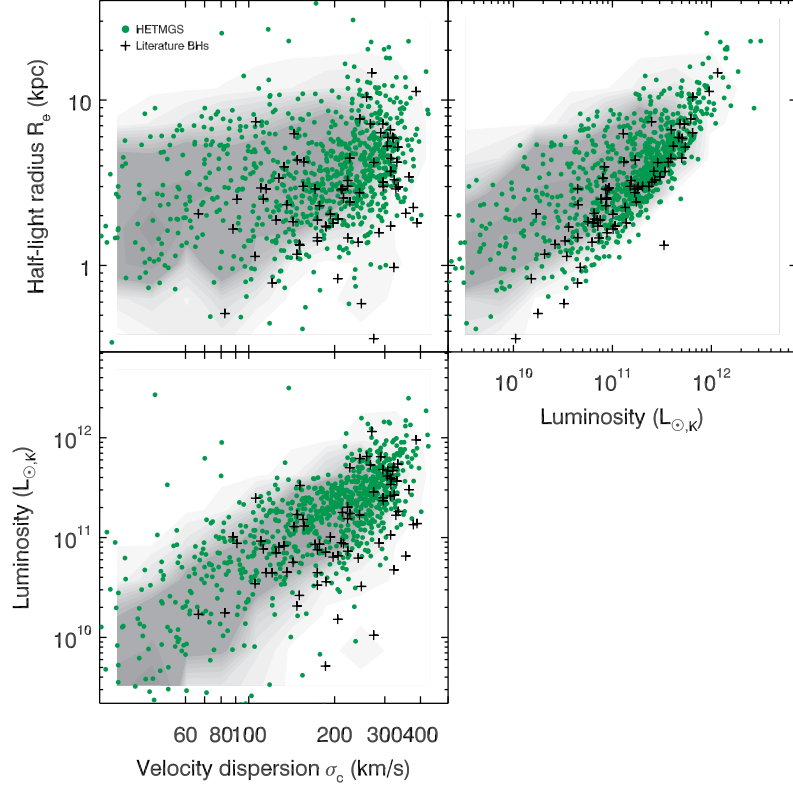


Figure 8. Demographics of the HETMGS galaxies and the literature black hole host galaxies shown as green circles and black crosses, resp. The shaded background represents number density of the global galaxy population, based on the representative SDSS sample of nearby galaxies. The **top left** panel shows the velocity dispersion versus half-light radius. The **right** panel shows the total luminosity versus half-light radius. The **bottom** panel shows the velocity dispersion versus luminosity, i.e. the Faber-Jackson relation. The HETMGS covers all of the galaxy parameter space, whereas the galaxies with a known black hole mass are not representative.

cosmic variance. The comparison of galaxy properties between HETMGS and CALIFA and ATLAS^{3D} is shown in Figure 3.

Emission lines are quite common in the centers of galaxies, often caused by star formation, shocks or accreting black holes. These phenomena can occur at the same time (e.g. Singh et al. 2013). In one third of the survey, central emission lines are detected. This includes the 50 broad line AGNs, and 203, 140 and 290 objects of that are classified as Seyfert, LINER and HII star formation, according to the classification scheme devised by Kewley et al. (2006). But note that we do not specifically attempt to detect (weak) broad line components with the GANDALF. The AGNs can vary substantially on both long and short time scales. One such dramatic example, reported in Denney et al. (2014), is Mrk 590 in which the broad lines have all but disappeared. The HETMGS spectra could be used as baseline for other synoptic AGN studies.

7. CENTRAL DISPERSION OR AVERAGE DISPERSION?

What correlates better with black hole mass: the central dispersion σ_c or the luminosity weighted dispersion inside a half-light radius σ_e ? The first one is more easily measured, but probes an seemingly arbitrary scale of the galaxy, that depends on distance and instrumental effects. Whereas σ_e is measured⁹ inside a physically relevant aperture (R_e) and is also the quantity used for the fundamental plane and virial galaxy masses.

⁹ Note that method for measuring σ_e varies; the measurement requires integral field observations to get the 2D luminosity weighted dispersion and that is not always available. Also the definition of half-light radius varies; e.g. some authors only use the bulge R_e .

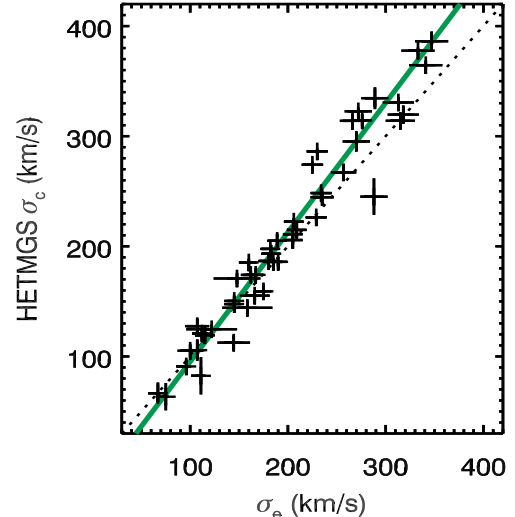


Figure 9. Comparison between the central dispersion σ_c and the luminosity weighted dispersion inside the half-light radius σ_e for the subset of 53 galaxies with black hole masses that are in the survey. A linear regression shows that $\sigma_e = (18 \pm 5) + (0.85 \pm 0.03)\sigma_c$ with an intrinsic scatter of $8 \pm 6 \text{ km s}^{-1}$. The slope is not consistent with unity. For high dispersion galaxies ($\sigma_c > 125 \text{ km s}^{-1}$), the central dispersions are higher than the half-light dispersions. See §7.

Different apertures for σ have been used in the literature. For example, McConnell et al. (2011) has suggested that the central region near the black hole should excluded from the σ_e

estimate, while Woo et al. (2013) argues for the use of a σ that only contains half of the second moment. Furthermore the known black hole masses themselves are strongly correlated with distance, with bigger black holes being further away. Given that σ_c is the most commonly available quantity it is useful to know if and how it correlates with black hole mass.

The difference between σ_c and σ_e is most interesting for disk galaxies where these two measurements probe very different things. Consider the broad-line AGNs in bulge-less disks galaxies (Greene et al. 2010; Simmons et al. 2013; Reines et al. 2013). For these systems, Kormendy et al. (2011) argues that neither $M_\bullet - \sigma$ and $M_\bullet - L_{\text{bul}}$ should apply to these galaxies, however their AGN is proof that they host a black hole. Is there perhaps another scaling relation that is applicable for these systems? If the black hole mass is solely linked to the bulge (e.g. Woo et al. 2013), then one would expect that the σ_e of a disk dominated galaxy should not correlate with black hole mass, whereas σ_c should correlate better as it is a good tracer of the (central) bulge component. A homogenous dataset allows for a systematic test of all such scenarios.

For the purpose of the survey, we are predominantly interested in whether the σ_c is a good predictor of black hole mass. Güttekin et al. (2009) found their dataset to be consistent with $\sigma_c = \sigma_e$, with an RMS scatter of 22 km s^{-1} . But this warrants repeating with the homogeneous dispersions from the HETMGS and the literature updates to σ_e (e.g. ATLAS^{3D}). For this comparison we use σ_c as measured in the central HETMGS 3.⁵ aperture (See §3) and σ_e as tabulated in Kormendy & Ho (2013) or McConnell & Ma (2013). There are 53 galaxies with a σ_c and a black hole mass in this survey. The comparison is shown in figure 9. Using a linear regression (LINMIXERR, Kelly 2007), we find $\sigma_e = (18 \pm 5) + (0.85 \pm 0.03)\sigma_c$ with an intrinsic scatter of $8 \pm 6 \text{ km s}^{-1}$. The slope is inconsistent with being unity and is also inconsistent with the regression from Güttekin et al. (2009). The σ_c is higher for higher dispersion galaxies and lower for the disk-dominated galaxies with low dispersions.

Using the same subset of 53 galaxies and LINMIXERR the $M_\bullet - \sigma_e$ and $M_\bullet - \sigma_c$ relations are: $(\alpha, \beta, \varepsilon_0) = (8.37 \pm 0.07, 5.49 \pm 0.40, 0.43 \pm 0.23)$ and $(8.24 \pm 0.06, 5.28 \pm 0.37, 0.40 \pm 0.21)$, with $\log(M_\bullet/M_\odot) = \alpha + \beta \log(\sigma/200 \text{ km s}^{-1})$, where ε_0 is the intrinsic scatter. The two relations are nearly identical, apart from a slightly shallower slope with the central dispersion, as expected from the correlation between σ_c and σ_e . So both velocity dispersion measures can be used to predict black hole mass. Our $M_\bullet - \sigma_e$ relation is not consistent with the $\beta = 4.38$ from Kormendy & Ho (2013), because we did not exclude pseudo-bulges (see their §6.6.2). Our $M_\bullet - \sigma_e$ relation is consistent with McConnell & Ma (2013).

We conclude that σ_c can indeed be used as a substitute in $M_\bullet - \sigma$, albeit with a steeper gradient. In the survey we used $M_\bullet - \sigma$ from Güttekin et al. (2009) for the target selection (§2.3), which has a shallower slope. The difference with $M_\bullet - \sigma_c$ is not very big, as seen in figure 10. If we had $M_\bullet - \sigma_c$ for target selection instead, the survey would have favored higher dispersion galaxies at larger distances, as this relation predicts bigger black holes for the highest dispersion galaxies. However those galaxies were already included in the survey, as they already have the largest spheres of influence anyways. The completeness statistics therefor would not differ appreciably with the $M_\bullet - \sigma_c$. The biggest change would be a decrease of $\sim 30\%$ of the θ_i of low dispersion galaxies in the survey ($\sigma_c < 150 \text{ km s}^{-1}$).

8. BLACK HOLE DEMOGRAPHY

Galaxies with black hole measurements, hereafter referred to as host galaxies, have properties that are biased in comparison to the galaxy population as a whole. This is evident from the distribution of host galaxy properties versus the galaxy population, shown in figure 8. It is striking how the host galaxies trace out a very narrow locus in this parameter space. This is most obvious in the luminosity-size panel, where they lie along a narrow line, sampling preferentially the densest galaxies. Notice that the black hole host galaxies are typically denser than the average (early-type) galaxies. This severely hinders a robust measurement of the coefficients of higher dimensional scaling relations or non-linear scaling relations.

Target galaxies that can challenge the scaling relations are most interesting, especially if they can be shown to have black holes smaller than predicted from the scaling relations. For a given spatial resolution θ_t , the black hole mass detection threshold M_t can be defined as $M_t \equiv G^{-1} \theta_t D \sigma_c^{-2}$ by inverting the sphere of influence criterion (§2.2). This inversion is independent of any scaling relation and can thus be used to select galaxies that can challenge a particular scaling relation. Note that for a given host galaxy it is easier to detect an over-massive black hole, as its sphere of influence is exponentially easier to resolve.

In figure 10 these lower limits are shown for $M_\bullet - \sigma$ and $M_\bullet - L_{\text{tot}}$. It is notable that the detection threshold overlaps with the existing black hole measurements on $M_\bullet - \sigma$. This fact raises the question of whether or not the $M_\bullet - \sigma$ relation can indeed be constrained at all. In particular, Batcheldor (2010) posed that the $M_\bullet - \sigma$ could just be an upper envelope relation. Güttekin et al. (2011b) argued that such analysis does not take into account the relative scarcity of upper limits to black hole masses compared to the number of detections. Because the value of the black hole mass is unknown before measuring it, an upper envelope relation would predict many more upper limits than detections at a fixed velocity dispersion and distance; instead the opposite is found. When using information from upper limits and detected black hole masses, Güttekin et al. (2011b) found the relation to be best described by a ridge-line relation and could rule out the upper envelope relation at $> 99\%$ confidence. It is also clear that highly accurate black hole masses are needed to secure $M_\bullet - \sigma$ at the low dispersion end. There is not a significant number of new galaxies in the survey with extremely large spheres of influence to help discriminate between these two scenarios. There are no galaxies with a sphere of influence bigger than $0.1''$ and a dispersion below 90 km s^{-1} . Hence very few mass measurements exist for such low dispersion galaxies (but see Sarzi et al. 2002; Beifiori et al. 2009).

The $M_\bullet - L_{\text{tot}}$ and $M_\bullet - L_{\text{bul}}$ relation have a similar issue at high luminosity. There are no high luminosity galaxies nearby enough for the detection of an under-massive black hole. In figure 10 we show the lowest black hole masses that can be detected as a function of total luminosity. This is conservative, as only considering the bulge would decrease the luminosity, but does not change the black hole mass detection threshold¹⁰. If luminous early types with small $10^6 M_\odot$ black holes exist, we would not be able to detect them (e.g. Güttekin et al. 2011a). There is a distinct lack of high luminosity galaxies in which

¹⁰ Bulge fractions are not known for the 2MASS and HETMGS galaxies, and thus we will only consider total luminosity here. Nonetheless, the $M_\bullet - L_{\text{tot}}$ has been shown to be a good proxy for black hole mass by Lasker et al. (2014b)

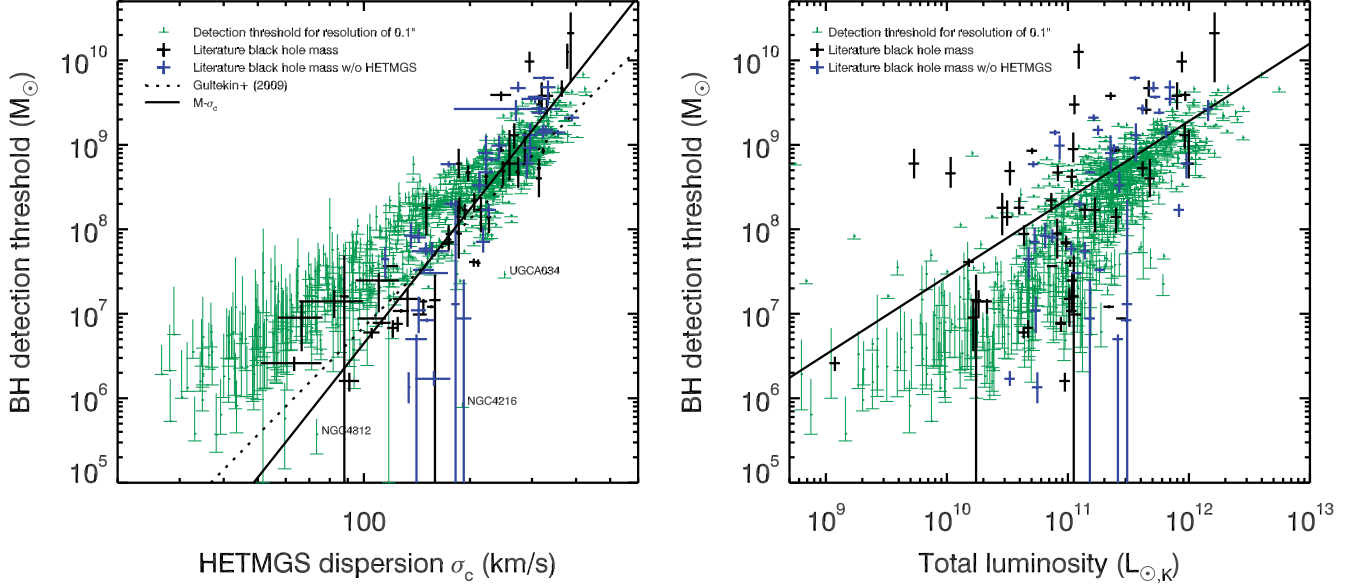


Figure 10. The black hole mass detection threshold of the HETMGS galaxies in comparison to the $M_{\bullet}-\sigma$ and $M_{\bullet}-L_{\text{tot}}$ scaling relation (Läsker et al. 2014b). This detection limit $M_t \equiv G^{-1} \theta_t D \sigma_c^{-2}$ assumes an angular resolution limit of a $\theta_t = 0.1''$ and the uncertainty in M_t is derived from the uncertainty in σ_c . Known black hole masses are over-plotted. These thresholds are expected upper detection limits on possible black hole measurements: When the black hole is smaller than the threshold, its sphere of influence would not be resolved by current generation optical and infrared telescopes. It is apparent that very few low-dispersion galaxies exist that can constrain the $M_{\bullet}-\sigma$. There are also no large-dispersion galaxies that could leverage on $M_{\bullet}-\sigma$ with an under-massive black hole. The right panel shows the same, but now for total luminosity. Here the situation is different and many objects can be used to discriminate different $M_{\bullet}-L_{\text{tot}}$ relations. See §8 for details.

a low mass black hole could be detected. This is because the closest large luminosity ellipticals are in Virgo at a distance of 14 Mpc, with the exception of Maffei I (UGCA034). The $M_{\bullet}-L_{\text{tot}}$ predicts relatively massive black holes for the nearby spirals. These galaxies do not host large bulges (Kormendy et al. 2010) and are thus ideal to distinguish between $M_{\bullet}-L_{\text{tot}}$, $M_{\bullet}-L_{\text{bul}}$ and $M_{\bullet}-\sigma$, as even an upper-limit would provide strongly leverage on $M_{\bullet}-L_{\text{tot}}$.

9. LOOKING AHEAD

This paper introduces the HET Massive Galaxy Survey, which consists of long slit spectroscopy of 1022 nearby galaxies. The surveyed galaxies were specifically chosen for their potential for a direct dynamical black hole mass measurement. By selecting galaxies with large spheres of influence, the survey provides the most complete prerequisite sample for future dynamical black hole mass measurements in the local volume. Other nearby galaxy surveys do not (specifically) probe galaxies that are nearby enough for black hole mass measurements and the HETMGS is thus complementary. The survey improves many velocity dispersion measurements present in the HyperLeda catalog (§4), which is often used as the basis for black hole mass measurements. The sample is very diverse and spans a large range in luminosity, size, dispersion and galaxy morphology (§6). The central stellar kinematics and emission line ratios are the survey’s primary data products and are presented in table 1. The HET observations have been used in the following papers van den Bosch et al. (2012), Läsker et al. (2013), Walsh et al. (2015 subm.) and Yıldırım et al. (2015 subm.).

Currently there are only 90 galaxies with direct black hole masses measurements and the existing data do not favor a specific black hole scaling relation over another (Kormendy & Ho 2013). This in part a result of the fact that the host galaxies are heavily biased and sample only the densest of galaxies, which is not representative of the galaxy population

at large (§8). They are also strongly clustered in luminosity and size. Expanding black hole mass measurements to be more representative of the galaxy population, will greatly extend the leverage on the black hole scaling relations. This is currently an active field, with different teams pursuing different parts of parameter space (McConnell et al. 2012; Nowak et al. 2010; Rusli et al. 2013; Krajnović et al. 2009; van den Bosch et al. 2012; Seth et al. 2014; Kuo et al. 2011; Walsh et al. 2015 subm.). Even with all the progress, the current crop of black hole masses is still confined to a narrow range of host galaxy properties. Unfortunately, the HETMGS survey shows that the potential targets are not very numerous. The black hole scaling relations are thus strongly limited by the detection thresholds set by angular resolution of telescopes. The increased spatial resolution offered by VLBI (Kuo et al. 2011), ALMA (Davis 2014) and the ELTs (Do et al. 2014) are crucial to resolve the sphere of influence of low-mass black holes.

Also important are the cross-calibrations between methods. These are crucial to independently verify the intrinsic uncertainties. Unfortunately, there are few objects where two or more of the main methods—gas dynamics, stellar dynamics, megamasers, and reverberation mapping—can be applied. The lack of such comparable measurements is a result of the different requirements that each method has concerning host galaxy properties. Comparisons between gas and stellar dynamical black hole masses have been done for only six objects (Walsh et al. 2013, and references therein). In half of those cases the gas dynamical masses are lower by at least a factor of two for reasons yet unknown. So far only NGC 4151 has both a dynamical and reverberation mass. However its stellar kinematics are strongly affected by the spiral perturbations and complex bar kinematics (Onken et al. 2007, 2014). Comparison targets of megamasers galaxies are similarly rare (Sicopis et al. 2009). The HETMGS can be the starting point for finding new cross-calibration targets.

The first result of the HETMGS survey was the discovery

of six extremely compact, high-dispersion, galaxies which are candidates to host black holes that are too large for their galaxy mass (van den Bosch et al. 2012; Fabian et al. 2013; Emsellem 2013). Apart from NGC1277, Walsh et al. (2015 subm.) found another compact galaxy with a over-massive black hole in the HETMGS sample. And there are hints for Mrk 1216 (Yıldırım et al. 2015 subm.) and b19 (Läsker et al. 2013). As the HETMGS survey is extremely suitable to find the densest galaxies in the nearby volume, because it is heavily biased towards the densest systems. These highly compact galaxies are very interesting, because they could be the passively evolved ancestors of the quiescent galaxies at $z \sim 2$ (red nuggets), sub-mm galaxies and quasars found at high redshift $z > 4$ (van den Bosch et al. 2012; Trujillo et al. 2014; Toft et al. 2014). A detailed study of these curious objects is outside the scope of this paper.

The HETMGS only contains Northern galaxies and an extension of the survey to the South would double the viable targets. This is very worthwhile given the rarity of suitable targets for dynamical black hole mass measurements and the availability of high resolution Southern facilities. In the South, galaxies with $m_{ks} < 11.7$ already have low resolution, single aperture, spectroscopy from the 6dF Galaxy Survey (Jones et al. 2009; Campbell et al. 2014) and the follow up can thus be planned efficiently.

In conclusion, this paper describes the HET Massive Galaxy Survey, including the sample selection, data reduction and derived quantities of 1022 galaxies. We also show that the current crop of black hole masses is strongly biased and that this survey is ideally suited to plan the next generation of direct black hole mass measurements.

ACKNOWLEDGMENTS

It is a pleasure to thank the Telescope Operators Frank Deglman, Vicki Riley, Eusebio Terrazas, Amy Westfall and Resident Astronomers, John Caldwell, Stephen Odewahn, Sergey Rostopchin, Matthew Shetrone. We thank Arjen van der Wel, Ronald Läsker and Glenn van de Ven for discussions and suggestions that improved the survey.

The Hobby-Eberly Telescope (HET) is a joint project of the University of Texas at Austin, the Pennsylvania State University, Ludwig-Maximilians-Universität München, and Georg-August-Universität Göttingen. The HET is named in honor of its principal benefactors, William P. Hobby and Robert E. Eberly. The Marcario Low Resolution Spectrograph is named for Mike Marcario of High Lonesome Optics who fabricated several optics for the instrument but died before its completion. The LRS is a joint project of the Hobby-Eberly Telescope partnership and the Instituto de Astronomía de la Universidad Nacional Autónoma de México.

J.L.W. has been supported by an NSF Astronomy and Astrophysics Postdoctoral Fellowship under Award No. 1102845. This material is based upon work supported by the National Science Foundation under Grant No. AST-1107675.

The work greatly depended on the public databases, [HyperLeda](#), NASA's Astrophysics Data System and the NASA/IPAC Extragalactic Database (NED), which is operated by the Jet Propulsion Laboratory, California Institute of Technology, under contract with the National Aeronautics and Space Administration. This research has made use of NASA's Astrophysics Data System.

This publication makes use of data products from the Two Micron All Sky Survey, which is a joint project of the University of Massachusetts and the Infrared Processing and Analysis

Center/California Institute of Technology, funded by the National Aeronautics and Space Administration and the National Science Foundation.

Funding for the [Sloan Digital Sky Survey](#) (SDSS) has been provided by the Alfred P. Sloan Foundation, the Participating Institutions, the National Aeronautics and Space Administration, the National Science Foundation, the U.S. Department of Energy, the Japanese Monbukagakusho, and the Max Planck Society. The SDSS is managed by the Astrophysical Research Consortium (ARC) for the Participating Institutions. The Participating Institutions are The University of Chicago, Fermilab, the Institute for Advanced Study, the Japan Participation Group, The Johns Hopkins University, Los Alamos National Laboratory, the Max-Planck-Institute for Astronomy (MPIA), the Max-Planck-Institute for Astrophysics (MPA), New Mexico State University, University of Pittsburgh, Princeton University, the United States Naval Observatory, and the University of Washington.

REFERENCES

- Adelman-McCarthy, J. K. et al. 2008, ApJS, 175, 297
- Aller, M. C. & Richstone, D. O. 2007, ApJ, 665, 120
- Batcheldor, D. 2010, ApJ, 711, L108
- Beifiori, A. et al. 2009, ApJ, 692, 856
- Blanton, M. R. et al. 2005, AJ, 129, 2562
- Campbell, L. A. et al. 2014, MNRAS, 443, 1231
- Cappellari, M. & Emsellem, E. 2004, PASP, 116, 138
- Cappellari, M. et al. 2011, MNRAS, 413, 813
- Davis, T. A. 2014, preprint (1406.2555)
- de Zeeuw, P. T. et al. 2002, MNRAS, 329, 513
- Denney, K. D. et al. 2014, preprint (1404.4879)
- Do, T. et al. 2014, AJ, 147, 93
- Emsellem, E. 2013, MNRAS, 433, 1862
- Fabian, A. C. 1999, MNRAS, 308, L39
- Fabian, A. C. et al. 2013, MNRAS, 431, L38
- Falcón-Barroso, J. et al. 2011a, A&A, 532, A95
- . 2011b, MNRAS, 417, 1787
- Ferrarese, L. & Merritt, D. 2000, ApJ, 539, L9
- Gebhardt, K. et al. 2000, ApJ, 539, L13
- Graham, A. W. 2012, ApJ, 746, 113
- Graham, A. W. & Scott, N. 2013, ApJ, 764, 151
- Greene, J. E. et al. 2010, ApJ, 721, 26
- Gültekin, K. et al. 2011a, ApJ, 741, 38
- . 2009, ApJ, 698, 198
- . 2011b, ApJ, 738, 17
- Häring, N. & Rix, H.-W. 2004, ApJ, 604, L89
- Hill, G. J. et al. 1998, in Society of Photo-Optical Instrumentation Engineers (SPIE) Conference Series, Vol. 3355, Proc. SPIE, ed. S. D'Odorico, 375–386
- Ho, L. C. et al. 2009, ApJS, 183, 1
- Hopkins, P. F. et al. 2007, ApJ, 669, 67
- Huchra, J. P. et al. 2012, ApJS, 199, 26
- Husemann, B. et al. 2012, A&A, 545, A137
- Jahnke, K. & Macciò, A. V. 2011, ApJ, 734, 92
- Jarrett, T. H. et al. 2000, AJ, 119, 2498
- . 2003, AJ, 125, 525
- Jones, D. H. et al. 2009, MNRAS, 399, 683
- Kelly, B. C. 2007, ApJ, 665, 1489
- Kewley, L. J. et al. 2006, MNRAS, 372, 961
- Komatsu, E. et al. 2009, ApJS, 180, 330
- Kormendy, J. et al. 2011, Nature, 469, 374
- . 2010, ApJ, 723, 54
- Kormendy, J. & Ho, L. C. 2013, ARA&A, 51, 511
- Krajnović, D. et al. 2009, MNRAS, 399, 1839
- Kuo, C. Y. et al. 2011, ApJ, 727, 20
- Landsman, W. B. 1993, in Astronomical Society of the Pacific Conference Series, Vol. 52, Astronomical Data Analysis Software and Systems II, ed. R. J. Hanisch, R. J. V. Brissenden, & J. Barnes, 246
- Läsker, R. et al. 2014a, ApJ, 780, 69
- . 2014b, ApJ, 780, 70
- . 2013, MNRAS, 434, L31

- Lauer, T. R. et al. 2007, ApJ, 670, 249
 Magoulas, C. et al. 2012, MNRAS, 427, 245
 Markwardt, C. B. 2009, in Astronomical Society of the Pacific Conference Series, Vol. 411, Astronomical Data Analysis Software and Systems XVIII, ed. D. A. Bohlender, D. Durand, & P. Dowler, 251
 McConnell, N. J. & Ma, C.-P. 2013, ApJ, 764, 184
 McConnell, N. J. et al. 2011, Nature, 480, 215
 —. 2012, ApJ, 756, 179
 McElroy, D. B. 1995, ApJS, 100, 105
 Mould, J. R. et al. 2000, ApJ, 529, 786
 Nowak, N. et al. 2010, MNRAS, 403, 646
 Onken, C. A. et al. 2014, ApJ, 791, 37
 —. 2007, ApJ, 670, 105
 Pahre, M. A. et al. 1998, AJ, 116, 1591
 Paturel, G. et al. 2003, A&A, 412, 45
 Peebles, P. J. E. 1972, ApJ, 178, 371
 Ramsey, L. W. et al. 1998, in Society of Photo-Optical Instrumentation Engineers (SPIE) Conference Series, Vol. 3352, Proc. SPIE, ed. L. M. Stepp, 34–42
 Reines, A. E. et al. 2013, ApJ, 775, 116
 Rusli, S. P. et al. 2013, AJ, 146, 45
 Sánchez, S. F. et al. 2012, A&A, 538, A8
 Sánchez-Blázquez, P. et al. 2006, MNRAS, 371, 703
 Sani, E. et al. 2011, MNRAS, 413, 1479
 Sarzi, M. et al. 2006, MNRAS, 366, 1151
 —. 2002, ApJ, 567, 237
 Schlegel, D. J. et al. 1998, ApJ, 500, 525
 Seth, A. C. et al. 2014, Nature, 513, 398
 Shetrone, M. et al. 2007, PASP, 119, 556
 Simmons, B. D. et al. 2013, MNRAS, 429, 2199
 Singh, R. et al. 2013, A&A, 558, A43
 Siopis, C. et al. 2009, ApJ, 693, 946
 Toft, S. et al. 2014, ApJ, 782, 68
 Trujillo, I. et al. 2014, ApJ, 780, L20
 Valluri, M. et al. 2004, ApJ, 602, 66
 van den Bosch, R. C. E. et al. 2012, Nature, 491, 729
 Walcher, C. J. et al. 2014, preprint (1407.2939)
 Walsh, J. L. et al. 2013, ApJ, 770, 86
 —. 2015 subm.
 Wegner, G. et al. 1999, MNRAS, 305, 259
 Woo, J.-H. et al. 2013, ApJ, 772, 49
 —. 2010, ApJ, 716, 269
 Yıldırım, A. et al. 2015 subm.

2MASS ID	Name	Frame	MJD	PA (°)	slit (")	V_{hel} (km s $^{-1}$)	σ_c (km s $^{-1}$)	[NII]/H α	[OIII]/H β	AoN
	NGC5623	050570	55309.407	197	2.0	3417.0±13.7	260.8±6.7	0.24±0.04	1.29±0.43	23,1
	NGC5623	050571	55309.418	197	2.0	3406.8±14.0	262.2±7.0	0.18±0.04	0.59±0.13	26,3
	NGC5623	051125	55327.364	197	2.0	3463.9±12.5	250.5±6.4	0.19±0.04	0.53±0.10	31,4
	NGC5623	051126	55327.375	197	2.0	3471.1±14.5	249.3±6.8	0.15±0.03	0.59±0.12	31,3
	NGC5846A	341486	56329.472	90	1.0	2196.8±11.3	195.3±3.5	-0.17±0.56	0.12±0.50	2,1
0223114+425931	UGC01841	060058	55413.410	90	2.0	6245.8±19.9	241.9±11.4	0.49±0.03	0.74±0.17	26,2
0223114+425931	UGC01841	060059	55413.422	90	2.0	6244.0±17.5	248.5±9.7	0.52±0.03	0.92±0.29	28,2
0223114+425931	UGC01841	060162	55418.384	90	2.0	6271.6±13.0	258.0±8.0	0.48±0.04	1.21±0.50	21,1
0223114+425931	UGC01841	060193	55419.383	83	2.0	6272.1±14.8	242.3±8.1	0.48±0.04	0.83±0.23	17,2
0249454+465834	IC0257	062826	55508.150	76	2.0	7659.8±13.4	351.2±8.8	-	0.26±0.39	1,2
0301141+445350	NGC1161	140346	55539.321	370	2.0	1900.6±13.1	257.5±5.9	0.11±0.05	0.28±0.18	23,3
0318158+415127	NGC1265	062149	55495.437	350	2.0	-	-	-	-	-
0318158+415127	NGC1265	140201	55536.329	365	2.0	7694.2±11.6	290.2±7.4	-	-	0,0
1353267+401809	NGC5354	143840	55644.235	87	2.0	2525.8±13.0	230.5±6.5	0.20±0.05	0.73±0.14	20,3
00000168+4716282	UGC12889	161195	55887.235	350	1.0	4945.0±13.1	154.7±8.5	0.23±0.04	0.59±0.25	29,2
00000914+3244182	IC5370	351996	56456.442	120	1.0	10133.7±14.0	238.3±4.3	0.04±0.20	-0.51±0.19	4,3
00004696+2824071	UGC12899	062173	55496.313	230	2.0	8616.0±18.0	263.1±12.6	-	-	1,0
00021916+1258176	NGC7810	261972	56237.247	260	1.0	5392.1±13.2	127.4±6.7	-0.34±0.01	-0.32±0.03	101,11
00031494+1608428	NGC7814	153358	55810.425	150	1.0	990.4±13.9	192.6±5.9	-	-	0,0
00043079+0512009	NGC7820	152909	55799.428	165	2.0	3043.2±13.1	143.5±10.5	-	-	0,3
00050624+0655122	NGC7824	151812	55742.437	165	2.0	6018.4±13.5	229.7±6.2	0.38±0.03	0.71±0.12	33,3
00095341+2555254	NGC0023	141442	55571.100	330	2.0	4486.0±14.2	158.5±12.0	-0.17±0.00	-0.12±0.01	184,24
00110106+3003072	UGC00102	153789	55829.382	258	2.0	6662.4±11.5	196.8±7.3	0.32±0.02	0.59±0.08	56,8
00112231+0623212	NGC0036	160684	55865.253	170	1.0	5936.8±10.1	142.1±6.9	0.34±0.10	-	13,0
00114314+2058320	MRK0337	252919	56103.427	140	1.0	7820.2±13.8	137.8±5.5	-	-	0,0
00133440-0505352	PGC000902	161006	55881.145	185	1.0	5344.1±14.0	84.1±18.6	-0.46±0.02	-0.47±0.14	50,4
00144455-0720423	NGC0050	060900	55450.316	180	2.0	5374.8±14.3	274.8±8.7	0.26±0.11	-	9,1
00153087+1719422	NGC0057	060896	55450.220	49	2.0	5360.4±15.1	298.6±8.8	-0.05±0.36	-	3,0
00153087+1719422	NGC0057	060897	55450.233	49	2.0	5358.6±15.2	314.5±12.4	-	-	0,1
00162493+3022252	PGC001084	261626	56223.100	60	1.0	6275.9±13.1	256.1±8.4	-1.19±0.64	-	2,1
00182359+3003475	NGC0071	161378	55893.227	285	1.0	6605.2±13.0	206.9±6.4	0.04±0.11	0.25±0.53	12,2
00193596-0440105	PGC1055035	262081	56239.170	205	1.0	6052.8±10.9	148.9±4.5	-0.09±0.01	1.08±0.02	82,16
00211086+2221261	NGC0080	060969	55452.427	248	2.0	5646.3±14.2	235.0±7.5	-0.34±0.32	-	2,0
00212239+2226011	NGC0083	262794	56262.196	295	1.0	6149.8±15.7	271.0±8.9	-0.03±0.06	0.31±0.27	22,2
00220321+2224291	NGC0093	160115	55847.134	55	2.0	5497.2±16.6	182.4±10.3	0.13±0.07	0.45±0.26	18,2
00270291+1135017	UGC00260	161413	55894.216	200	1.0	2098.7±18.2	72.8±29.5	-0.46±0.04	0.20±0.15	34,6
00271620-0146487	NGC0118	153306	55808.380	250	2.0	10935.8±15.0	125.7±20.8	-0.37±0.01	0.04±0.03	75,20
00305921+0509350	NGC0138	141341	55569.090	165	2.0	11649.7±13.8	259.4±6.5	0.50±0.11	0.61±0.27	13,2
00314572-0509095	NGC0145	153672	55827.301	170	1.0	4087.4±17.4	74.1±30.5	-0.46±0.01	-0.21±0.03	138,20
00344675-0823473	NGC0157	262190	56243.163	205	1.0	1606.9±12.6	81.6±10.5	-0.23±0.01	0.10±0.00	39,7
00355984-1007183	NGC0163	161347	55892.128	255	2.0	5850.4±14.7	267.2±8.4	0.14±0.14	-	7,0
00370548+2541564	UGC00367	161414	55894.239	185	2.0	9512.5±14.0	282.3±7.1	-0.04±0.13	-	10,1
00373345-0655202	2M00373	161150	55884.157	240	1.0	3277.7±11.5	208.0±4.7	-	-	1,0
00375413-0624462	PGC089884	262242	56246.160	235	1.0	7631.6±15.0	138.8±12.7	-0.35±0.00	-0.48±0.05	174,10
00375769+0838068	NGC0180	153607	55825.388	155	1.0	5203.3±13.9	118.9±10.3	-0.46±0.01	-0.52±0.08	101,6
00393486+0253145	NGC0200	161374	55893.074	135	1.0	5080.7±12.4	111.0±9.5	-0.19±0.01	0.29±0.03	127,18
00395598+0650550	IC1568	152418	55777.367	85	2.0	11694.3±14.6	285.4±8.7	0.24±0.11	0.40±0.35	13,1
00402207+4141070	NGC0205	161950	55932.138	250	1.0	-291.2±15.1	24.8±25.4	-	-	1,0
00423684-0131436	NGC0227	153551	55822.370	160	2.0	5368.4±15.0	269.2±6.1	-0.04±0.17	-	3,0
004244182+4051546	NGC0221	261443	56218.357	345	1.0	-231.1±13.7	63.4±12.4	-	-	0,0
00424433+4116074	NGC0224	161565	55909.211	274	1.0	-358.1±14.6	185.3±3.4	-	-	0,0
00432844-0620554	PGC002598	160931	55873.195	100	2.0	5784.5±18.7	140.2±29.8	0.05±0.20	-	7,1

Table continues on next page

2MASS ID	Name	Frame	MJD	PA	slit ('')	V_{hel} (km s^{-1})	σ_c (km s^{-1})	[NII]/H α	[OIII]/H β	AoN
00433238+1420334	NGC0234	261630	56223.314	235	1.0	4396.4 \pm 13.1	74.7 \pm 18.2	-0.34 \pm 0.01	-0.29 \pm 0.06	83,9
00435075+3251121	UGC00465	161379	55893.252	181	1.0	4696.3 \pm 12.2	144.1 \pm 5.6	0.43 \pm 0.13	-	9,0
00471856+2749398	IC1584	153901	55833.403	275	1.0	4663.2 \pm 14.7	87.6 \pm 9.2	0.18 \pm 0.13	-	10,0
00494779+3216398	NGC0266	153360	55810.484	275	2.0	4565.3 \pm 15.3	238.9 \pm 7.6	0.43 \pm 0.03	0.54 \pm 0.12	20,4
00520430+4733019	NGC0278	160601	55864.329	210	1.0	590.9 \pm 13.7	55.3 \pm 13.5	-0.27 \pm 0.01	-0.26 \pm 0.06	82,6
00563259-0146189	NGC0307	152308	55772.439	80	2.0	3905.1 \pm 12.6	239.4 \pm 7.5	-	-2.14 \pm 0.12	0,2
00564266-0954500	NGC0309	153673	55827.325	100	1.0	5579.7 \pm 11.2	117.5 \pm 8.0	-0.13 \pm 0.03	0.26 \pm 0.16	46,4
00573274+3016508	NGC0311	061546	55478.390	295	2.0	4943.4 \pm 13.5	250.6 \pm 6.9	0.29 \pm 0.12	-	8,1
00574891+3021083	NGC0315	060751	55445.240	45	2.0	4885.0 \pm 13.5	339.0 \pm 7.5	0.37 \pm 0.04	0.83 \pm 0.25	31,2
00574891+3021083	NGC0315	060752	55445.254	45	2.0	4887.0 \pm 13.9	328.3 \pm 6.2	0.37 \pm 0.03	0.58 \pm 0.13	36,3
00574891+3021083	NGC0315	062731	55506.313	258	2.0	4880.4 \pm 14.0	335.5 \pm 5.8	0.41 \pm 0.02	0.69 \pm 0.12	38,3
01002812+4759428	UGC00622	153937	55835.411	330	1.0	2648.3 \pm 14.5	34.9 \pm 25.5	-0.32 \pm 0.01	-0.38 \pm 0.13	123,4
01015784-0156124	NGC0351	160679	55865.178	125	1.0	4159.4 \pm 12.8	121.9 \pm 6.8	-0.16 \pm 0.01	0.09 \pm 0.05	82,12
01071757+3228581	NGC0380	061286	55471.407	225	2.0	4420.3 \pm 14.0	281.0 \pm 7.2	0.20 \pm 0.06	0.64 \pm 0.28	11,1
01071757+3228581	NGC0380	061287	55471.419	225	2.0	4421.7 \pm 13.8	284.7 \pm 5.8	0.32 \pm 0.05	0.63 \pm 0.19	11,2
01072180+1416240	PGC003963	141582	55575.108	315	2.0	21678.0 \pm 16.2	369.0 \pm 11.8	-	-	0,1
01072493+3224452	NGC0383	060971	55452.456	261	2.0	4994.1 \pm 14.9	326.1 \pm 9.0	0.29 \pm 0.03	0.52 \pm 0.12	33,3
01072493+3224452	NGC0383	062005	55488.142	98	2.0	4958.7 \pm 14.7	291.5 \pm 8.8	0.33 \pm 0.02	0.59 \pm 0.12	37,4
01072493+3224452	NGC0383	062361	55500.330	261	2.0	4977.1 \pm 14.9	300.5 \pm 6.7	0.30 \pm 0.03	0.57 \pm 0.15	33,3
01072503+3217341	NGC0384	140342	55539.229	315	2.0	4180.1 \pm 13.2	262.1 \pm 5.9	0.39 \pm 0.11	-	8,0
01072503+3217341	NGC0384	261482	56219.369	315	1.0	4188.2 \pm 13.4	266.4 \pm 3.9	0.23 \pm 0.07	-	13,0
01072503+3217341	NGC0384	340749	56293.167	315	1.0	4183.0 \pm 13.9	250.1 \pm 6.5	0.08 \pm 0.17	-	8,0
01082344+3308008	NGC0392	153902	55833.422	235	2.0	4581.5 \pm 12.5	235.6 \pm 6.6	-	-0.42 \pm 0.23	0,2
01105887+3309072	NGC0410	060972	55452.471	262	2.0	5204.2 \pm 15.2	310.6 \pm 5.8	0.13 \pm 0.04	-0.07 \pm 0.12	16,3
01124858-0017246	NGC0426	062216	55497.272	140	2.0	5187.4 \pm 15.1	297.4 \pm 7.6	0.31 \pm 0.01	0.40 \pm 0.04	72,11
01125570+0058536	NGC0428	340872	56305.079	275	1.0	1130.5 \pm 14.1	55.8 \pm 26.4	-0.42 \pm 0.36	-	3,0
01125992-0015087	NGC0430	061901	55485.225	153	2.0	5220.6 \pm 13.6	242.4 \pm 6.4	0.28 \pm 0.06	-	10,0
01155335+0519325	PGC004568	262083	56239.270	190	1.0	4969.6 \pm 13.3	207.9 \pm 6.3	-	-	0,2
01160360+0417385	NGC0446	153670	55827.263	115	2.0	5363.4 \pm 13.7	173.0 \pm 7.4	0.06 \pm 0.01	0.36 \pm 0.06	65,4
01160722+3305218	NGC0449	161951	55932.155	262	1.0	4689.1 \pm 31.2	250.1 \pm 86.3	-	-	AGN
01191813+0434411	MRK0567	253521	56140.411	70	1.0	9527.9 \pm 16.6	142.2 \pm 13.2	-0.35 \pm 0.00	-0.53 \pm 0.00	137,8
01193304+1452147	NGC0469	062354	55500.152	170	2.0	3984.0 \pm 23.4	31.0 \pm 44.7	-0.77 \pm 0.01	0.35 \pm 0.01	94,85
01193304+1452147	NGC0469	062355	55500.164	170	2.0	4028.0 \pm 41.6	20.6 \pm 53.7	-0.76 \pm 0.02	0.34 \pm 0.03	45,39
01195507+1632407	NGC0473	161415	55894.258	160	1.0	2083.7 \pm 12.7	62.3 \pm 10.3	-0.17 \pm 0.02	0.35 \pm 0.08	55,7
01195962+1447107	NGC0471	262026	56238.314	245	1.0	4121.7 \pm 12.5	127.5 \pm 5.4	-0.20 \pm 0.00	-0.25 \pm 0.01	271,23
01195962+1447107	NGC0471	262084	56239.294	245	1.0	4117.0 \pm 13.3	127.4 \pm 6.0	-0.20 \pm 0.00	-0.30 \pm 0.02	281,25
01202867+3242322	NGC0472	161013	55881.301	305	2.0	5178.0 \pm 12.5	247.1 \pm 6.6	-	-	0,0
01202867+3242322	NGC0472	261319	56214.394	305	1.0	5213.1 \pm 13.2	245.6 \pm 5.0	-	-	1,0
01202867+3242322	NGC0472	340608	56285.199	305	1.0	5200.9 \pm 16.3	253.1 \pm 5.5	-	-	0,0
01202867+3242322	NGC0472	341331	56323.089	305	1.0	5202.5 \pm 13.2	256.7 \pm 5.4	-	-	0,0
01212039+4029176	NGC0477	161325	55890.280	300	1.0	5768.0 \pm 17.3	108.4 \pm 18.2	-0.44 \pm 0.03	-0.25 \pm 0.16	39,4
01214684+0515241	NGC0488	153638	55826.267	185	2.0	2205.5 \pm 15.2	201.0 \pm 7.0	0.26 \pm 0.04	0.50 \pm 0.16	15,2
01225395-0438353	ICO100	153427	55811.383	260	2.0	5153.0 \pm 13.2	186.2 \pm 9.3	-	-	0,0
01225533+3310261	NGC0494	153938	55835.426	280	2.0	5349.9 \pm 13.8	121.7 \pm 14.1	0.22 \pm 0.02	1.02 \pm 0.05	60,9
01231145+3327362	NGC0499	140927	55555.203	250	2.0	4292.5 \pm 14.9	276.9 \pm 7.4	0.35 \pm 0.12	-	7,1
01232787+3312152	NGC0504	141953	55590.111	225	2.0	4147.6 \pm 13.1	181.7 \pm 9.0	-	-0.32 \pm 0.45	0,2
01233995+3315222	NGC0507	060934	55451.255	97	2.0	4859.7 \pm 13.8	282.7 \pm 6.2	-0.22 \pm 0.30	-	2,0
01243377+0143532	NGC0521	260482	56177.439	145	1.0	4947.7 \pm 11.9	222.8 \pm 4.8	0.38 \pm 0.05	0.70 \pm 0.27	16,2
01244505+3209565	UGC00959	153875	55832.435	260	2.0	10315.4 \pm 15.1	195.6 \pm 11.2	-0.14 \pm 0.02	-0.03 \pm 0.07	66,9
01244770+0932196	NGC0524	261973	56237.310	235	1.0	2339.3 \pm 12.5	244.6 \pm 5.2	-0.26 \pm 0.09	-0.94 \pm 0.20	15,3
01250764+0841576	IC1695	162757	55959.068	295	2.0	14324.3 \pm 17.2	387.3 \pm 12.9	-	-	0,1
01253143+0145335	NGC0533	152352	55775.420	55	2.0	5469.3 \pm 15.2	288.7 \pm 6.4	0.25 \pm 0.04	0.88 \pm 0.35	18,1
01253359+3340165	NGC0528	161104	55883.290	240	2.0	4710.4 \pm 14.0	267.5 \pm 6.1	0.42 \pm 0.04	0.61 \pm 0.18	21,3
01254030+3442465	NGC0529	153508	55821.470	340	2.0	4721.3 \pm 15.4	239.5 \pm 11.0	-	-	0,0
01254430-0122461	NGC0541	262023	56238.249	240	1.0	5338.9 \pm 13.6	237.6 \pm 5.1	0.01 \pm 0.05	0.39 \pm 0.26	25,2
01260057-0120424	NGC0547	060968	55452.318	130	2.0	5470.0 \pm 15.5	250.2 \pm 7.4	0.39 \pm 0.07	-	9,0
01264255+0201205	NGC0550	141198	55565.110	300	2.0	5788.6 \pm 12.5	217.6 \pm 8.1	0.20 \pm 0.05	-	21,1
01265610-0722240	PGC1020086	140117	55534.151	180	2.0	10000.7 \pm 14.2	215.7 \pm 9.1	-0.05 \pm 0.33	-0.10 \pm 0.41	6,6
01274302-0108225	UGC01043	153304	55808.343	200	1.0	5152.0 \pm 11.4	95.3 \pm 8.5	-	-	0,0
01312075-0652050	NGC0584	060867	55449.376	242	2.0	1802.1 \pm 13.4	220.1 \pm 6.6	0.25 \pm 0.09	-	6,0
01312075-0652050	NGC0584	060939	55451.362	232	2.0	1782.7 \pm 13.1	219.0 \pm 6.8	0.38 \pm 0.06	-	6,1
01312075-0652050	NGC0584	060940	55451.376	232	2.0	1789.6 \pm 13.4	212.9 \pm 6.7	0.38 \pm 0.07	-	6,1
01314889+1835498	ARK052	152268	55770.402	55	2.0	12560.0 \pm 15.4	248.4 \pm 7.9	-	-	2,0
01325190-0701535	NGC0596	262793	56262.149	230	1.0	1820.3 \pm 13.6	154.9 \pm 4.1	-	-	0,0
01333122+3540055	NGC0591	162708	55958.114	315	1.0	4427.0 \pm 15.4	123.0 \pm 7.7	0.05 \pm 0.00	1.04 \pm 0.01	301,36
01390652-0730453	NGC0636	152862	55798.428	240	1.0	1810.1 \pm 13.9	173.3 \pm 3.9	-	-	0,0
01390902+4816574	PGC006116	152858	55798.326	50	2.0	5351.2 \pm 13.6	331.6 \pm 6.7	0.28 \pm 0.03	0.44 \pm 0.08	32,4
01390902+4816574	PGC006116	161326	55890.301	230	1.0	5377.7 \pm 13.4	337.5 \pm 7.4	0.26 \pm 0.05	0.36 \pm 0.12	28,4
01430234+1338444	NGC0660	261974	56237.327	221	1.0	819.				

2MASS ID	Name	Frame	MJD	PA	slit ('')	V_{hel} (km s^{-1})	σ_c (km s^{-1})	[NII]/H α	[OIII]/H β	AoN
01501400+2738444	NGC0684	161014	55881.318	265	2.0	3474.6±14.2	179.2±9.0	0.37±0.03	1.22±0.28	20,1
01504172+2145356	NGC0691	262027	56238.338	280	1.0	2610.5±10.2	104.2±6.0	0.26±0.11	-	11,1
01504172+2145356	NGC0691	262086	56239.338	280	1.0	2610.0±7.7	131.2±6.7	0.26±0.25	-	6,0
01504172+2145356	NGC0691	262113	56240.327	280	1.0	2604.8±13.0	98.4±8.6	0.37±0.22	-	8,0
01511756+2221286	NGC0697	153678	55827.471	283	2.0	3066.8±14.4	85.1±22.0	-0.15±0.04	0.15±0.23	33,2
01512719-0215317	PGC006858	061904	55485.332	199	2.0	13551.9±15.0	242.7±8.7	-	-0.50±0.20	0.4
01523770+3607362	NGC0704	253322	56124.418	85	1.0	4658.5±12.5	166.8±5.7	0.01±0.49	-	1,1
01524648+3609065	NGC0708	162188	55942.170	220	2.0	4762.4±14.7	242.7±9.8	0.35±0.02	0.46±0.12	57,4
01530843+3649115	NGC0712	161100	55883.108	80	2.0	5291.3±15.1	227.9±9.0	-0.12±0.09	0.16±0.25	16,3
01532965+3613167	NGC0714	142529	55609.087	290	2.0	4324.2±15.5	223.8±15.0	0.25±0.17	-	7,1
01552201+0636421	UGC01395	261521	56220.356	140	1.0	5079.1±12.9	69.7±12.8	-0.02±0.01	1.06±0.02	94,12
01562095+0537437	NGC0741	060847	55448.317	90	2.0	5484.5±13.1	292.2±7.0	-0.19±0.14	-	7,1
01562095+0537437	NGC0741	060848	55448.328	90	2.0	5487.3±15.2	284.0±7.1	-0.09±0.13	-	6,0
01564087+3302366	NGC0736	160677	55865.139	135	2.0	4265.1±14.0	263.3±5.8	-1.28±0.17	-1.96±0.17	5,2
01564822+3559412	PGC007302	141443	55571.175	285	2.0	-	-	-	-	-
01564822+3559412	PGC007302	142409	55605.071	270	2.0	13965.9±23.1	46.9±51.5	-	-	0,1
01575032+3620351	NGC0759	140307	55538.265	225	2.0	4583.7±14.9	259.2±7.2	-0.11±0.01	-0.05±0.05	84,10
01575100+4455069	NGC0746	253480	56138.411	20	1.0	651.0±23.8	50.8±37.4	-0.76±0.04	0.49±0.07	14,14
01583589-0127259	ARK069	261367	56215.255	230	1.0	4938.7±13.3	214.3±6.3	-	-	2,0
01584199+0820482	NGC0766	062176	55496.365	155	2.0	7801.5±16.9	270.7±12.5	-0.15±0.09	-	8,1
01591364+1857169	NGC0770	262137	56241.334	190	1.0	2505.8±13.6	96.9±7.1	-	-	0,0
01591958+1900271	NGC0772	262736	56261.268	315	1.0	2430.2±11.2	123.9±5.6	-0.07±0.02	0.18±0.11	59,6
02001493+3125457	NGC0777	060002	55411.382	145	2.0	4905.1±14.9	321.5±9.1	0.46±0.13	-	4,0
02001493+3125457	NGC0777	060003	55411.394	145	2.0	4914.0±14.7	327.4±8.9	0.49±0.21	-	3,1
02001493+3125457	NGC0777	0600473	55427.346	145	2.0	4916.7±14.4	340.6±5.4	-0.20±0.10	-0.89±0.17	7,1
02001493+3125457	NGC0777	0600474	55427.358	145	2.0	4925.7±13.0	330.6±6.3	0.71±0.41	-	1,0
02005846+5423427	PGC2468432	261483	56219.388	240	1.0	4746.1±13.8	267.8±4.3	0.02±0.02	0.75±0.10	56,4
02010947-5030254	UGC01493A	261524	56220.410	320	1.0	4790.3±13.2	111.7±9.3	-0.09±0.01	0.46±0.05	73,10
02060402+2947350	UGC01590	140928	55555.220	310	2.0	4909.2±14.0	226.3±7.9	-0.91±0.73	-1.78±0.18	3,4
02060402+2947350	UGC01590	141015	55558.214	310	2.0	4867.9±13.8	230.0±6.9	-	-	0,0
02082114+1059415	NGC0821	153639	55826.285	210	2.0	1629.8±13.4	214.9±6.8	-0.50±0.19	-0.61±0.21	2,1
02092458-1008091	NGC0835	153485	55818.392	175	2.0	3949.5±14.3	125.0±15.0	0.00±0.01	0.36±0.07	67,4
02093856+3547499	UGC01651	153573	55823.270	105	2.0	10964.0±14.5	268.6±8.4	0.53±0.07	1.13±0.62	12,1
02100957+3911253	NGC0828	140308	55538.282	315	2.0	5216.9±14.1	146.6±14.9	-0.29±0.01	-0.19±0.08	108,6
02111449+1407144	ARK078	142328	55604.075	275	2.0	7546.2±15.9	180.6±8.1	-0.97±0.30	-0.95±0.35	5,3
02113142+7046204	PGC137982	141012	55558.103	370	2.0	3187.8±16.5	296.6±12.8	0.15±0.05	0.04±0.36	20,2
02132233-0220322	PGC170027	153099	55804.405	145	2.0	10902.3±13.4	255.6±6.5	0.23±0.06	0.42±0.13	12,3
02140361+2752378	NGC0855	262138	56241.350	247	1.0	552.0±15.9	51.5±23.5	-0.76±0.01	0.46±0.01	63,43
02140361+2752378	NGC0855	262191	56243.344	247	1.0	563.2±15.6	42.7±20.7	-0.78±0.01	0.45±0.01	68,54
02143357-0046002	NGC0863	262022	56238.202	215	1.0	7757.8±12.9	174.9±4.4	0.25±0.01	1.17±0.03	65,11
02161335+7041194	PGC138040	141581	55575.065	395	2.0	3409.1±17.7	292.0±15.0	-0.60±0.40	-	3,1
02190516-0647271	NGC0883	061747	55482.324	182	2.0	5337.9±14.3	277.9±6.6	0.24±0.19	-	4,1
02220100+3315579	NGC0890	060846	55448.301	97	2.0	3946.4±14.4	211.7±8.0	-0.27±0.36	-0.16±0.69	1,1
02232039+4157052	NGC0898	141711	55580.167	353	2.0	5392.8±13.2	206.0±10.0	0.22±0.05	0.49±0.23	18,2
02232199+3211492	MRK1034	261976	56237.381	255	1.0	9954.1±14.4	181.3±9.5	-0.07±0.01	0.45±0.02	227,24
02240801+4758108	UGC01845	152307	55772.421	140	2.0	4539.5±16.0	136.7±21.0	-0.19±0.01	-0.15±0.07	210,5
02244441+4237225	UGC01859	060004	55411.411	36	2.0	5849.1±15.9	353.4±7.2	0.15±0.03	0.60±0.09	29,4
02244441+4237225	UGC01859	060005	55411.422	36	2.0	5861.8±15.9	347.1±8.2	0.18±0.03	0.49±0.10	26,5
02244441+4237225	UGC01859	060230	55420.382	36	2.0	5843.4±14.2	352.5±7.0	0.07±0.03	0.59±0.10	21,4
02244441+4237225	UGC01859	060231	55420.395	36	2.0	5858.3±13.9	357.3±8.7	0.06±0.03	0.34±0.09	23,6
02244441+4237225	UGC01859	062006	55488.192	84	2.0	5891.2±16.7	320.2±8.2	0.19±0.04	0.42±0.11	25,6
02244441+4237225	UGC01859	062321	55499.372	274	2.0	5868.5±14.4	381.9±8.2	0.20±0.02	0.50±0.07	42,7
02244441+4237225	UGC01859	160678	55865.161	45	1.0	5858.2±14.1	350.9±8.0	0.16±0.04	0.61±0.13	31,4
02250460+2213021	UGC01871	253446	56133.438	50	1.0	9936.4±14.3	222.9±10.4	-0.24±0.03	-0.12±0.11	46,5
02252677+4149275	NGC0910	162710	55958.151	215	2.0	5115.2±14.4	254.5±7.8	0.18±0.33	-	3,0
02264683+2029507	NGC0924	153574	55823.288	55	2.0	4430.7±14.6	201.6±8.5	0.38±0.05	1.00±0.21	12,2
02273746-0109226	NGC0936	260565	56186.365	105	1.0	1379.0±13.1	194.4±3.6	0.15±0.05	0.53±0.13	16,3
02280361+2810312	IC0227	153671	55827.282	70	2.0	10131.3±17.1	245.2±9.6	0.34±0.18	0.22±0.46	6,2
02291399+2304579	IC1802	141444	55571.192	300	2.0	9397.0±14.8	371.5±8.5	-0.59±0.35	-	2,0
02303311-0106305	NGC0955	153214	55806.403	200	1.0	1430.8±13.1	92.4±10.4	0.18±0.21	-	8,0
02304283-0256204	NGC0958	153428	55811.400	195	2.0	5559.7±13.8	169.8±10.1	-0.05±0.05	0.79±0.50	28,1
02304865+3708124	NGC0949	162189	55942.194	325	1.0	577.5±13.7	18.4±25.9	-0.41±0.01	-0.04±0.04	72,18
02322394+3529408	NGC0959	262088	56239.383	215	1.0	557.4±19.3	40.0±31.7	-0.43±0.02	0.34±0.09	49,9
02341338+2918404	NGC0972	153259	55807.335	150	2.0	1504.2±14.6	69.2±24.7	-0.35±0.00	0.08±0.01	218,27
02342010+3230200	NGC0973	141733	55581.167	225	2.0	4702.3±30.2	151.9±45.4	0.11±0.07	0.92±0.36	18,2
02343788-0847170	NGC0985	152791	55796.470	257	2.0	12608.8±42.3	290.7±33.5	-	-	AGN
02352485+4052109	NGC0982	141734	55581.191	310	2.0	5645.1±17.7	200.3±13.1	0.27±0.02	0.91±0.21	35,2
02352485+4052109	UGC02066	141445	55571.210	310	2.0	5668.9±10.7	214.8±7.5	0.26±0.03	0.76±0.12	40,3
02363546+5939165	UGCA034	153261	55807.370	47	2.0	11.7±16.3	250.6±11.8	-0.08±0.12	-	11,0
02364960+3319381	NGC0987	141849	55585.169	220	2.0	4520.8±14.3	260.9±8.1	-0.19±0.02	0.21±0.14	34,4
02364960+3319381	NGC0987	141850	55585.183	220	2.0	4567.1±13.1	251.8±8.6	-0.16±0.03	0.30±0.22	31,2
02372549+2106030	NGC0992	153074	55803.351	185	2.0	4148.1±13.5	104.1±23.9	-0.35±0.01	-0.43±0.04	174,10
02374759+3225114	PGC3088862	262180	56242.379	200	1.0	10691.6±13.0	212.7±7.9	0.72±0.24	-	6,0
02381955+0207091	NGC1016	061220	55470.307	235	2.0	6484.5±13.7	293.2±6.3	-	-	0,0
02381955+0207091	NGC1016	061221	55470.321	235	2.0	6482.2±14.4	314.4±7.3	-	-0.45±0.41	0,2
02383270-0640386	NGC1022	262024	56238.269	260	1.0	1399.4±11.9	81.5±10.6	-0.27±0.00	-0.42±0.00	332,15
02383270-0640386	NGC1022	262082	56239.249	260	1.0	1388.6±14.5	72.0±11.8	-0.25±0.00	-0.46±0.00	434,18

Table continues on next page

2MASS ID	Name	Frame	MJD	PA	slit ('')	V_{hel} (km s^{-1})	σ_c (km s^{-1})	[NII]/H α	[OIII]/H β	AoN
02383986+4138512	NGC0996	142576	55611.093	295	2.0	4303.7±13.8	239.3±8.6	0.24±0.23	-0.03±0.28	4,3
02384973+4127352	NGC1000	161327	55890.320	270	1.0	4316.2±21.4	195.2±17.6	-	-	0,0
02391496+3009060	NGC1012	160325	55857.187	20	1.0	949.8±19.4	56.4±32.0	-0.84±0.01	0.64±0.02	65,34
02391689+4052202	NGC1003	261975	56237.365	267	1.0	582.2±16.7	48.9±30.0	-0.52±0.08	0.67±0.40	12,2
02392368+0105376	NGC1032	140992	55557.074	70	2.0	2656.2±14.6	210.7±7.0	0.16±0.09	0.49±0.31	12,2
02402401+3903477	NGC1023	262139	56241.388	280	1.0	570.5±13.1	211.0±3.2	-	0.20±0.30	1,2
02402898+1917494	NGC1036	262160	56242.155	195	1.0	754.9±4.7	13.8±29.7	-0.76±0.02	0.64±0.04	30,20
02402912-1116391	NGC1045	341082	56312.061	245	1.0	4553.6±13.5	269.4±5.0	0.22±0.07	0.61±0.18	14,3
02410480-0815209	NGC1052	141261	55566.108	120	2.0	1453.1±14.2	220.4±7.5	0.07±0.00	0.47±0.01	133,20
02413486+0711140	MRK0595	162758	55959.101	295	2.0	7987.6±13.2	31.8±45.0	-1.26±0.01	0.16±0.01	24,14
02414523+0026354	NGC1055	262568	56255.167	181	1.0	939.5±18.2	56.4±24.8	-0.16±0.04	-0.27±0.29	27,2
02422903+1809528	ARK090	162445	55950.156	295	2.0	9260.9±14.7	374.9±6.6	0.06±0.03	0.36±0.08	42,6
02422903+1809528	ARK090	162709	55958.133	295	1.0	9291.1±18.3	382.9±8.6	0.00±0.02	0.29±0.00	30,4
02422903+1809528	ARK090	163183	55976.085	205	1.0	9336.3±15.4	365.2±6.9	0.11±0.04	0.53±0.12	33,4
02431242+4130022	NGC1053	062007	55488.210	45	2.0	4709.8±15.1	294.8±7.1	-0.06±0.07	0.22±0.19	12,3
02431242+4130022	NGC1053	062772	55507.139	45	2.0	4778.2±12.9	291.1±7.7	-0.05±0.08	0.13±0.25	15,3
02431504+3225300	NGC1060	060936	55451.301	70	2.0	5063.7±14.1	326.1±6.9	0.32±0.09	-	9,0
02431504+3225300	NGC1060	060937	55451.316	70	2.0	5081.0±13.4	327.1±6.5	0.12±0.09	0.09±0.28	10,2
02431504+3225300	NGC1060	062020	55488.431	261	2.0	5076.7±14.5	315.1±5.5	0.16±0.07	-	11,1
02431504+3225300	NGC1060	062223	55497.409	261	2.0	5079.7±14.7	325.1±5.9	0.38±0.11	-	7,0
02433005+3720283	NGC1058	261969	56237.174	95	1.0	471.1±15.0	14.0±26.8	0.28±0.05	1.03±0.39	23,2
02433460+4749238	UGC02192	163184	55976.109	250	1.0	4980.9±14.0	177.0±10.9	-	-	AGN
02463391-0014493	NGC1090	153674	55827.343	105	1.0	2715.4±9.5	64.6±11.5	-0.22±0.07	-	16,1
02470218+0839080	UGC02255	153845	55831.320	85	2.0	7432.2±11.6	199.6±7.5	0.32±0.08	0.55±0.24	13,3
02481741+5048012	UGC02261	141320	55567.240	250	2.0	4803.3±17.2	326.8±13.1	0.35±0.10	0.38±0.36	15,2
02481741+5048012	UGC02261	141347	55569.227	250	2.0	4805.8±13.1	308.9±6.6	0.24±0.04	0.18±0.12	27,4
02491961+0805334	NGC1107	140339	55539.113	140	2.0	3318.2±12.4	228.2±8.0	0.29±0.12	0.37±0.25	12,2
02510087+4657175	ICO260	262442	56252.354	340	1.0	8512.3±12.7	289.3±6.6	0.35±0.16	0.16±0.31	9,3
02542739+4134467	NGC1129	060163	55418.401	100	2.0	5255.7±15.5	229.1±8.1	-	-	1,0
02542739+4134467	NGC1129	060164	55418.415	100	2.0	5272.4±16.3	232.1±7.8	-	-	0,0
02542739+4134467	NGC1129	060194	55419.399	85	2.0	5234.6±14.8	229.2±9.0	-	-	0,0
02542739+4134467	NGC1129	060195	55419.411	85	2.0	5237.9±14.1	233.2±9.8	-	-	1,0
02573365+0558371	PGC011179	152742	55795.412	150	2.0	6707.9±14.2	290.7±8.7	0.00±0.10	-0.33±0.21	11,2
02573365+0558371	PGC011179	260594	56187.336	150	1.0	6727.5±13.5	303.1±5.9	0.17±0.14	-0.07±0.36	10,2
02573365+0558371	PGC011179	340398	56279.246	150	1.0	6726.4±14.9	290.2±7.5	0.13±0.16	0.45±0.65	9,2
02581028+0321429	NGC1153	142171	55598.092	240	2.0	2990.7±14.2	232.6±5.8	0.33±0.07	-	11,1
02581392+1107596	ARK094	261971	56237.208	155	1.0	7633.9±11.0	239.2±5.4	-0.51±0.46	-0.46±0.37	2,2
02585781+1334583	UGC02450	153098	55804.387	215	2.0	21410.9±16.3	261.6±15.9	0.29±0.24	-	3,1
03005943+4301034	UGC02470	142607	55612.114	350	2.0	4696.9±14.3	164.7±10.7	-0.14±0.34	-0.37±0.37	3,3
03020668+4135371	UGC02495	142478	55608.138	280	2.0	8906.9±15.0	209.4±8.2	0.36±0.04	-	18,0
03033053-0214539	PGC011516	153825	55830.370	210	2.0	5983.8±13.4	138.4±11.7	-0.02±0.17	-	4,0
03034909-0106129	NGC1194	162707	55958.095	145	1.0	4011.1±12.1	170.8±4.9	-0.28±0.01	1.25±0.04	57,8
03044401+5406473	PGC011586	140713	55546.075	35	2.0	2467.1±28.9	47.8±69.3	-0.65±0.28	-	4,0
03053486+0608001	PGC011621	340876	56305.182	150	1.0	11197.0±17.0	256.1±11.3	0.50±0.21	-0.59±0.43	4,2
03055539+5415579	PGC011632	152821	55797.383	120	2.0	2172.3±14.4	221.3±13.0	-	-	1,0
03055539+5415579	PGC011632	152822	55797.394	120	2.0	2189.0±16.0	243.6±12.8	-2.02±0.33	-1.70±0.54	3,1
03060989+4222189	ICO284	261583	56221.447	195	1.0	2669.0±9.9	57.2±17.8	-0.43±0.03	-0.36±0.18	41,4
03061191-0932288	NGC1208	160685	55865.300	255	2.0	4401.9±14.3	218.1±7.4	0.58±0.06	-	12,0
03062435+5223459	PGC2418553	261484	56219.430	255	2.0	10647.7±14.1	172.1±15.9	0.69±0.39	-	4,0
03062848-0943518	IC1880	153790	55829.411	220	2.0	9656.4±15.6	241.4±12.7	0.40±0.04	0.51±0.12	36,7
03071837-0936454	NGC1216	160769	55866.303	245	2.0	5118.6±13.5	146.3±10.2	0.45±0.05	-	21,0
03073290+4223151	ICO288	140338	55539.070	40	2.0	5059.3±14.8	189.2±9.0	-0.33±0.37	-	2,0
03081551+3822557	NGC1207	153550	55822.298	181	2.0	4715.3±16.8	162.3±15.2	-0.28±0.01	-0.40±0.06	132,5
03082624+0406388	NGC1218	261444	56218.405	155	1.0	8484.8±14.6	341.8±9.6	0.59±0.08	-	16,1
03085519+7033477	UGC02542	141624	55576.074	-20	2.0	-	-	-	-	-
03104409+6106477	PGC2797416	140808	55549.279	335	2.0	-	-	-	-	-
03104409+6106477	PGC2797416	141848	55585.151	335	2.0	2432.4±21.9	279.5±19.1	-0.33±0.18	-	12,1
03111355+4121494	NGC1224	142554	55610.126	185	2.0	5032.3±15.5	213.0±13.8	-0.24±0.04	-0.13±0.25	13,3
03130881-0243191	PGC3095627	261522	56220.374	165	1.0	8101.0±17.0	164.9±14.2	0.26±0.03	1.19±0.07	71,7
03135317+6232589	PGC138608	152595	55783.456	30	2.0	2007.1±21.9	289.0±22.9	-0.03±0.06	0.40±0.26	27,1
03140848+4244570	PGC012039	161183	55886.133	170	2.0	5276.2±14.8	255.6±9.7	0.07±0.59	-	2,0
03160262+3706452	IC1901	162957	55968.152	345	1.0	5197.1±13.5	203.0±6.0	-	-	0,0
03170362+4138012	PGC012193	142946	55619.100	361	2.0	7112.1±13.1	254.0±7.3	-0.18±0.20	-	5,0
03184497+4128041	NGC1267	153788	55829.309	70	2.0	5241.1±16.0	267.9±11.1	-	-	AGN
03185814+4128121	NGC1270	060095	55415.418	18	2.0	4903.9±13.3	385.5±7.1	-0.04±0.15	-0.57±0.17	5,2
03185814+4128121	NGC1270	060096	55415.436	18	2.0	4909.6±14.5	391.8±6.2	-0.60±0.50	-	2,0
03185814+4128121	NGC1270	060097	55415.454	18	2.0	4917.6±14.8	389.5±6.9	-	-	0,0
03185814+4128121	NGC1270	062008	55488.229	85	2.0	4912.0±15.1	405.5±6.6	-0.52±0.27	-0.28±0.25	3,2
03185814+4128121	NGC1270	062773	55507.172	85	2.0	4892.8±12.5	422.2±8.3	-	-	1,1
03185814+4128121	NGC1270	153899	55833.279	34	1.0	4899.3±14.5	422.2±6.4	-0.22±0.33	-	4,0
03185814+4128121	NGC1270	153934	55835.274	124	1.0	4929.7±14.5	405.4±7.7	0.08±0.51	-	2,1
03191127+4121120	NGC1271	142530	55609.136	310	2.0	5867.0±16.2	325.3±11.2	-	-	0,1
03191127+4121120	NGC1271	161375	55893.120	130	1.0	5870.8±14.3	308.2±8.3	-0.90±0.26	-0.80±0.27	6,3
03191127+4121120	NGC1271	253481	56138.436	130	1.0	5877.9±14.6	314.6±9.6	-0.73±0.45	-0.29±0.53	2,1
03192129+4129261	NGC1272	060260	55421.395	12	2.0	3750.6±15.6	290.6±9.2	-0.68±0.35	-0.72±0.38	1,2
03192129+4129261	NGC1272	060261	55421.407	12	2.0	3742.8±14.5	295.6±7.8	-	-0.44±0.48	1,1
03192129+4129261	NGC1272	060331	55423.398	12	2.0	3721.6±16.2	287.4±7.8	-0.72±0.47	-1.27±0.20	1,2

Table continues on next page

2MASS ID	Name	Frame	MJD	PA	slit ('')	V_{hel} (km s^{-1})	σ_c (km s^{-1})	[NII]/H α	[OIII]/H β	AoN
03192129+4129261	NGC1272	060332	55423.411	12	2.0	3731.3±14.0	272.7±8.4	-	-	0,0
03194313+0945079	UGC02674	062732	55506.380	300	2.0	7323.2±10.8	194.2±7.5	-	-	0,0
03194823+4130420	NGC1275	060510	55428.385	100	2.0	5155.0±18.5	286.9±29.5	-	-	AGN
03194823+4130420	NGC1275	060511	55428.400	100	2.0	5209.6±20.2	277.6±20.2	-	-	AGN
03194823+4130420	NGC1275	060512	55428.419	100	2.0	5163.8±24.3	268.3±26.8	-	-	AGN
03194823+4130420	NGC1275	140052	55533.108	99	2.0	5118.1±22.9	269.3±32.3	-	-	AGN
03194823+4130420	NGC1275	140249	55537.323	325	2.0	5171.7±20.1	275.8±22.1	-	-	AGN
03195148+4134242	NGC1277	140600	55544.080	95	2.0	4960.9±14.0	400.4±6.5	-0.12±0.23	0.13±0.29	6,2
03195148+4134242	NGC1277	142332	55604.142	365	2.0	5002.1±15.0	344.0±7.7	-0.21±0.12	-0.21±0.18	7,3
03195148+4134242	NGC1277	153260	55807.352	95	1.0	4983.9±13.5	397.8±7.5	0.98±0.37	-0.31±0.21	2,2
03195148+4134242	NGC1277	153844	55831.301	185	1.0	5096.0±14.1	358.4±6.5	0.20±0.13	-	7,0
03195148+4134242	NGC1277	160930	55873.177	5	1.0	5056.1±18.5	319.7±11.7	-0.21±0.38	-	2,0
03195148+4134242	NGC1277	162542	55953.193	275	1.0	4974.1±14.8	387.2±5.9	-0.33±0.21	-0.49±0.34	6,2
03195148+4134242	NGC1277	163185	55976.127	300	1.0	4976.1±13.9	395.3±8.0	0.03±0.14	-0.43±0.31	9,2
03195416+4133482	NGC1278	162885	55966.157	320	1.0	5960.6±13.5	271.2±11.9	0.34±0.19	-	6,0
03200610+4137483	NGC1281	060475	55427.377	85	2.0	4186.4±14.8	298.9±6.3	-0.04±0.28	-	3,1
03200610+4137483	NGC1281	060476	55427.392	85	2.0	4206.0±14.8	287.9±7.3	-0.08±0.38	-	3,0
03200610+4137483	NGC1281	060477	55427.407	85	2.0	4205.0±15.1	291.3±7.7	-0.58±0.17	-	4,0
03201214+4122012	NGC1282	140665	55545.070	25	2.0	2168.6±14.6	204.0±10.1	0.12±0.56	-	2,1
03201214+4122012	NGC1282	261441	56218.222	25	1.0	2171.9±12.7	209.9±6.5	-0.68±0.38	-0.80±0.42	3,2
03205776+4130229	PGC012557	160331	55857.454	295	2.0	4915.2±13.3	302.4±7.3	1.10±0.26	0.31±0.18	2,3
03205786+4153377	IC0313	142680	55615.120	230	2.0	4371.9±13.3	240.4±7.8	0.28±0.08	0.50±0.36	13,2
03210041+4133449	PGC012562	161351	55892.353	260	2.0	4640.8±14.8	285.6±7.8	-	-	0,2
03210041+4133449	PGC012562	261366	56215.237	80	1.0	4634.0±16.2	298.7±7.7	0.58±0.70	-0.66±0.47	2,2
03210041+4133449	PGC012562	340553	56283.055	80	1.0	4655.1±16.0	282.7±7.5	0.11±0.35	-	4,1
03210915+6655186	PGC2797207	140721	55546.207	364	2.0	2360.2±22.5	247.1±18.6	-0.40±0.15	-0.55±0.42	15,2
03212081+4127359	PGC012580	153640	55826.303	95	2.0	4532.9±14.1	249.2±8.0	-	-	0,2
03212772+4048059	UGC02689	261970	56237.192	110	1.0	6041.4±12.7	187.3±6.6	0.33±0.22	-	7,0
03213647+4123340	NGC1293	153305	55808.362	1	2.0	4129.0±15.0	243.2±8.5	-	-	0,1
03220285+4051500	UGC02698	060232	55420.424	91	2.0	6380.4±13.5	384.4±9.1	-0.06±0.12	-	4,0
03220285+4051500	UGC02698	060233	55420.437	91	2.0	6360.9±13.1	375.2±9.5	-	-	0,0
03220285+4051500	UGC02698	060756	55445.342	91	2.0	6362.8±14.7	368.8±9.3	-	-	0,1
03220285+4051500	UGC02698	060757	55445.357	91	2.0	6350.8±15.8	364.0±9.7	-0.74±0.34	0.05±0.52	3,1
03220285+4051500	UGC02698	153935	55835.290	110	1.0	6338.5±14.2	368.4±9.3	-0.19±0.22	-0.41±0.49	6,2
03260309+4115084	UGC02733	142578	56511.129	240	2.0	5266.4±15.5	271.6±7.6	-0.10±0.21	-	4,0
03275526+3959497	PGC213218	163445	55981.115	361	2.0	7334.6±13.2	290.6±8.3	0.07±0.07	0.13±0.26	18,3
03280595-0823190	NGC1337	341121	56315.089	190	1.0	1178.0±27.6	36.0±39.1	-0.38±0.04	-	5,0
03292389+3947318	UGC02755	062827	55508.176	88	2.0	7204.8±15.0	280.5±8.3	0.51±0.11	0.45±0.35	10,3
03320732+4747385	UGC02773	261526	56220.462	285	1.0	169.3±22.6	58.3±36.1	-	-	AGN
03341837+3921243	UGC02783	140347	55539.342	290	2.0	6054.4±13.4	304.5±9.6	0.41±0.17	-	7,0
03370592-0502339	NGC1376	153732	55828.415	210	1.0	4084.7±16.1	56.0±20.4	-0.45±0.03	-0.64±0.20	34,3
03380124+6642455	2M03380	153359	55810.466	400	2.0	5833.6±27.3	289.3±21.2	-0.34±0.11	-	19,0
03381210+6642567	PGC2690279	153846	55831.379	455	2.0	5236.5±38.7	378.6±29.7	-0.20±0.21	-	12,0
03411752+1523477	PGC1483518	061973	55487.274	90	2.0	8673.3±17.8	305.8±10.9	0.52±0.43	-	3,0
03411752+1523477	PGC1483518	140340	55539.132	121	2.0	8696.0±17.8	330.0±10.3	-	-	0,0
03445844+4558030	UGC02844	140287	55538.130	40	2.0	4847.1±14.0	342.4±8.5	0.02±0.15	0.03±0.19	11,4
03445844+4558030	UGC02844	160683	55865.217	40	1.0	4864.2±12.3	319.6±9.3	-0.07±0.13	-0.10±0.19	15,4
03462726-0358075	NGC1453	060902	55450.446	199	2.0	3865.0±14.7	312.8±6.2	0.35±0.03	0.50±0.10	22,4
03462726-0358075	NGC1453	060903	55450.458	199	2.0	3873.4±14.4	323.1±6.5	0.31±0.03	0.34±0.07	25,5
03480074+3306417	PGC2023632	141765	55583.228	255	2.0	4143.4±27.0	272.3±26.4	-	-	0,0
03480074+3306417	PGC2023632	142531	55609.154	255	2.0	4121.7±23.1	225.1±26.1	-	-	0,0
03482073+7007583	UGC02855	153486	55818.470	360	2.0	1173.0±27.6	81.8±52.2	-0.31±0.01	-0.74±0.26	77,2
03501487+7005409	UGC02866	153608	55825.452	70	2.0	1272.9±16.9	128.9±24.1	-0.31±0.00	-0.42±0.02	475,15
03502828+5122423	PGC2393112	162958	55968.171	340	2.0	4754.1±51.1	253.1±79.8	-1.11±0.57	-	2,0
03521694+3614129	UGC02881	143484	55632.107	210	2.0	5626.8±13.1	188.5±14.7	0.15±0.06	0.68±0.37	25,1
03531336+6020218	PGC165379	142874	55618.094	260	2.0	5341.7±13.8	125.2±23.8	-0.23±0.02	0.09±0.17	43,3
03533191+3229343	NGC1465	060198	55419.437	163	2.0	4067.9±14.2	267.9±5.5	0.45±0.07	-	7,1
03533191+3229343	NGC1465	060199	55419.451	163	2.0	4032.5±13.8	260.8±7.4	0.40±0.06	-	8,1
03543327-0255046	PGC148580	261523	56220.392	260	1.0	4014.1±14.7	254.7±8.1	0.25±0.19	0.39±0.47	10,2
04002774+6834398	NGC1469	061656	55480.378	-30	2.0	1036.5±13.7	259.0±6.6	0.02±0.02	0.44±0.06	32,4
04002774+6834398	NGC1469	061657	55480.392	-30	2.0	1042.2±13.7	264.1±6.3	-0.01±0.02	0.45±0.07	31,3
04020678+2307585	NGC1497	261629	56223.257	55	1.0	6158.8±13.7	254.8±7.0	0.42±0.03	0.79±0.09	39,4
04034219+4643428	UGC02937	163600	55984.138	355	2.0	4450.1±14.0	234.8±11.2	0.01±0.21	0.13±0.29	7,2
04034287+1953415	IC0358	261375	56215.282	60	1.0	6696.0±30.2	287.1±25.8	-0.22±0.54	-	3,0
04034287+1953415	IC0358	261578	56221.274	60	1.0	6680.4±14.1	284.4±7.4	0.21±0.16	0.64±0.31	8,2
04035523-1110446	NGC1509	341241	56317.101	255	1.0	8693.8±16.0	153.5±11.5	-0.38±0.01	-0.61±0.03	120,13
04063774+3022344	PGC014467	060826	55447.381	101	2.0	5306.7±19.1	292.6±15.4	-0.86±0.84	-0.25±0.73	2,1
04074690+6948447	IC0356	153507	55821.452	285	1.0	861.8±12.7	162.5±6.5	0.28±0.05	0.49±0.23	21,2
04115279+3447522	PGC2054700	261577	56221.257	135	1.0	6235.1±10.7	120.3±10.6	0.14±0.13	-	17,0
04122834+2742065	IC0359	062774	55507.224	35	2.0	3904.7±13.6	219.5±8.2	0.27±0.04	0.52±0.16	29,4
04164020+3451101	PGC2055576	342692	56366.098	350	1.0	9921.4±13.9	173.9±7.7	-0.08±0.10	-	3,0
04191415+0320536	IC0365	141710	55580.079	210	2.0	7321.0±14.8	250.6±10.6	0.36±0.12	0.57±0.30	8,2
04193792+0224355	NGC1551	153310	55808.441	210	2.0	3718.2±17.5	334.5±9.9	-	-	0,2
04201768-0041336	NGC1552	061905	55485.354	110	2.0	4887.0±14.2	247.6±7.1	0.55±0.05	0.84±0.13	14,2
04212943+3656572	2M04212	152823	55797.416	130	2.0	5656.7±16.8	252.4±13.7	-0.44±0.15	-	7,1
04215763+0150202	UGC03023	060901	55450.427	80	2.0	3930.6±13.8	219.6±7.3	-1.75±0.15	-2.05±0.27	4,2
04222658+2717521	UGC03024	141862	55585.237	315	2.0	5174.3±18.3	290.5±15.4	0.09±0.44	-	14,2

Table continues on next page

2MASS ID	Name	Frame	MJD	PA	slit ('')	V_{hel} (km s^{-1})	σ_c (km s^{-1})	[NII]/H α	[OIII]/H β	AoN
04222658+2717521	UGC03024	143485	55632.125	315	2.0	5182.7±24.0	273.5±25.3	-0.21±0.20	-	7,1
04275732+2619180	PGC138729	260381	56165.425	106	1.0	-	-	-	-	-
04275732+2619180	PGC138729	340395	56279.118	120	1.0	-	-	-	-	-
04284494+6934458	PGC015211	141625	55576.144	50	2.0	4613.8±16.0	189.9±9.4	0.80±0.26	-	3,0
04303992+0039421	NGC1587	160773	55866.406	225	2.0	3627.8±13.7	239.3±6.0	0.28±0.04	0.93±0.12	19,3
04304545+0051491	NGC1589	262593	56256.344	160	1.0	3733.1±13.7	194.7±4.8	-0.05±0.02	1.10±0.15	52,2
04304918+6450525	NGC1569	261745	56229.328	-62	1.0	-105.7±22.3	93.8±35.0	-1.23±0.01	0.84±0.00	29,169
04310522+2324076	2M04310	152824	55797.434	150	2.0	5019.3±23.3	283.9±18.1	0.06±0.06	0.32±0.31	29,2
04313985+0505099	NGC1600	140343	55539.251	185	2.0	4651.6±14.8	343.6±7.6	-	-	0,2
04315707+5925473	PGC165398	163326	55978.120	260	2.0	4539.3±13.5	196.5±10.9	0.37±0.07	1.01±0.43	19,1
04324860+2929578	PGC089985	140525	55543.129	140	2.0	1983.5±34.3	34.0±54.6	-0.20±0.01	-0.40±0.12	337,4
04331106+0521151	3C120	140200	55536.206	139	2.0	-	-	-	-	AGN
04340002-0834445	NGC1614	262028	56238.357	200	1.0	4644.8±17.0	147.3±22.3	-0.01±0.00	-0.31±0.01	539,117
04350397+7315446	NGC1573	140120	55534.272	390	2.0	4160.1±13.3	305.5±8.7	-	-1.64±0.47	1,1
04360101+1957008	NGC1615	060760	55445.409	120	2.0	3354.8±14.3	137.5±9.9	-	-	1,0
04360101+1957008	NGC1615	060761	55445.423	120	2.0	3329.8±14.0	143.3±10.8	-	-	1,0
04362230-1022346	MRK0618	153903	55833.454	178	2.0	10428.2±23.9	84.9±54.8	-	-	AGN
04362230-1022346	MRK0618	162540	55953.127	178	2.0	10431.5±28.0	134.4±38.8	-	-	AGN
04363734-0008370	NGC1620	162297	55946.202	200	1.0	3463.0±14.5	73.7±14.2	-0.08±0.07	0.25±0.35	20,2
04370366+2456067	2M04370	341482	56329.205	210	1.0	4780.2±16.9	95.2±18.3	0.15±0.03	1.17±0.15	43,4
04370757-0218166	UGC03105	062148	55495.418	245	2.0	8667.9±16.9	302.1±15.3	0.08±0.19	0.09±0.43	7,2
04371939+2447120	PGC3097125	142555	55610.185	175	2.0	5036.2±40.1	308.6±32.0	0.02±0.10	0.09±0.35	17,2
04381542+4841393	PGC015704	143572	55635.132	275	2.0	5638.4±49.5	138.7±94.4	-	-	AGN
04395859+2454274	PGC3097126	141793	55584.253	165	2.0	3790.8±23.3	187.6±22.8	-0.00±0.16	-	11,0
04412822-0251289	NGC1637	260947	56201.418	212	1.0	686.4±15.0	34.3±17.2	-0.21±0.00	-0.49±0.02	289,15
04454736-0223340	NGC1653	142796	55617.078	175	2.0	4277.6±13.0	240.1±6.4	0.22±0.04	0.71±0.13	20,3
04473623-0109428	UGC03170	261580	56221.355	120	1.0	8820.3±14.6	203.4±4.9	0.27±0.10	0.90±0.54	12,1
04483720-0619114	NGC1667	261582	56221.390	181	1.0	4496.9±10.4	160.1±4.6	0.39±0.01	1.15±0.03	99,12
04493401+0015103	NGC1671	262569	56255.261	130	1.0	6279.6±14.2	244.9±6.2	0.31±0.06	0.65±0.24	20,3
04500668+4503057	PGC016124	142736	55616.174	245	2.0	5982.6±56.9	328.5±108.6	0.17±1.29	-	3,0
04500668+4503057	PGC016124	142737	55616.186	245	2.0	5932.2±53.3	239.0±85.3	-	-	0,0
04513544-0237235	NGC1678	142945	55619.081	250	2.0	4585.1±12.3	263.3±7.8	-	-	0,2
04520479+4932446	PGC168563	152910	55799.448	15	2.0	8302.8±69.2	461.5±110.7	-	-	AGN
04523116-0306220	NGC1684	061547	55478.410	135	2.0	4448.2±13.3	268.6±6.4	-0.02±0.02	0.39±0.15	30,3
04523116-0306220	NGC1684	061548	55478.422	135	2.0	4468.8±13.8	269.8±6.8	-0.06±0.02	0.13±0.12	30,4
04525281+5204476	PGC016235	260552	56181.397	-10	2.0	9652.7±121.5	693.7±176.3	-	-	AGN
04525281+5204476	PGC016235	340495	56282.125	-10	2.0	9508.0±76.3	365.6±51.8	-	-	AGN
04532576+0403416	PGC016263	341332	56323.184	215	1.0	8632.7±14.6	137.5±15.2	-0.45±0.00	1.11±0.00	80,37
04543832+0316045	NGC1691	140726	55546.307	210	2.0	4535.4±15.7	172.0±11.4	-0.20±0.00	-0.24±0.02	187,16
04565634-0451566	NGC1700	160328	55857.409	265	2.0	3844.7±13.6	243.9±5.4	-	-	0,0
04594189-0745185	NGC1726	142116	55597.118	185	2.0	3920.9±11.8	256.3±6.0	0.33±0.09	-	9,1
05025822+2259520	PGC097068	153677	55827.388	105	2.0	16627.5±69.7	158.9±93.3	-	-	AGN
05051802-0908500	NGC1779	153939	55835.469	130	2.0	3272.7±13.8	163.6±10.4	0.34±0.02	0.64±0.13	33,2
05063500+0735385	2M05063	262025	56238.294	95	1.0	12989.1±14.8	250.4±5.3	0.40±0.48	-	16,0
05081967+1721483	PGC1530971	142810	55617.166	265	2.0	5240.1±22.8	236.3±21.5	-	-	AGN
05114519+6729174	UGC03252	262399	56251.312	35	1.0	6011.4±10.8	92.7±7.2	0.18±0.01	1.20±0.04	90,11
05122970+5117149	UGC03260	062217	55497.290	115	2.0	6507.1±13.4	201.6±9.7	0.21±0.06	0.03±0.29	22,3
05140614-1037366	NGC1843	160772	55866.388	105	1.0	2554.3±11.2	23.5±24.6	-	-0.81±0.38	1,2
05161139-0008596	UGC03271	261581	56221.374	200	1.0	9580.5±22.5	202.2±24.3	-	-	AGN
05214155+7219533	PGC017169	142435	55606.140	405	2.0	4908.1±16.6	231.5±9.8	-	-	0,1
05312581+6743497	PGC017387	262401	56251.349	430	1.0	4960.4±14.3	316.8±7.5	0.33±0.17	0.36±0.32	8,2
05374496+2428294	PGC3097142	262112	56240.271	30	1.0	7476.7±15.1	154.3±15.4	0.07±0.19	-0.49±0.36	9,2
05414221+0640502	PGC017603	262085	56239.319	145	1.0	490.6±21.4	17.8±29.8	-0.82±0.01	0.59±0.06	39,17
05420477+6922421	NGC1961	153904	55833.473	452	2.0	3864.9±13.0	239.6±7.8	0.23±0.01	0.23±0.06	122,8
05420477+6922421	NGC1961	162045	55937.228	275	2.0	3900.0±16.6	220.5±16.8	0.23±0.01	0.21±0.08	87,6
05420477+6922421	NGC1961	162046	55937.243	275	2.0	3885.2±17.3	234.0±18.3	0.21±0.02	0.25±0.11	66,4
05420477+6922421	NGC1961	162047	55937.260	275	2.0	3880.8±15.8	206.9±13.5	0.21±0.01	0.19±0.09	79,5
05430850+6036100	PGC2604391	341681	56335.203	260	1.0	16427.7±18.8	423.6±17.9	-	-	0,1
05454783+5842038	UGC03351	142811	55617.184	345	2.0	4384.5±20.0	178.2±23.3	0.06±0.02	0.08±0.16	97,5
05471117+1733467	PGC213322	342267	56353.177	270	1.0	5522.8±17.5	65.0±30.2	-0.36±0.00	0.07±0.01	428,57
05512589-1014438	PGC148081	262115	56240.400	240	1.0	787.1±51.2	102.2±60.6	-0.70±0.10	0.43±0.36	9,3
05521140-0727222	NGC2110	141626	55576.215	160	2.0	2292.5±18.8	233.2±17.1	-	-	AGN
05572695+1156572	NGC2119	141014	55558.166	155	2.0	3462.0±14.8	249.4±8.1	0.57±0.15	-	5,0
06023793+6522161	UGC03386	142434	55606.107	45	2.0	4522.3±13.7	168.9±10.9	0.39±0.01	1.08±0.04	67,6
06043422+5737401	NGC2128	060942	55451.445	65	2.0	2925.1±14.3	251.3±8.6	0.01±0.03	0.67±0.18	32,2
06043422+5737401	NGC2128	060943	55451.458	65	2.0	2916.1±12.5	236.5±7.0	0.03±0.02	0.45±0.10	33,3
06045758-0635165	2M06045	262475	56253.386	130	1.0	-	-	-	-	-
06084688+3229032	PGC1999078	142745	55616.229	260	2.0	7280.3±16.1	277.6±14.6	-0.15±0.30	-0.17±0.72	5,2
06153645+7102152	UGC03426	062421	55501.420	380	2.0	3957.5±16.8	253.2±14.6	-	-	AGN
06153645+7102152	UGC03426	062422	55501.432	380	2.0	3940.6±15.4	233.7±12.8	-	-	AGN
06190264+0309512	PGC086285	140312	55538.407	273	2.0	2820.7±16.4	188.4±15.2	-0.11±0.10	0.27±0.59	13,1
06201164+6635058	UGC03438	161345	55890.382	280	1.0	4138.9±18.5	102.4±26.5	-0.40±0.08	-	14,1
06205573-0829441	UGCA127	262090	56239.421	110	1.0	690.7±14.9	30.4±27.5	-0.34±0.06	-	20,1
06215050+0021581	UGC03457	140345	55539.287	230	2.0	2680.3±13.1	191.2±8.1	0.30±0.17	-	6,0
06222832+6634428	UGC03448	160962	55873.433	405	1.0	4349.9±12.5	176.9±7.9	0.45±0.22	-	6,0
06255550+6444265	UGC03458	142437	55606.234	310	2.0	4132.2±31.7	226.6±43.2	-0.03±0.21	-0.84±0.73	9,1
06265562+5904483	IC2166	161242	55888.306	115	1.0	2621.0±13.9	68.4±16.1	-0.33±0.07	-0.22±0.52	18,2

Table continues on next page

2MASS ID	Name	Frame	MJD	PA	slit ('')	V_{hel} (km s^{-1})	σ_c (km s^{-1})	[NII]/H α	[OIII]/H β	AoN
06283061+2132595	PGC019111	140722	55546.226	184	2.0	4409.9±16.5	337.0±12.0	0.07±0.10	0.07±0.34	14,2
06283061+2132595	PGC019111	161196	55887.270	200	1.0	4392.7±15.6	300.6±10.3	-0.07±0.09	0.21±0.41	18,2
06325201+4731326	PGC019232	162539	55953.098	70	2.0	10281.7±14.0	331.5±9.6	0.52±0.52	-	3,0
06345941+0653184	PGC019278	142812	55617.209	270	2.0	3486.6±18.1	189.4±21.5	-0.87±0.20	-	5,0
06391085-0130277	PGC085930	160605	55864.412	95	2.0	2759.3±16.4	231.8±12.6	-0.16±0.15	-	12,1
06454107+7120378	IC0449	163484	55982.142	440	2.0	3837.6±14.7	240.3±8.4	-	-	0,1
06471737+3334021	NGC2274	140074	55533.253	97	2.0	5032.0±14.3	290.3±6.9	-	-0.22±0.23	1,3
06471737+3334021	NGC2274	140527	55543.218	170	2.0	4949.4±15.6	284.8±6.9	-	-0.53±0.38	1,1
06500866+6050445	NGC2273	162543	55953.292	260	1.0	1812.3±12.7	112.5±6.6	-0.07±0.00	0.91±0.00	336,37
06501768-0251397	PGC076120	161353	55892.431	240	2.0	2548.0±20.7	285.0±18.4	-0.10±0.10	0.08±0.28	22,2
06515795+1617407	PGC019750	161416	55894.291	195	1.0	2582.3±12.3	123.3±6.8	-	-	0,0
06552767+3316495	PGC019864	142563	55610.273	305	2.0	5175.3±13.0	269.9±6.7	0.17±0.07	0.30±0.13	16,4
06553570+3945526	UGC03596	262570	56255.279	130	1.0	5146.2±14.0	168.7±6.2	0.59±0.18	-	5,0
06584610+5946393	PGC3096769	260949	56201.456	-25	1.0	20467.2±189.1	922.5±132.7	-	-	AGN
07033226+0117074	PGC076449	262114	56240.383	160	1.0	9276.4±12.9	197.3±7.6	-0.45±0.33	-0.23±0.38	2,2
070542202+5034519	NGC2320	062056	55491.383	140	2.0	5738.4±16.1	324.3±11.3	0.27±0.04	0.53±0.12	29,4
07081396+4606569	UGC03683	140344	55539.268	50	2.0	5812.0±15.1	280.2±7.3	-	-	0,0
07090595+6135438	UGC03685	161509	55896.305	135	1.0	1759.0±12.9	42.1±19.2	-0.04±0.00	1.11±0.00	176,21
07111080+5010288	NGC2340	341480	56329.087	85	1.0	5836.6±12.9	243.9±6.0	0.11±0.12	-	9,1
07114179+4952003	UGC03725	142746	55616.285	288	2.0	6043.1±13.2	285.3±10.9	0.54±0.13	-	7,0
07122870+4710004	NGC2344	144394	55660.150	325	1.0	922.8±15.2	55.1±16.9	0.05±0.25	-0.07±0.35	4,3
07122870+4710004	NGC2344	144395	55660.162	325	1.0	919.3±13.7	48.8±16.6	-0.30±0.36	-0.81±0.50	1,2
07140387+3516455	UGC03752	260948	56201.436	75	1.0	4594.4±15.0	88.6±8.1	-0.16±0.00	0.78±0.00	140,32
07141510+4541557	MRK0376	160771	55866.358	170	2.0	16315.5±38.7	250.8±42.7	-	-	AGN
07164122+5323091	PGC020561	262087	56239.359	135	1.0	18515.1±17.0	309.7±13.2	-	-	0,1
07180060+4405271	PGC020607	262571	56255.301	20	1.0	18445.1±170.1	92.0±187.0	-	-	AGN
07193089+5921184	UGC03789	162711	55958.169	-20	1.0	3184.5±9.6	127.5±6.7	-0.07±0.00	1.10±0.01	369,55
07202668+5623271	UGC03800	161349	55892.316	30	2.0	13218.2±12.9	234.3±9.9	-	-	0,0
07221089-0555472	PGC020827	140787	55548.348	100	2.0	1547.6±13.9	133.7±14.0	0.42±0.02	-	34,0
07225814-0357344	PGC077133	262408	56251.445	225	1.0	19893.0±14.0	138.1±17.0	-0.09±0.32	0.15±0.88	7,2
07231243+5803532	UGC03816	061549	55478.445	52	2.0	3274.9±14.0	297.5±6.1	0.27±0.05	0.41±0.17	19,3
07231243+5803532	UGC03816	061550	55478.456	52	2.0	3249.7±13.8	299.3±5.8	0.32±0.05	0.61±0.17	16,2
07231243+5803532	UGC03816	061589	55479.424	52	2.0	3280.5±13.0	305.7±5.9	0.31±0.09	0.58±0.36	12,2
07231243+5803532	UGC03816	061590	55479.436	52	2.0	3279.3±13.2	307.5±5.5	0.29±0.07	0.58±0.31	12,2
07243578+5758029	UGC03828	262400	56251.330	-20	1.0	3449.2±12.4	78.6±10.7	-0.32±0.00	-0.27±0.03	147,16
07252090+1910387	UGC03840	142587	55611.280	310	2.0	8313.0±14.0	298.2±8.1	-0.73±0.29	-	2,0
07281299+5830242	UGC03855	161417	55894.307	55	1.0	3110.8±13.3	143.6±5.6	0.15±0.11	-	13,0
07285341+3349084	NGC2388	142564	55610.289	240	2.0	4028.8±21.6	55.9±42.3	-0.22±0.00	-0.52±0.06	231,6
07312264+1854217	PGC021204	162541	55953.146	130	2.0	8128.0±14.5	222.8±9.4	0.36±0.18	-	8,0
07330464+6504446	UGC03894	142486	55608.228	380	2.0	6628.7±13.5	302.0±7.0	0.16±0.13	0.39±0.45	8,2
07330464+6504446	UGC03894	142586	55611.226	380	2.0	6644.2±13.8	308.9±8.1	0.18±0.16	-0.43±0.29	6,2
07343635+1816534	NGC2411	142411	55605.307	230	2.0	4959.3±13.5	276.5±6.9	0.47±0.11	-	7,0
07363752+1753023	NGC2418	262572	56255.319	65	1.0	4995.0±13.5	254.5±4.9	0.43±0.07	-	15,1
07365707+5846134	PGC021400	140667	55545.298	35	2.0	11733.0±18.1	91.7±44.9	-	-	AGN
07405822+5525379	UGC03957	142543	55609.290	280	2.0	9985.6±17.2	304.8±12.1	-0.21±0.59	-0.33±1.07	2,1
07424170+6510378	MRK0078	161981	55933.274	80	1.0	10881.2±25.4	96.4±40.4	-	-	AGN
07435033+4936515	IC0472	262192	56243.362	25	1.0	5578.4±11.5	140.8±6.4	0.39±0.08	0.59±0.27	19,3
07441362+3139045	NGC2435	140374	55539.512	215	2.0	4121.7±14.0	192.1±8.4	0.27±0.05	0.61±0.30	19,2
07511761+5010459	UGC04051	162759	55959.144	10	2.0	6178.5±13.8	300.5±7.3	0.05±0.18	-	5,0
07570191+4934021	UGC04107	340520	56282.472	295	1.0	3440.7±16.3	64.7±22.4	-0.45±0.02	-0.65±0.11	70,5
07594014+1523122	UGC04145	142577	55611.111	130	2.0	4546.3±14.6	164.6±12.9	0.15±0.00	0.95±0.02	125,13
08002366+3949494	NGC2493	140723	55546.279	30	2.0	3889.6±13.8	225.8±8.4	0.33±0.05	0.60±0.15	18,3
08014590+5631320	NGC2488	142588	55611.297	275	2.0	8488.1±14.9	290.1±8.6	0.38±0.23	1.04±0.81	4,1
08015724+0833064	NGC2508	160986	55876.398	130	2.0	4224.9±24.6	310.2±29.7	-0.13±0.20	-0.86±0.46	4,1
08015724+0833064	NGC2508	162712	55958.184	130	2.0	4284.6±12.6	263.7±5.9	0.49±0.05	0.80±0.18	15,2
08022465+0924489	NGC2513	141016	55558.272	170	2.0	4619.5±14.4	297.0±6.5	-	-	1,0
08040584+0506498	UGC04203	341484	56329.314	325	1.0	3976.1±15.4	74.5±22.3	-	-	AGN
08053779-058174	PGC022720	261705	56225.480	156	1.0	25649.9±14.2	418.6±17.5	-	-	
08061345+1742231	NGC2522	142439	55606.329	215	2.0	4648.1±15.9	289.1±10.8	0.21±0.07	-	13,1
08071471+0428106	PGC022798	162511	55951.353	230	2.0	9152.8±14.9	198.5±8.4	-	-	0,1
08095257+5754458	PGC022906	142545	55609.324	365	2.0	7741.8±18.0	280.5±13.4	0.23±0.08	0.36±0.21	13,3
08102329+4216262	PGC2195631	161350	55892.336	110	2.0	18422.0±16.4	363.4±12.7	-	-	0,1
08102329+4216262	PGC2195631	161418	55894.325	110	2.0	18438.5±16.2	318.6±16.0	-	-0.42±0.45	1,2
08110158+0505143	IC2231	142640	55613.278	300	2.0	8876.0±15.0	267.6±8.8	0.43±0.29	0.02±0.45	2,3
08131464+4559232	NGC2537	261746	56229.407	165	1.0	-	-	-	-	
08144007+4903411	NGC2541	261485	56219.448	-5	1.0	526.6±21.3	71.1±31.0	-0.54±0.05	0.00±0.14	16,8
08154484+5819159	UGC04289	341481	56329.178	95	1.0	7983.9±14.1	239.8±6.3	0.46±0.12	-	10,0
08172577+2141080	UGC04308	262402	56251.365	100	1.0	3518.3±12.2	77.9±16.6	-0.41±0.01	-0.53±0.06	113,8
08173676+3526455	UGC04306	161151	55884.357	135	1.0	2321.9±15.4	49.4±26.7	-0.38±0.01	-0.24±0.06	127,8
08175347+2328195	NGC2554	163598	55984.090	160	1.0	4045.4±12.2	188.0±4.5	0.28±0.02	0.87±0.27	39,2
08185834+5748111	NGC2549	261725	56228.435	1	1.0	1022.8±13.5	147.5±3.8	0.01±0.14	-	3,0
08194833+2201531	NGC2565	160960	55873.398	175	1.0	3523.5±11.3	156.2±6.1	0.26±0.08	-	16,0
08202368+2107533	NGC2562	142589	55611.314	181	2.0	4996.0±13.8	176.9±10.0	1.19±1.18	-	2,1
08203567+2104042	NGC2563	140734	55546.502	250	2.0	4441.0±13.5	286.9±6.0	-	-	0,3
08223394+5619455	UGC04357	161419	55894.343	90	1.0	8433.5±13.0	147.3±7.4	-0.21±0.02	-0.25±0.13	48,4
08224347+2233109	NGC2577	261445	56218.440	105	1.0	2003.6±12.7	215.9±5.8	0.14±0.14	-	11,1
08262485+5953433	PGC023680	161352	55892.373	90	2.0	7856.6±14.3	301.4±15.7	0.16±0.06	0.42±0.30	19,2

Table continues on next page

2MASS ID	Name	Frame	MJD	PA	slit ('')	V_{hel} (km s^{-1})	σ_c (km s^{-1})	[NII]/H α	[OIII]/H β	AoN
08270808+2558132	NGC2592	261410	56217.447	55	1.0	1944.6±12.0	232.6±4.5	-0.28±0.21	-0.49±0.18	4,3
08270808+2558132	NGC2592	340877	56305.200	55	1.0	1941.2±14.1	240.0±4.6	0.10±0.18	0.15±0.51	7,1
08284712-0656246	MRK1216	142410	55605.243	250	2.0	6331.8±15.6	343.1±9.2	0.27±0.06	0.11±0.21	17,3
08284712-0656246	MRK1216	161426	55894.454	160	1.0	6363.0±12.0	356.2±7.4	0.24±0.05	0.20±0.19	27,3
08284712-0656246	MRK1216	161511	55896.450	250	1.0	6373.0±13.7	341.3±10.1	0.25±0.06	0.68±0.57	22,1
08355356+0042259	NGC2618	163418	55980.173	145	1.0	3983.4±12.5	148.8±7.6	-	-	3,0
08424792+7258352	NGC2614	262410	56251.482	330	1.0	3394.8±13.5	58.3±23.3	0.29±0.57	-	4,0
08433809+5012199	NGC2639	163599	55984.109	123	1.0	3121.5±12.9	188.6±5.3	0.48±0.01	0.83±0.05	81,5
08442146+5850307	UGC04549	341683	56335.346	330	1.0	1262.8±15.9	16.0±26.9	-0.36±0.05	-0.21±0.18	25,5
08471585+7259082	NGC2629	141416	55570.368	455	2.0	3584.3±12.4	298.6±6.5	0.28±0.02	0.48±0.07	46,7
08492189+1904298	NGC2672	140309	55538.343	120	2.0	4290.0±14.6	283.0±5.7	-	0.03±0.50	1,3
08524134+3325184	NGC2683	160961	55873.415	97	1.0	372.5±14.7	108.3±17.8	0.16±0.05	0.46±0.17	24,3
08533273+5118493	NGC2681	262089	56239.402	70	1.0	641.6±12.8	103.3±5.7	0.67±0.02	-	15,0
08542706-0304015	NGC2695	161510	55896.428	170	1.0	1784.8±13.3	222.8±3.6	-	-	0,0
08565924+5120504	NGC2693	140492	55542.321	160	2.0	4821.6±13.5	331.4±5.8	-0.07±0.09	-0.27±0.16	9,3
08572051+0255171	NGC2713	140318	55538.505	295	2.0	3869.5±13.5	235.9±6.1	0.40±0.05	0.89±0.27	18,2
08590808+1108566	NGC2720	142641	55613.324	205	2.0	8709.1±15.1	324.3±9.2	0.22±0.46	-	2,0
09015837+6009062	UGC04730	162713	55958.243	95	1.0	3292.4±13.3	101.9±9.5	-0.43±0.00	0.35±0.01	167,43
09052131+1818472	NGC2749	142184	55598.379	245	2.0	4140.4±14.1	268.0±7.4	0.26±0.02	0.58±0.11	32,4
09073352+6028454	NGC2816	162219	55943.406	265	1.0	1238.4±14.2	69.9±16.4	-0.38±0.00	-0.34±0.00	37,3
09083728+3737174	NGC2759	142642	55613.356	230	2.0	6855.6±15.0	283.3±7.6	0.08±0.10	-	8,1
09085837-0935587	PGC025752	341352	56323.290	173	1.0	14994.1±19.1	317.8±14.7	-	-	0,1
09101187+5024048	NGC2767	142414	55605.393	355	2.0	4870.3±14.7	244.5±7.6	0.45±0.10	1.44±0.77	7,1
09101187+5024048	NGC2767	251846	56064.138	355	1.0	4879.5±13.1	248.5±5.8	0.40±0.14	-	8,1
09101187+5024048	NGC2767	261584	56221.466	-5	1.0	4875.4±12.8	248.1±4.9	0.40±0.12	-	7,0
09102011+0702165	NGC2775	161215	55887.422	160	1.0	1316.4±13.4	166.1±4.0	-0.05±0.23	-	3,0
09113750+6002139	NGC2768	261748	56229.468	93	1.0	1318.0±13.0	172.8±4.0	0.17±0.02	0.43±0.08	40,5
09122439+3501387	NGC2778	340804	56294.493	230	1.0	1979.6±15.8	159.1±5.9	0.05±0.16	0.88±0.43	8,1
09133949+2959340	NGC2783	142639	55612.377	170	2.0	6674.9±16.3	241.7±10.4	0.27±0.04	0.25±0.14	20,6
09145961+2943492	NGC2789	142413	55605.375	220	2.0	6265.2±14.0	183.0±11.6	-0.19±0.01	-0.13±0.06	107,10
09164777+4946491	PGC026193	341439	56327.416	255	1.0	8424.3±12.9	305.4±6.8	0.15±0.31	0.27±0.86	4,3
09165350+1727271	PGC026204	140493	55542.342	183	2.0	8398.3±13.7	237.3±8.9	-1.18±0.59	-1.15±0.34	1,2
09180931+1611526	NGC2819	141420	55570.456	225	2.0	8813.7±14.5	312.4±7.5	-	-	0,0
09182597+1618196	PGC026292	140310	55538.363	65	2.0	8581.9±22.2	282.6±20.3	-	-	AGN
09191853+6912122	NGC2787	140373	55539.473	300	2.0	627.3±13.2	205.0±6.3	0.19±0.02	0.53±0.08	30,4
09194687+3344594	NGC2832	140121	55534.354	165	2.0	6740.6±13.3	340.4±7.1	0.40±0.16	0.41±0.51	5,2
09220265+5058353	NGC2841	144503	55670.216	290	2.0	599.5±13.1	230.1±8.3	0.25±0.01	0.42±0.04	43,7
09234300+2254324	PGC026614	251034	56024.242	335	1.0	9757.3±53.4	96.6±84.3	-	-	AGN
09234300+2254324	PGC026614	261446	56218.493	165	1.0	9671.8±24.4	148.3±29.0	-	-	AGN
09241854+3430481	NGC2859	261806	56231.455	157	1.0	1627.1±14.1	172.8±3.5	0.33±0.06	-	16,1
09251217-0649476	IC2471	142488	55608.274	145	2.0	6105.7±14.4	181.2±10.2	-	-	0,1
09254253+1125557	NGC2872	140122	55534.384	45	2.0	3207.1±13.8	293.3±5.8	0.39±0.19	0.07±0.33	4,4
09260324+1244041	UGC05025	163186	55976.180	80	2.0	8472.3±22.2	197.5±30.3	-	-	AGN
09301694+2932339	NGC2893	342011	56342.158	165	1.0	1663.4±13.8	41.5±16.7	-0.21±0.00	-0.13±0.00	196,16
09321011+2130029	NGC2903	160963	55873.451	102	1.0	506.0±12.8	75.2±8.4	-0.39±0.00	-0.44±0.02	181,11
09325289+6737026	NGC2892	142438	55606.312	361	2.0	6732.8±16.2	272.6±9.1	0.68±0.16	0.16±0.29	5,3
09380516+0936598	NGC2940	141456	55571.454	295	2.0	8417.3±12.9	218.6±7.9	-	0.09±0.87	0,2
09380516+0936598	NGC2940	141457	55571.465	295	2.0	8417.5±14.6	200.4±9.4	-0.16±0.37	-0.36±0.37	2,2
09383289+1701527	NGC2943	142688	55615.359	305	2.0	8239.7±15.2	259.2±8.4	0.53±0.17	-	5,0
09403637+0334369	NGC2960	162714	55958.269	210	1.0	4870.3±12.1	155.2±4.2	0.48±0.01	1.07±0.04	60,10
09420333+0020113	NGC2967	144555	55673.167	135	2.0	1862.4±13.1	77.9±27.4	-0.26±0.08	0.37±0.59	12,1
09420333+0020113	NGC2967	144556	55673.181	135	2.0	1851.9±15.7	93.3±24.0	-0.40±0.06	0.07±0.30	12,3
09423511+5851043	NGC2950	262031	56238.459	135	1.0	1275.6±14.3	168.9±3.7	0.55±0.11	-	4,0
09425425+3150499	NGC2964	343049	56378.279	270	1.0	1283.6±14.7	82.3±14.4	-0.30±0.00	-0.24±0.02	183,18
09430865-1022596	NGC2979	162301	55946.353	205	1.0	2641.1±13.3	92.3±11.4	0.24±0.03	0.95±0.10	60,5
09431201+3155438	NGC2968	161346	55890.412	40	1.0	1524.9±42.1	221.5±65.8	-	-	0,1
09483604+3325173	NGC3003	340609	56285.319	79	1.0	1491.8±17.2	99.6±19.1	-0.56±0.00	-0.03±0.00	105,31
09505711+3333124	NGC3021	262186	56242.447	105	1.0	1603.1±18.1	68.3±31.3	-0.42±0.01	-0.27±0.11	68,6
09530714+1640396	NGC3041	163187	55976.197	100	1.0	1378.0±13.9	50.3±16.7	-0.12±0.00	0.44±0.00	14,1
09534088+0134467	NGC3044	342469	56360.309	304	1.0	1218.2±15.0	28.1±28.0	-0.49±0.01	0.01±0.02	178,60
09542701-0657122	IC0574	341578	56331.329	185	1.0	6047.1±15.1	354.6±10.3	-0.15±0.39	-	6,2
095444965-0916179	NGC3049	340610	56285.351	215	1.0	1344.8±27.3	97.3±41.4	0.18±0.01	-0.46±0.00	427,104
09551804+0416122	NGC3055	262215	56245.479	60	1.0	1779.7±13.3	32.7±18.3	-0.17±0.00	-0.03±0.01	477,98
09555243+6940469	NGC3034	144552	55673.121	360	1.0	179.9±15.1	93.1±12.5	-0.07±0.00	-0.37±0.01	1113,42
09562016+2713393	IC2520	162225	55943.492	185	1.0	1200.8±15.1	44.5±21.0	-0.41±0.01	0.06±0.03	117,26
09580691+1021353	NGC3070	262594	56256.426	215	1.0	5329.7±11.6	224.0±4.9	-0.11±0.41	-	1,0
09582105+3222119	NGC3067	163609	55984.385	285	1.0	1435.6±14.2	71.2±16.6	-0.43±0.00	-0.40±0.00	145,9
10015792+5540480	NGC3079	163698	55987.357	359	1.0	1107.7±14.6	160.6±10.8	0.37±0.03	0.65±0.18	54,3
10031907+6844022	NGC3077	161627	55916.452	425	1.0	-43.5±13.8	43.5±17.9	-0.63±0.00	0.03±0.00	232,133
10035880+2216334	UGC05420	051118	55327.166	243	2.0	6055.8±12.2	265.4±7.2	-	-	2,0
10035880+2216334	UGC05420	051119	55327.177	243	2.0	6057.8±13.6	266.5±7.0	0.67±0.30	-	3,0
10051397-0743068	NGC3115	250604	56012.187	90	1.0	637.5±12.9	286.2±2.4	-0.13±0.10	-0.25±0.16	4,3
10054161-0758532	PGC029300	340519	56282.450	225	1.0	680.6±14.1	43.2±21.2	-	-	0,0
10055999+5848443	UGC05435	351384	56430.135	400	1.0	2799.0±14.3	220.0±4.0	-	-	0,1
10133157+2244152	NGC3162	262116	56240.469	165	1.0	1250.6±11.9	41.3±18.4	-0.43±0.00	-0.40±0.00	91,10
10133829-0055319	UGC05515	142964	55619.247	110	2.0	12989.6±16.2	329.4±11.1	-	-	1,0
10134567+0325288	NGC3166	163603	55984.213	84	1.0	1302.0±14.1	147.3±4.1	0.44±0.02	-	31,1

Table continues on next page

2MASS ID	Name	Frame	MJD	PA	slit ('')	V_{hel} (km s^{-1})	σ_c (km s^{-1})	[NII]/H α	[OIII]/H β	AoN
10135049+3845536	NGC3158	140091	55533.408	183	2.0	6774.0±12.6	289.7±6.2	-0.06±0.19	-0.06±0.44	4,2
10141509+0327580	NGC3169	340522	56282.522	232	1.0	1212.9±12.2	163.6±4.9	0.24±0.02	0.75±0.12	44,3
10163416+2107223	NGC3177	342013	56342.197	125	1.0	1275.5±11.1	121.2±13.0	-0.20±0.00	-0.29±0.00	80,6
10165363+7324023	NGC3147	142491	55608.303	325	2.0	2780.2±13.5	233.1±8.0	0.42±0.03	0.87±0.09	40,3
10180564+2149549	NGC3190	140811	55549.368	118	2.0	1188.4±13.9	163.6±10.1	0.29±0.03	0.71±0.19	23,2
10182488+2153383	NGC3193	262140	56241.461	200	1.0	1342.7±12.7	208.1±3.5	-0.02±0.09	-	8,0
10203840+2530177	NGC3209	144235	55656.281	265	2.0	6122.2±14.0	308.9±8.2	0.05±0.40	-	4,1
10211787+2755484	IC2565	342012	56342.177	190	1.0	14589.6±16.3	249.3±7.8	-	-	0,1
10232701+1953543	NGC3226	262214	56245.459	205	1.0	1260.7±12.4	202.6±4.4	0.15±0.02	0.54±0.05	60,7
10233060+1951538	NGC3227	162548	55953.469	305	1.0	1107.7±15.8	141.8±11.0	-	-	AGN
10262836+2013417	IC0610	350990	56418.203	210	1.0	1127.8±16.3	81.3±27.8	-0.44±0.00	-0.49±0.00	44,2
10271019-0319082	PGC030732	142440	55606.352	115	2.0	8957.6±14.8	207.0±12.1	-	-	1,0
10271836+2830267	NGC3245	160964	55873.475	175	1.0	1276.0±14.0	205.7±4.2	0.01±0.05	0.37±0.21	30,3
10291992+2929291	NGC3254	351489	56433.169	243	1.0	1318.0±12.5	105.3±6.0	0.06±0.00	1.07±0.00	38,3
10301064-0309488	PGC030960	140207	55536.489	230	2.0	11166.7±12.9	330.2±6.8	0.38±0.12	0.56±0.27	8,2
10313885+2559023	UGC05713	341483	56329.226	185	1.0	6191.5±12.5	162.1±5.9	0.18±0.03	0.96±0.13	45,4
10323195+5424035	UGC05720	351023	56419.211	330	1.0	1357.2±18.6	20.1±28.5	-0.76±0.00	0.44±0.00	219,170
10323481+6502277	NGC3259	341684	56335.365	375	1.0	1644.0±14.3	40.8±18.5	0.01±0.04	1.05±0.18	39,3
10325545+2830422	NGC3277	062579	55504.481	20	2.0	1421.7±14.0	127.3±14.1	-0.02±0.02	0.59±0.07	43,6
10325545+2830422	NGC3277	062580	55504.492	20	2.0	1416.7±13.6	138.3±10.2	-0.00±0.02	0.60±0.06	44,6
10341978+1345165	UGC05739	262409	56251.463	150	1.0	2873.7±14.6	17.0±26.7	-0.32±0.01	-0.43±0.04	176,13
10344477-0158088	UGC05745	342033	56343.349	200	1.0	892.6±12.7	73.3±10.6	-0.19±0.00	-0.28±0.04	149,10
10361516-0820021	IC0624	142183	55598.349	220	2.0	4927.2±14.3	228.3±8.6	0.43±0.12	-	7,0
10361626+3719285	NGC3294	262187	56242.466	115	1.0	1522.0±13.6	79.0±14.1	-0.30±0.01	0.19±0.00	46,9
10362128+5837124	NGC3286	051086	55324.199	400	2.0	8004.2±12.5	271.1±7.4	0.22±0.51	0.61±0.42	1,1
10362128+5837124	NGC3286	051087	55324.210	400	2.0	8001.4±12.6	254.3±8.5	-	0.27±0.37	1,3
10362128+5837124	NGC3286	051385	55336.149	400	2.0	7975.5±14.2	246.1±7.5	-	-	0,1
10362128+5837124	NGC3286	051386	55336.166	400	2.0	7986.8±13.6	241.0±7.7	-	-	0,1
10362128+5837124	NGC3286	051387	55336.183	400	2.0	8005.6±13.4	265.8±6.9	-	-	0,0
10362128+5837124	NGC3286	051582	55347.135	400	2.0	8013.2±14.1	261.3±7.5	-	-	0,0
10362128+5837124	NGC3286	051583	55347.146	400	2.0	8024.6±13.3	260.7±8.0	-	-0.16±0.66	1,2
10384585+5330118	NGC3310	162582	55955.293	170	1.0	952.7±12.6	80.3±10.0	-0.26±0.00	0.51±0.01	226,20
10390953+4141127	NGC3319	250212	56000.125	85	1.0	699.7±20.2	39.6±27.1	-0.63±0.18	-	6,1
10390953+4141127	NGC3319	252271	56078.155	270	1.0	719.6±19.9	27.7±33.2	-0.48±0.21	-	5,0
10433114+2455199	NGC3344	163610	55984.402	330	1.0	529.6±13.9	53.1±12.8	-0.22±0.00	0.01±0.01	288,76
10435773+1142129	NGC3351	162304	55946.491	163	1.0	712.6±13.3	83.3±7.8	-0.43±0.00	-0.70±0.02	210,12
10461264+0148479	NGC3365	262798	56262.473	164	1.0	988.9±17.2	21.2±33.0	-0.55±0.01	0.08±0.06	45,11
10463496+1345026	NGC3367	262573	56255.461	70	1.0	2988.1±14.0	115.5±12.8	-0.04±0.00	-0.21±0.01	423,32
10464574+1149117	NGC3368	163119	55972.419	315	1.0	867.5±12.5	124.7±4.3	0.17±0.01	0.61±0.10	47,3
10470999+7250228	NGC3348	140795	55548.495	425	2.0	2736.9±12.6	253.6±6.4	0.18±0.11	-	10,0
10474048+3855533	UGC05893	140728	55546.381	85	2.0	10419.0±15.2	310.6±7.4	-	-	0,0
10474143+1104376	UGC05897	162716	55958.303	70	1.0	2653.6±18.7	45.2±30.0	-0.30±0.12	-	9,0
10474239+1359083	NGC3377	262694	56260.439	47	1.0	653.4±14.7	150.4±4.0	0.75±0.36	-	1,0
10474959+1234538	NGC3379	262660	56259.448	67	1.0	874.8±13.9	222.4±3.1	0.12±0.07	0.45±0.15	11,2
10495938+0021115	PGC032447	141321	55567.408	70	2.0	11045.0±20.7	122.1±33.3	0.46±0.37	-	6,0
10495938+0021115	PGC032447	141968	55590.435	250	2.0	11033.1±14.8	148.7±15.0	0.10±0.12	-	13,0
10505331+1324437	NGC3412	262661	56259.464	155	1.0	816.0±13.4	99.6±5.2	-	-	0,0
10511624+2758298	NGC3414	262188	56242.486	195	1.0	1435.3±15.2	239.1±4.7	0.17±0.03	0.62±0.09	30,4
10511799+4434185	UGC05953	160965	55873.493	80	1.0	3176.7±12.6	129.8±6.9	0.87±0.27	-	4,0
10521141+3257015	NGC3430	163188	55976.217	35	1.0	1547.7±13.7	70.0±12.9	-0.41±0.00	-0.49±0.00	82,6
10523113+3637076	NGC3432	252363	56081.151	213	1.0	440.6±70.7	51.1±46.2	-	-	AGN
10535485+7341253	NGC3403	351022	56419.126	435	1.0	1192.7±49.4	91.1±72.8	-0.35±0.00	-	12,0
10561600+4219591	PGC032873	161354	55892.451	40	2.0	7353.7±14.8	325.8±7.1	0.29±0.05	0.78±0.43	14,1
10561600+4219591	PGC032873	251790	56063.211	220	1.0	7366.6±13.0	348.5±5.3	0.20±0.06	0.16±0.20	22,3
10561600+4219591	PGC032873	262117	56240.485	40	1.0	7352.8±12.7	343.8±5.7	0.27±0.06	0.46±0.29	14,2
11000239+1450295	NGC3485	262595	56256.465	50	1.0	1393.2±11.5	52.9±16.5	-0.24±0.02	-0.15±0.07	71,10
11001858+1354045	NGC3489	342035	56343.420	250	1.0	656.1±12.4	105.2±5.6	0.33±0.02	-	22,0
11002394+2858293	NGC3486	250802	56017.318	225	1.0	640.2±13.1	56.5±11.3	0.10±0.02	0.91±0.06	48,6
11004538+1033117	IC0664	142182	55598.270	50	2.0	9960.2±15.3	304.3±7.3	-0.61±0.27	-0.47±0.64	3,2
11004795+1043417	UGC06093	341460	56328.446	205	1.0	10580.3±11.9	179.6±8.5	0.43±0.03	0.76±0.09	34,7
11031119+2758207	NGC3504	163611	55984.419	330	1.0	1458.9±13.0	109.7±6.2	0.19±0.00	-0.26±0.00	455,74
11032539+1808072	NGC3507	162227	55943.532	300	1.0	906.7±13.9	60.8±14.8	0.11±0.01	0.28±0.05	124,10
11042732+3812320	UGC06132	141415	55570.349	85	2.0	8788.7±26.3	162.8±55.0	-	-	AGN
11042732+3812320	UGC06132	141794	55584.299	95	2.0	-	-	-	-	AGN
11054859-0002092	NGC3521	162055	55937.380	211	1.0	752.6±14.3	122.0±4.8	0.55±0.05	-	5,0
11064749+7234066	NGC3516	340521	56282.490	367	1.0	2582.6±15.0	179.1±9.5	-	-	AGN
11143700+1249048	NGC3593	262615	56257.474	89	1.0	592.7±15.5	75.5±9.1	-0.21±0.01	0.27±0.03	108,16
11150623+1447136	NGC3596	144326	55659.108	65	1.0	1154.0±14.9	37.0±16.6	-0.32±0.00	-0.14±0.00	84,7
11155197+4135289	NGC3600	262516	56254.470	10	1.0	674.6±15.6	52.2±25.0	-0.87±0.01	0.44±0.02	43,56
11165465+1803065	NGC3607	262695	56260.455	125	1.0	916.3±13.6	226.3±3.7	0.38±0.05	0.78±0.27	16,2
11165896+1808547	NGC3608	262216	56245.498	80	1.0	1189.3±13.1	197.6±3.3	0.03±0.07	-	10,0
11183613+5759597	NGC3613	262738	56261.461	100	1.0	2006.5±13.6	214.2±3.6	-0.76±0.37	-	2,0
11185595+1305319	NGC3623	162723	55958.485	234	1.0	748.1±12.9	152.2±3.8	0.29±0.03	0.81±0.18	26,2
11201502+1259286	NGC3627	163427	55980.238	45	1.0	696.3±12.7	121.3±4.7	0.24±0.01	1.06±0.12	59,2
11201701+1335221	NGC3628	162965	55968.459	185	1.0	804.1±16.6	84.4±28.9	-0.14±0.09	-0.33±0.29	16,2
11205383+5656366	PGC034754	342958	56374.335	315	1.0	13757.0±15.8	373.3±8.3	-	-	0,1
11210685+0314051	NGC3640	340780	56293.415	100	1.0	1257.9±14.1	180.1±4.2	-	-	0,2

Table continues on next page

2MASS ID	Name	Frame	MJD	PA	slit ('')	V_{hel} (km s^{-1})	σ_c (km s^{-1})	[NII]/H α	[OIII]/H β	AoN
11211226-0259029	PGC034786	342034	56343.366	270	1.0	7283.3±12.6	140.5±12.6	-0.20±0.01	0.11±0.06	158,12
11212841+3432394	PGC094177	140494	55542.412	170	2.0	12180.0±15.9	297.3±10.9	-0.80±0.55	-	3,1
11221801+5904272	NGC3642	250705	56015.181	49	1.0	1536.8±14.7	84.9±10.5	-0.24±0.00	0.07±0.00	77,17
11233229-0839308	NGC3660	340587	56284.500	110	1.0	3603.5±12.5	94.6±9.7	-0.21±0.01	0.76±0.03	86,18
11244363+3845460	NGC3665	262737	56261.443	25	1.0	2030.9±15.6	224.0±5.0	-0.21±0.04	0.21±0.19	21,3
11260858+4335093	NGC3675	262797	56262.442	1	1.0	728.2±14.9	110.9±5.2	0.29±0.03	-	22,0
11262660+5702538	NGC3674	262638	56258.499	30	1.0	2015.3±13.7	213.3±6.2	-	-	2,0
11271117+1701491	NGC3684	250709	56015.353	295	1.0	1117.7±13.0	25.3±25.9	-0.41±0.00	-0.38±0.00	41,4
11273188+5652361	NGC3683	251033	56024.107	126	1.0	1658.8±22.1	79.0±25.9	-0.35±0.05	-	18,1
11284198+0432222	b22	162719	55958.413	150	2.0	37498.4±16.1	349.7±19.3	-	-	-
11284198+0432222	b22	162720	55958.425	150	2.0	37491.2±12.6	368.8±17.0	-	-	-
11284198+0432222	b22	162721	55958.436	150	2.0	37530.2±17.7	373.9±20.2	-	-	-
11284198+0432222	b22	250521	56010.419	150	1.0	37553.4±15.4	373.3±18.8	-	-	-
11300745+0916358	NGC3705	262518	56254.508	122	1.0	980.7±13.3	103.3±8.7	-0.04±0.03	0.47±0.19	41,3
11323494+5304041	NGC3718	163279	55977.237	45	1.0	951.5±14.0	176.9±6.2	-0.01±0.02	0.56±0.09	53,4
11335553+2338375	UGC06548	250151	55999.188	40	1.0	-	-	-	-	-
11344932+4904388	IC0712	142200	55598.481	280	2.0	9826.4±15.7	313.7±8.2	0.12±0.34	-0.08±0.43	4,2
11355732+7032081	NGC3735	142412	55605.357	355	2.0	2639.4±13.8	147.9±13.9	-0.07±0.01	1.01±0.03	106,13
11364797+5417372	NGC3756	163695	55987.222	1	1.0	1254.2±13.5	23.8±26.2	-0.35±0.05	-	21,0
11380904-0936257	NGC3789	162059	55937.478	175	1.0	5483.2±16.6	179.4±11.9	0.27±0.13	0.46±0.61	11,1
11400684+5836473	NGC3795	351548	56441.162	415	1.0	1176.8±19.1	60.0±39.8	-0.32±0.00	-0.01±0.00	10,3
11401689+1743404	NGC3801	250803	56017.347	300	1.0	3426.4±12.3	187.0±10.0	-0.02±0.06	0.54±0.20	28,3
11404166+2020348	NGC3805	163510	55982.442	245	2.0	6479.9±13.5	294.5±6.1	-0.11±0.04	0.15±0.15	29,4
11405873+1128160	NGC3810	161626	55916.432	215	1.0	950.5±13.0	68.9±8.2	-0.16±0.02	-0.03±0.18	42,3
11415735-0609203	NGC3818	143961	55648.271	105	2.0	1637.4±13.9	192.9±6.9	-	-	0,0
11421107+1016398	NGC3822	141628	55576.376	175	2.0	6047.8±15.6	126.3±17.1	0.04±0.02	0.85±0.06	51,4
11422942+1819580	UGC06670	163612	55984.436	170	1.0	878.6±18.5	48.3±29.7	-0.58±0.03	0.42±0.08	27,11
11440217+1956593	NGC3842	150532	55700.219	175	2.0	6173.1±20.0	295.2±9.3	-	-	0,2
11452766+2048257	PGC036650	144239	55656.342	245	2.0	6848.3±11.1	270.4±6.9	0.19±0.08	0.49±0.27	12,2
11453317+5858408	UGC06732	161514	55896.501	5	1.0	2356.9±12.8	94.2±7.5	0.34±0.03	-	33,0
11454556+1049286	NGC3869	161355	55892.496	136	2.0	2972.4±13.6	232.7±6.8	0.12±0.05	0.80±0.26	30,2
11454906+1346000	NGC3872	142835	55617.449	205	2.0	3078.2±14.7	336.7±5.6	-0.27±0.25	-0.42±0.30	3,3
11483820+4842388	NGC3893	262517	56254.490	-5	1.0	918.6±13.8	67.3±11.3	-0.40±0.01	-0.50±0.09	61,5
11484595+2938285	PGC036880	350403	56395.330	190	1.0	6739.2±14.0	143.0±13.8	0.07±0.03	0.50±0.16	61,5
11485036+5924561	NGC3894	141028	55558.428	20	2.0	3229.7±14.7	326.0±10.1	0.34±0.05	0.90±0.16	22,3
11491536+5605036	NGC3898	144558	55673.286	290	2.0	1142.7±13.9	213.6±7.2	0.15±0.02	0.66±0.05	27,4
11504150+2000544	NGC3919	151268	55724.168	330	2.0	6008.8±14.5	287.7±9.8	0.34±0.08	0.75±0.35	12,2
11504548+5149271	NGC3917	341355	56323.519	244	1.0	906.9±2.4	11.9±29.5	-0.02±0.23	-	5,0
11514768+4840593	NGC3928	342276	56353.442	361	1.0	933.8±13.1	55.2±12.3	-0.31±0.00	-0.06±0.01	210,49
11524264+2037527	NGC3937	151027	55714.194	215	2.0	6574.6±14.2	298.5±9.0	0.14±0.37	-	2,0
11525536+3659109	NGC3941	262637	56258.482	10	1.0	887.2±14.3	132.9±4.2	0.19±0.03	0.89±0.14	21,2
11534174+4751316	NGC3949	351491	56433.225	305	1.0	766.7±13.3	60.0±15.3	-0.28±0.01	-0.14±0.00	30,5
11534902+5219355	NGC3953	162545	55953.325	100	1.0	1014.5±12.4	123.9±5.1	0.20±0.04	1.00±0.33	31,1
11541224+0008116	IC0745	351805	56449.136	185	1.0	1092.3±14.2	25.1±25.7	-0.56±0.00	0.10±0.00	156,62
11554511+5519144	NGC3972	163566	55983.258	115	1.0	726.5±25.9	57.0±35.7	-0.54±0.04	-	27,1
11555729+0644580	NGC3976	163406	55979.437	235	1.0	2454.8±11.8	172.0±4.0	0.40±0.04	1.42±0.40	25,1
11562816+5507313	NGC3982	163407	55979.458	375	1.0	1077.3±12.4	62.9±9.0	0.01±0.00	1.33±0.01	191,20
11573359+5527318	NGC3990	142770	55616.466	220	2.0	668.0±13.6	122.9±12.7	-	-	1,0
11573559+5527318	NGC3990	163696	55987.239	10	1.0	651.2±13.2	117.5±5.2	-	-	1,0
11573559+5527318	NGC3990	251059	56028.305	220	1.0	653.4±13.2	118.4±5.3	-	-	2,0
11573598+5322282	NGC3992	250603	56012.167	128	1.0	989.3±14.3	137.6±5.0	0.16±0.03	0.80±0.14	27,2
11573685+3216400	NGC3994	151530	55735.153	190	2.0	3062.5±13.5	148.0±9.2	-0.04±0.00	0.27±0.02	137,17
11575616+5527128	NGC3998	343093	56380.340	310	1.0	1006.9±15.3	322.6±3.4	0.10±0.00	0.17±0.01	113,19
11575902+2307300	NGC4003	150215	55689.275	325	2.0	6363.8±14.8	157.5±11.9	-0.05±0.01	0.19±0.08	91,9
11592518+5057420	NGC4026	342923	56373.388	343	1.0	918.0±13.9	186.7±3.5	-0.11±0.16	-	4,0
12002364+0105598	NGC4030	163568	55983.308	220	2.0	1411.2±13.0	121.1±12.7	-0.20±0.02	0.15±0.11	38,4
12021217+6208142	NGC4041	162724	55958.503	250	1.0	1179.9±12.3	93.1±8.9	-0.22±0.01	-0.05±0.04	129,14
12030968+4431525	NGC4051	350068	56388.357	323	1.0	663.6±12.5	83.0±13.4	-	-	AGN
12031320+0157029	ARK344	144329	55659.193	210	2.0	5602.1±11.7	253.8±6.2	-0.33±0.28	-	3,1
12040140+2013559	NGC4055	141417	55570.386	170	2.0	7211.6±14.4	263.1±8.3	-0.03±0.06	-0.01±0.21	18,4
12040383+3153449	NGC4062	162717	55958.321	120	1.0	729.4±15.8	42.9±21.5	-0.29±0.05	-0.02±0.34	23,3
12042705+0153456	NGC4073	341654	56333.454	260	1.0	5838.5±13.3	288.6±6.9	0.23±0.68	-	3,0
12042964+2018581	NGC4074	162963	55968.302	100	1.0	6672.1±14.5	160.3±10.2	0.02±0.00	1.08±0.01	147,21
12044762+1035439	NGC4078	163191	55976.295	195	1.0	2496.9±12.4	179.8±4.1	0.42±0.27	-	5,0
12051554+4310079	PGC038276	151231	55723.190	215	2.0	15430.3±15.5	354.1±9.0	-	-	0,1
12053418+5032205	NGC4088	342269	56353.230	20	1.0	759.4±13.5	72.9±14.1	-0.42±0.02	-0.36±0.08	56,7
12060116+4728420	NGC4096	262616	56257.491	76	1.0	517.6±12.4	70.7±12.8	-0.45±0.02	-0.54±0.12	50,4
12060860+4934563	NGC4100	351808	56449.198	325	1.0	1041.0±15.0	99.5±10.6	-0.45±0.00	-0.60±0.00	195,12
12062311+5242394	NGC4102	144667	55676.110	38	2.0	841.9±13.3	151.4±11.8	-0.09±0.00	-0.13±0.02	412,22
12070312+4303554	NGC4111	262739	56261.479	160	1.0	739.3±14.9	150.1±3.8	0.37±0.02	-	29,0
12080557+2514141	UGC07115	350688	56408.299	215	1.0	6668.3±13.0	238.3±8.9	0.30±0.12	-	8,1
12080601+6510268	NGC4125	140796	55548.526	82	2.0	1253.8±13.8	224.5±7.8	0.25±0.01	0.52±0.07	33,3
12080601+6510268	NGC4125	141796	55584.424	82	2.0	1281.1±13.8	225.1±7.2	0.30±0.02	0.45±0.07	29,4
12080601+6510268	NGC4125	142590	55611.417	262	2.0	1279.9±14.3	220.7±8.8	0.29±0.02	0.42±0.07	33,5
12083235+6846034	NGC4128	144504	55670.232	425	2.0	2231.2±15.2	234.2±6.8	0.09±0.09	0.63±0.18	9,2
12091770+2955393	NGC4136	252844	56101.148	210	1.0	573.2±14.9	34.8±19.2	-0.43±0.01	0.10±0.04	70,23
12092978+4341071	NGC4138	341459	56328.286	150	1.0	833.3±13.7	120.9±5.1	0.14±0.01	0.93±0.04	51,6

Table continues on next page

2MASS ID	Name	Frame	MJD	PA	slit ('')	V_{hel} (km s^{-1})	σ_c (km s^{-1})	[NII]/H α	[OIII]/H β	AoN
12093608+4232031	NGC4143	262696	56260.473	145	1.0	904.8±15.7	223.7±3.7	0.25±0.02	0.61±0.06	28,6
12095860+4627258	NGC4144	252403	56084.212	284	1.0	-	-	-	-	-
12095860+4627258	NGC4144	262697	56260.488	70	1.0	163.0±0.0	10.3±27.9	-0.87±0.15	0.63±0.38	2,2
12103265+3924207	NGC4151	162510	55951.332	130	1.0	949.5±13.0	111.8±8.0	-	-	AGN
12103285+5818137	NGC4149	250706	56015.198	85	1.0	3017.7±15.9	141.2±13.7	-0.11±0.06	-	25,0
12104427+3820103	PGC038759	163281	55977.269	10	1.0	6812.1±17.8	106.0±18.4	-	-	AGN
12110436+5029048	NGC4157	252364	56081.197	243	1.0	715.8±28.2	85.7±41.8	-0.40±0.13	0.41±0.75	5,2
12150502+3311500	NGC4203	140731	55546.449	50	2.0	1031.3±13.7	166.0±8.6	0.14±0.01	0.72±0.03	45,6
12150502+3311500	NGC4203	141352	55569.392	5	2.0	1044.1±13.8	175.3±8.3	0.07±0.01	0.66±0.04	43,6
12150502+3311500	NGC4203	250710	56015.379	225	1.0	1049.6±14.0	176.8±3.3	0.05±0.01	0.66±0.03	47,5
12150502+3311500	NGC4203	250905	56019.371	181	1.0	1051.1±13.9	168.8±3.8	0.07±0.02	0.68±0.05	49,5
12150502+3311500	NGC4203	251351	56037.102	25	1.0	1059.4±14.6	169.1±3.7	0.07±0.02	0.64±0.05	44,5
12153917+3619368	NGC4214	340585	56284.420	128	1.0	229.6±36.6	40.2±103.5	-	-	AGN
12153917+3619368	NGC4214	340586	56284.433	128	1.0	-	-	-	-	AGN
12153937+1354053	NGC4212	250015	55989.432	255	1.0	-131.6±14.1	51.7±15.8	-0.38±0.01	-0.55±0.04	200,10
12155089+4705304	NGC4217	252906	56103.157	247	1.0	994.9±14.6	117.3±17.2	-0.26±0.01	0.06±0.00	28,4
12155444+1308578	NGC4216	140732	55546.466	125	2.0	115.5±13.6	190.3±6.9	0.35±0.03	0.72±0.10	17,2
12155451+0624040	NGC4215	342956	56374.213	175	1.0	1973.2±13.3	140.4±4.5	-	-	1,0
12162252+1318254	NGC4222	163282	55977.287	60	1.0	196.0±23.1	59.6±37.3	-0.59±0.02	-0.06±0.07	38,12
12172630+7048094	NGC4250	141322	55567.480	355	2.0	1997.6±13.1	132.1±13.3	0.18±0.02	0.98±0.07	64,7
12173678+2936288	NGC4245	150859	55708.226	315	1.0	834.6±12.5	91.8±6.9	-0.12±0.04	0.40±0.19	19,3
12174990+4724329	NGC4248	351845	56450.200	285	1.0	445.9±20.7	48.3±33.7	-0.41±0.14	-	6,1
12182648+2948461	NGC4253	251054	56024.368	290	1.0	3619.5±35.8	101.9±41.4	-	-	AGN
12184303+6553530	NGC4256	162722	55958.469	402	1.0	2489.3±13.2	181.4±6.8	0.35±0.11	-	12,0
12184303+6553530	NGC4256	250801	56017.292	400	1.0	2471.8±14.6	196.6±5.2	0.42±0.08	-	13,0
12184962+1424593	NGC4254	251062	56028.334	203	1.0	2360.5±13.1	70.1±10.2	-0.21±0.01	0.59±0.04	81,9
12185618+0447093	NGC4255	341274	56317.380	140	1.0	1939.5±15.1	177.7±14.1	-0.14±0.25	-	4,0
12185761+4718133	NGC4258	161983	55933.406	76	1.0	416.0±14.7	119.2±5.8	-0.15±0.01	0.81±0.04	64,7
12192224+0605556	NGC4260	341526	56330.336	225	1.0	1734.9±12.3	148.3±5.1	0.53±0.09	-	11,0
12192326+0549289	NGC4261	351779	56448.173	173	1.0	2177.0±13.0	314.0±4.1	0.42±0.02	0.63±0.11	28,2
12195066+2936529	NGC4274	350329	56394.127	160	1.0	841.2±13.1	97.2±6.6	-0.05±0.01	0.22±0.10	56,4
12200679+2916502	NGC4278	262799	56262.492	35	1.0	592.9±14.4	262.2±4.5	0.11±0.01	0.40±0.02	93,11
12204209+2920454	NGC4286	262617	56257.507	115	1.0	623.9±17.5	48.7±29.5	-0.07±0.06	-	20,1
12211289+1822566	NGC4293	144601	55674.114	77	1.0	895.6±14.7	106.0±9.3	0.23±0.02	0.92±0.22	63,2
12213279+1436217	NGC4298	144531	55671.122	123	1.0	1093.9±16.0	74.2±16.6	-0.46±0.00	-0.46±0.03	162,15
12213279+1436217	NGC4298	144532	55671.134	123	1.0	1090.8±14.5	29.2±27.5	-0.46±0.00	-0.49±0.00	161,14
12221234+0708398	NGC4309	144533	55671.151	70	1.0	1015.2±15.7	35.7±19.9	-0.15±0.00	0.15±0.00	38,5
12221234+0708398	NGC4309	144534	55671.162	70	1.0	1001.9±20.5	32.7±32.3	-0.19±0.08	0.42±0.77	15,2
12223135+1532165	NGC4312	342466	56360.240	173	1.0	124.6±13.8	73.4±17.2	-0.47±0.02	-0.38±0.15	49,4
12230190+5826409	NGC4335	142836	55617.467	325	2.0	4530.5±13.4	293.5±6.9	0.47±0.05	0.93±0.33	16,2
12232410+0240449	MRK0050	342468	56360.276	175	1.0	6987.8±23.1	117.8±25.6	-	-	AGN
12233902+0703141	NGC4342	350231	56391.326	165	1.0	734.1±12.7	274.1±2.7	-0.14±0.41	-	2,0
12235781+1641360	NGC4350	350597	56403.126	210	1.0	1060.9±13.7	130.0±6.7	-	-	0,2
12245493+0726404	NGC4370	351807	56449.179	260	1.0	761.6±14.9	104.8±16.2	0.11±0.13	-	16,1
12253509+4541048	NGC4389	351259	56426.274	280	1.0	684.7±16.3	18.0±28.2	-0.54±0.00	-0.65±0.03	164,15
12254682+1239434	NGC4388	163613	55984.454	269	1.0	2464.1±14.7	105.7±9.8	-0.19±0.00	1.20±0.01	274,45
12255562+1812501	NGC4394	342277	56353.461	325	1.0	868.6±13.3	77.6±7.8	0.24±0.03	1.10±0.25	23,1
12261279-0741059	NGC4403	142442	55606.393	210	2.0	5151.6±13.9	185.5±10.8	0.24±0.11	0.64±0.34	14,3
12262708+3113247	NGC4414	252272	56078.224	340	1.0	660.6±14.7	115.6±5.1	0.44±0.04	-	12,0
12265643+1502507	NGC4419	163567	55983.275	130	1.0	-238.7±14.0	118.9±5.2	0.07±0.01	0.44±0.07	107,5
12272040+6448056	NGC4441	341353	56323.396	-10	1.0	2665.8±16.8	87.7±23.0	-0.33±0.01	-0.05±0.03	203,29
12281111+4405368	NGC4449	252236	56077.238	230	1.0	145.0±16.4	17.4±26.9	-0.87±0.00	0.61±0.00	60,60
12281542+2837130	NGC4448	144425	55660.368	272	1.0	616.6±14.6	96.4±7.9	-0.31±0.00	-0.37±0.05	120,8
12282963+1705058	NGC4450	163429	55980.284	188	1.0	1911.7±13.0	118.2±4.7	0.20±0.02	0.62±0.07	34,4
12284555+4451512	NGC4460	250804	56017.382	220	1.0	441.6±15.1	17.3±26.4	-0.60±0.01	0.26±0.02	80,41
12290002+1358428	NGC4459	350804	56411.309	285	1.0	1139.2±14.5	174.1±5.8	0.15±0.07	-	16,0
12292799+0845006	NGC4469	341083	56312.386	85	1.0	562.5±13.5	97.5±7.9	-0.21±0.02	0.53±0.17	42,3
12294887+1325455	NGC4473	342993	56376.208	95	1.0	2204.3±14.1	185.9±4.0	-	-	1,0
12303198+1229248	NGC4486B	151588	55736.137	200	1.0	1519.9±13.0	185.8±3.6	-0.21±0.28	-	2,0
12303636+4138370	NGC4490	252845	56101.165	255	1.0	539.3±14.6	49.8±19.7	-0.55±0.03	0.67±0.10	22,7
12305772+1216132	NGC4486A	151589	55736.154	185	1.0	673.4±13.8	82.4±16.9	-0.33±0.16	-	5,0
12315921+1425134	NGC4501	162056	55937.403	210	1.0	2233.7±14.5	146.5±5.4	0.36±0.01	0.78±0.05	61,7
12321745-0733483	NGC4504	163203	55976.397	145	1.0	975.1±16.1	31.5±27.2	-0.24±0.05	0.00±0.37	24,3
12340849+0239137	NGC4527	144502	55670.175	145	2.0	1650.5±14.1	132.5±14.6	-0.16±0.01	0.09±0.06	70,8
12342712+0211163	NGC4536	250167	55999.398	275	1.0	1742.3±14.7	97.3±7.9	-0.30±0.00	-0.28±0.00	298,23
12352642+1429467	NGC4548	162966	55968.517	300	1.0	425.3±14.1	104.4±5.9	0.34±0.03	0.63±0.12	28,3
12353249+7340294	UGC07767	341354	56323.445	420	1.0	1281.1±15.5	79.4±10.3	-	-	0,0
12354118+2631227	NGC4555	140092	55533.493	120	2.0	6560.9±14.7	318.9±5.4	0.06±0.48	-	2,1
12362080+2559146	NGC4565	252365	56081.217	337	1.0	1179.5±15.2	166.4±4.8	0.18±0.02	0.73±0.07	33,4
12362699+1126215	NGC4564	342467	56360.257	230	1.0	1105.9±13.6	174.0±3.4	-0.34±0.28	-	2,0
12363035+2612009	IC3582	162762	55959.340	40	2.0	6998.0±14.4	126.6±16.5	0.49±0.02	-	39,0
12364981+1309463	NGC4569	250879	56019.190	135	1.0	-255.7±14.0	117.6±4.2	0.01±0.00	0.42±0.03	159,9
12374359+1149051	NGC4579	162057	55937.427	75	1.0	1476.9±15.2	161.5±4.6	0.27±0.01	0.56±0.03	84,9
12382843+0419087	NGC4586	144338	55659.347	295	1.0	745.8±14.9	62.0±13.4	-0.01±0.02	0.97±0.10	68,5
12395938+6136330	NGC4605	252517	56088.160	300	1.0	110.5±16.5	24.5±26.3	-0.59±0.02	0.20±0.05	40,17
12413284+4109027	NGC4618	252237	56077.255	245	1.0	-	-	-	-	-
12415270+4116253	NGC4625	262639	56258.516	27	1.0	570.9±17.2	44.9±27.9	-0.27±0.03	-0.15±0.17	26,5

Table continues on next page

2MASS ID	Name	Frame	MJD	PA	slit ('')	V_{hel} (km s^{-1})	σ_c (km s^{-1})	[NII]/H α	[OIII]/H β	AoN
12424098+1417451	NGC4634	163703	55987.485	156	1.0	79.7±19.7	38.1±29.1	-0.41±0.02	-0.09±0.22	60,4
12425218+5451215	NGC4646	142887	55618.275	20	2.0	4514.1±14.0	268.0±6.6	0.23±0.09	1.26±0.90	10,1
12434000+1133093	NGC4649	150889	55709.225	288	2.0	1070.1±12.4	364.5±4.0	-0.03±0.14	-	4,1
12442937+1329552	NGC4659	342924	56373.405	170	1.0	401.4±16.3	39.2±24.7	-	-	0,0
12450867-0027428	NGC4666	142248	55600.380	151	2.0	1465.7±12.7	110.2±16.4	-0.22±0.01	0.19±0.04	82,12
12451714+2707317	NGC4670	351780	56448.228	260	1.0	1028.1±15.2	34.6±22.5	-1.10±0.00	0.75±0.00	54,73
12453470+2703386	NGC4673	252328	56080.229	170	1.0	6721.4±12.6	216.2±5.0	0.28±0.12	-	7,0
12463982+5432030	NGC4686	142965	55619.265	5	2.0	4902.7±13.8	276.2±5.9	0.49±0.03	1.25±0.24	23,2
12471526+1012124	IC3773	341961	56341.320	200	1.0	1054.4±13.7	37.1±17.4	-	-	0,0
12482293+0829140	NGC4698	250108	55998.270	170	1.0	963.6±14.1	128.9±5.2	0.12±0.02	0.94±0.06	51,5
12490218-0839514	NGC4699	150361	55694.176	215	2.0	1319.8±15.0	153.4±11.8	-	-	0,0
12495381-0643027	IC3812	150579	55701.165	185	2.0	3357.5±12.1	115.8±14.7	-0.29±0.01	-0.11±0.09	46,6
12505314+4107125	NGC4736	162718	55958.337	85	1.0	265.4±14.1	120.8±4.4	0.49±0.02	-	17,0
12514803-1027172	NGC4742	162060	55937.505	260	1.0	1243.4±17.3	98.1±7.3	0.47±0.18	-	2,0
12530567-0912141	NGC4761	341962	56341.412	230	1.0	4214.2±13.4	251.7±5.4	0.31±0.11	0.56±0.37	14,2
12543242-0651339	NGC4786	142443	55606.431	160	2.0	4526.3±14.4	305.1±7.3	0.11±0.12	-	10,1
12543777+4631521	NGC4800	251359	56037.343	380	1.0	836.4±12.3	101.7±6.0	-0.24±0.02	-0.03±0.09	50,5
12561432+5652244	UGC08058	144501	55670.149	25	2.0	13682.6±97.4	299.8±113.6	-	-	AGN
12564369+2140575	NGC4826	350689	56408.330	200	1.0	378.3±13.9	90.9±6.0	0.13±0.01	0.33±0.04	69,6
12592713+1410157	NGC4866	141418	55570.422	45	2.0	1926.7±14.2	205.1±6.9	0.27±0.06	0.51±0.14	16,3
12593570+2757338	NGC4874	144340	55659.400	235	2.0	7067.0±14.2	266.2±8.3	-	-0.46±0.59	1,1
13000809+2758372	NGC4884	144426	55660.392	200	2.0	6396.3±14.6	386.2±8.9	-	-	0,2
13004296+3718552	NGC4914	252366	56081.235	335	1.0	4583.0±15.3	233.3±4.5	-	-	0,1
13045839+2907204	NGC4952	150174	55688.329	205	2.0	5838.1±15.0	296.8±6.4	0.26±0.20	-	4,0
13054887-0801129	NGC4958	163509	55982.402	195	1.0	1429.2±13.1	156.4±3.7	0.19±0.02	0.76±0.11	29,2
13084873-0646392	NGC4981	162226	55943.512	145	1.0	1643.5±11.2	104.4±5.9	-0.25±0.00	-0.11±0.00	88,9
13092704-0718450	PGC1021091	162767	55959.468	130	2.0	6561.5±13.6	249.6±6.7	0.24±0.09	0.86±0.39	13,2
13092704-0718450	PGC1021091	251847	56064.176	130	1.0	6530.0±12.4	258.4±4.6	0.27±0.08	0.77±0.32	14,2
13105631+3703321	NGC5005	140208	55536.510	157	2.0	928.1±14.5	213.9±6.6	0.35±0.01	0.43±0.04	94,7
13212311+0020333	NGC5104	142142	55597.418	165	2.0	5497.1±15.5	157.5±15.9	-0.11±0.01	0.12±0.08	103,9
13234497+3133568	NGC5127	351029	56419.327	260	1.0	4801.6±11.8	194.1±5.3	0.64±0.11	-	7,0
13245144+3622424	NGC5141	252908	56103.203	255	1.0	5197.5±13.2	247.8±4.8	0.39±0.06	0.92±0.27	17,2
13245289-0404550	NGC5133	163571	55983.423	210	2.0	6139.1±13.4	316.8±7.2	0.38±0.05	0.85±0.27	17,2
13245289-0404550	NGC5133	350402	56395.281	210	1.0	6152.1±11.1	338.3±8.1	0.24±0.08	0.47±0.22	17,3
13315259+2000042	UGC08516	351710	56447.242	225	1.0	982.7±15.6	46.1±26.7	-0.64±0.00	-0.08±0.00	68,34
13322790+0718599	NGC5208	143875	55646.266	165	2.0	6688.3±14.7	267.2±6.0	0.12±0.04	0.44±0.34	21,2
13343506+3446405	NGC5228	140733	55546.484	15	2.0	7583.7±12.6	221.0±7.3	0.16±0.07	-	13,0
13360823-0829519	NGC5232	143843	55644.324	250	2.0	6755.2±15.0	265.0±6.9	0.44±0.03	0.92±0.19	30,2
13362618+0722109	NGC5239	151531	55735.181	150	1.0	6931.0±12.1	96.0±10.2	-	-	1,2
13373206+0853062	NGC5248	341275	56317.413	95	1.0	1109.4±15.4	71.1±13.3	-0.23±0.02	-0.14±0.10	45,5
13381586+0432330	NGC5252	162461	55950.445	195	1.0	6788.9±14.3	235.9±6.8	-0.09±0.00	0.74±0.01	73,21
13410573+6740197	NGC5283	350654	56407.247	460	1.0	3041.4±14.6	124.6±5.2	-0.03±0.00	1.02±0.01	205,40
13412423+5538347	UGC08671	144441	55665.200	90	2.0	7424.2±16.2	182.0±11.3	-0.03±0.33	-	4,2
13412423+5538347	UGC08671	144442	55665.213	90	2.0	7442.6±15.9	186.4±14.6	-0.42±0.36	-0.66±0.60	2,1
13444207+20553131	UGC08696	252691	56096.208	355	1.0	10952.9±27.3	208.6±30.8	-	-	AGN
13451913+4142444	NGC5290	140319	55538.524	85	2.0	2539.4±15.8	118.2±18.6	-0.06±0.02	0.64±0.10	59,6
13461863+4351046	NGC5296	143490	55632.260	130	2.0	2236.4±21.3	92.9±43.4	-0.51±0.03	-0.17±0.04	51,22
13470039+6058229	NGC5308	340782	56293.510	60	1.0	1821.2±15.0	133.1±9.5	-	-	0,0
13522671+1405281	IC0948	250169	55999.487	155	1.0	6799.1±15.6	322.6±5.6	0.51±0.26	0.39±0.54	4,2
13523859+4620591	PGC049293	342957	56374.250	35	1.0	18106.4±16.3	389.0±13.4	-	-	0,1
13531785+3329267	NGC5347	350903	56416.131	100	1.0	2345.5±13.6	78.4±13.8	-0.10±0.01	1.13±0.02	82,12
13532674+4016592	NGC5353	051436	55337.314	308	2.0	2180.5±14.3	300.1±5.0	0.22±0.03	0.45±0.10	22,3
13532674+4016592	NGC5353	051437	55337.326	308	2.0	2168.5±14.5	294.2±5.0	0.24±0.03	0.38±0.10	19,3
13532674+4016592	NGC5353	051806	55356.247	308	2.0	2148.4±13.5	301.3±4.7	0.21±0.03	0.29±0.10	20,4
13532674+4016592	NGC5353	051807	55356.261	308	2.0	2139.2±14.6	300.7±5.5	0.20±0.02	0.27±0.08	25,4
13532674+4016592	NGC5353	051981	55363.226	308	2.0	2142.0±14.6	294.1±5.6	0.17±0.03	0.26±0.08	24,4
13532674+4016592	NGC5353	051982	55363.242	308	2.0	2138.4±13.7	303.3±5.5	0.22±0.03	0.38±0.09	22,3
13532674+4016592	NGC5353	051983	55363.258	308	2.0	2146.2±13.7	300.7±5.7	0.21±0.06	0.25±0.15	14,3
13560288+1822188	UGC08850	150201	55689.131	200	2.0	14761.7±33.6	265.2±60.5	-	-	AGN
13560636+5944311	NGC5389	351810	56449.243	361	1.0	1804.5±13.2	135.3±5.2	0.12±0.05	-	19,1
13560724+0515169	NGC5363	150890	55709.253	310	2.0	1000.7±13.3	225.8±5.9	0.00±0.01	0.20±0.03	109,14
13561200+0500520	NGC5364	340805	56294.510	102	1.0	-	-	-	-	-
13561200+0500520	NGC5364	340806	56294.514	90	1.0	1213.4±16.3	86.2±18.8	-0.21±0.03	-	9,1
13580605+2140206	PGC097421	162058	55937.452	113	2.0	19251.4±18.8	317.1±16.9	-	-	1,1
13581486+0615318	NGC5382	163570	55983.367	195	1.0	4270.7±12.6	241.3±3.4	-0.03±0.24	0.93±0.50	5,1
14003719-0251281	NGC5400	142199	55984.463	85	2.0	7329.3±13.8	257.2±6.7	0.29±0.04	0.73±0.21	18,2
14014186-1136251	PGC049940	342922	56373.370	225	1.0	11082.6±21.5	245.1±16.6	0.41±0.21	0.15±0.40	8,3
14061051+0921122	NGC5463	144243	55656.412	230	2.0	7089.9±14.3	202.6±7.9	0.54±0.11	-	7,1
14062152+5043299	NGC5480	141546	55574.449	1	2.0	1845.8±14.6	61.7±27.1	-0.42±0.00	-0.52±0.02	171,14
14063199+0601458	NGC5470	350531	56402.362	250	1.0	985.1±33.0	26.7±35.5	-0.42±0.08	-0.26±0.71	13,2
14095733+1732435	NGC5490	143117	55623.340	184	2.0	4837.7±14.4	353.1±6.3	0.13±0.10	-	10,0
14100154+5452547	PGC050564	162303	55946.433	110	2.0	12316.3±14.2	362.9±8.2	-0.29±0.35	-0.02±0.50	7,2
14113785-0109313	NGC5496	351809	56449.216	168	1.0	1475.9±19.1	84.3±34.7	-0.51±0.04	0.14±0.14	24,8
14131490-0312272	NGC5506	350529	56402.268	90	1.0	1750.4±16.7	131.0±18.4	-	-	AGN
14145230+2519034	NGC5523	351712	56447.280	260	1.0	975.6±11.8	36.3±20.3	-0.41±0.00	-0.37±0.00	37,6
14165292+1048264	NGC5532	162547	55953.443	150	2.0	7287.8±15.2	342.7±6.1	0.53±0.05	-	14,0
14182570+3629372	NGC5557	260041	56145.127	270	1.0	3189.4±12.9	289.2±2.9	-1.28±0.27	-1.32±0.11	1,3

Table continues on next page

2MASS ID	Name	Frame	MJD	PA	slit ('')	V_{hel} (km s^{-1})	σ_c (km s^{-1})	[NII]/H α	[OIII]/H β	AoN
14194820+5643445	NGC5585	250880	56019.263	1	1.0	226.1 \pm 29.4	183.5 \pm 35.3	-0.81 \pm 0.02	0.53 \pm 0.04	24,18
14201994+0356009	NGC5566	141712	55580.486	107	2.0	1465.5 \pm 13.7	103.7 \pm 18.0	0.30 \pm 0.04	-	11,0
14202592-0920019	PGC992360	350459	56397.317	190	1.0	13034.1 \pm 15.5	384.6 \pm 11.0	0.26 \pm 0.52	-0.18 \pm 0.35	6,2
14205100+0419547	PGC051260	163508	55982.383	120	2.0	7974.0 \pm 12.5	196.5 \pm 7.7	-	-	0,4
14210369+0316157	NGC5576	152028	55753.138	275	1.0	1460.2 \pm 14.6	193.3 \pm 3.5	-	-	0,0
14211311+0326087	NGC5577	342470	56360.340	240	1.0	1462.6 \pm 13.8	58.7 \pm 20.5	-0.36 \pm 0.00	-0.49 \pm 0.00	33,4
14240759+3451320	NGC5614	141967	55590.415	185	2.0	3808.6 \pm 12.4	211.7 \pm 7.3	0.44 \pm 0.03	0.97 \pm 0.21	24,2
14281635+2550557	NGC5629	162964	55968.386	110	2.0	4442.6 \pm 14.8	256.6 \pm 7.6	-0.37 \pm 0.56	-0.67 \pm 0.36	2,2
14283173+2724326	NGC5635	340588	56284.519	65	1.0	4222.6 \pm 13.9	232.2 \pm 11.5	0.18 \pm 0.05	1.05 \pm 0.48	20,1
14294980+4937214	NGC5660	163196	55976.364	30	1.0	2282.1 \pm 13.0	36.8 \pm 18.1	-0.36 \pm 0.01	-0.44 \pm 0.07	102,7
14310477+2817143	MRK0684	341124	56315.446	145	1.0	13481.8 \pm 26.7	179.4 \pm 33.1	-	-	AGN
14352967+4844293	NGC5689	253401	56131.181	270	1.0	2165.3 \pm 13.6	161.9 \pm 4.8	0.22 \pm 0.08	-	11,0
14372214+3634040	NGC5695	340909	56305.466	140	1.0	4182.4 \pm 11.1	137.5 \pm 5.8	0.15 \pm 0.01	1.33 \pm 0.06	78,7
14401152-0017211	NGC5713	342994	56376.330	160	1.0	1846.2 \pm 14.5	101.4 \pm 18.8	-0.33 \pm 0.01	-0.00 \pm 0.02	184,45
14422885+4150321	NGC5739	050572	55309.435	214	2.0	5411.4 \pm 13.3	307.3 \pm 5.7	0.31 \pm 0.02	0.55 \pm 0.09	47,6
14422885+4150321	NGC5739	050573	55309.446	214	2.0	5415.2 \pm 13.5	317.9 \pm 6.4	0.31 \pm 0.03	0.56 \pm 0.10	42,4
14422885+4150321	NGC5739	050941	55322.157	34	2.0	5407.4 \pm 15.0	317.7 \pm 6.9	0.28 \pm 0.02	0.43 \pm 0.05	49,9
14422885+4150321	NGC5739	050942	55322.170	34	2.0	5418.9 \pm 12.5	326.2 \pm 5.8	0.26 \pm 0.02	0.39 \pm 0.05	53,9
14422885+4150321	NGC5739	051316	55333.119	34	2.0	5392.0 \pm 13.8	317.9 \pm 5.8	0.28 \pm 0.02	0.41 \pm 0.05	43,8
14422885+4150321	NGC5739	051317	55333.130	34	2.0	5394.3 \pm 14.0	317.7 \pm 6.0	0.24 \pm 0.02	0.37 \pm 0.04	50,9
14445600+0157170	NGC5746	341203	56316.492	195	1.0	1665.5 \pm 13.5	190.0 \pm 6.3	0.12 \pm 0.06	0.38 \pm 0.25	25,2
14454510+5134509	PGC052708	163569	55983.337	70	2.0	8778.7 \pm 14.0	204.9 \pm 11.4	-0.03 \pm 0.01	0.13 \pm 0.09	150,9
14461110-0013229	NGC5750	351847	56450.239	255	1.0	1623.7 \pm 14.4	106.0 \pm 6.3	0.14 \pm 0.03	1.18 \pm 0.37	36,1
14505151+0506522	NGC5765B	253124	56116.168	174	1.0	8127.8 \pm 10.8	133.1 \pm 12.4	-0.19 \pm 0.00	0.84 \pm 0.00	313,74
14505151+0506522	NGC5765B	253158	56121.149	170	1.0	8127.8 \pm 12.8	129.2 \pm 13.5	-0.18 \pm 0.00	0.85 \pm 0.00	341,63
14535765+0332401	NGC5775	144244	55656.429	216	2.0	1628.0 \pm 14.0	105.7 \pm 19.6	-0.24 \pm 0.03	0.09 \pm 0.13	40,5
14555524+1151407	UGC09602	142198	55598.439	127	2.0	9306.3 \pm 13.4	286.7 \pm 7.4	0.28 \pm 0.15	-	9,0
14570066+2437026	UGC09618	163118	55972.399	185	2.0	9943.4 \pm 18.7	80.0 \pm 40.2	-0.12 \pm 0.02	0.27 \pm 0.08	67,7
14582270-0105278	NGC5792	142834	55617.431	181	2.0	1838.0 \pm 13.7	112.6 \pm 14.9	-0.37 \pm 0.01	-0.30 \pm 0.04	110,12
14583982+5353100	NGC5820	252911	56103.263	270	1.0	3215.3 \pm 13.5	180.6 \pm 5.4	0.25 \pm 0.15	-	8,0
15005570-0727263	NGC5812	142496	55608.497	270	2.0	1855.7 \pm 13.4	225.4 \pm 7.5	-0.37 \pm 0.15	0.21 \pm 0.29	3,1
15005570-0727263	NGC5812	142592	55611.492	90	2.0	1880.2 \pm 13.6	213.3 \pm 8.1	-0.40 \pm 0.14	-0.60 \pm 0.14	2,3
15021965+0538479	UGC09667	141714	55580.521	90	2.0	10660.6 \pm 22.7	198.7 \pm 34.7	0.30 \pm 0.29	-	4,1
15021965+0538479	UGC09667	142495	55608.426	90	2.0	10685.5 \pm 14.1	251.3 \pm 10.2	0.39 \pm 0.11	-	9,0
15060078+0138017	NGC5845	342036	56343.442	145	1.0	1437.2 \pm 13.0	248.3 \pm 3.8	-	-	0,1
15062956+5545479	NGC5866	260021	56144.143	303	1.0	728.0 \pm 14.7	135.7 \pm 8.5	0.07 \pm 0.06	-	30,0
15065641+1250485	NGC5852	152416	55777.148	305	2.0	6583.0 \pm 14.4	223.7 \pm 7.3	0.13 \pm 0.01	0.25 \pm 0.02	113,15
15091320+5231418	NGC5875	150254	55690.186	140	1.0	3448.6 \pm 14.6	105.2 \pm 10.0	0.05 \pm 0.01	0.79 \pm 0.02	323,32
15094675+5700007	NGC5879	351385	56430.165	-15	1.0	733.3 \pm 13.7	66.0 \pm 13.9	0.07 \pm 0.04	0.51 \pm 0.20	35,3
15105568-1128477	NGC5872	351456	56432.252	190	1.0	7361.6 \pm 11.8	331.0 \pm 7.6	0.36 \pm 0.07	0.64 \pm 0.33	17,2
15105610+0544416	IC1101	143288	55629.381	225	2.0	22442.3 \pm 22.7	376.1 \pm 21.0	-	-	0,0
15105610+0544416	IC1101	341485	56329.453	195	1.0	22500.3 \pm 23.9	350.1 \pm 21.3	-	-	0,0
15150414-1005101	NGC5885	351846	56450.220	165	1.0	1947.8 \pm 13.9	85.3 \pm 15.1	-0.41 \pm 0.02	-0.21 \pm 0.12	60,5
15152332+5531015	NGC5905	251380	56037.450	385	1.0	3329.2 \pm 11.4	115.1 \pm 9.4	-0.36 \pm 0.01	-0.27 \pm 0.03	176,17
15152332+5531015	NGC5905	252912	56103.280	385	1.0	3325.2 \pm 13.9	96.7 \pm 8.1	-0.36 \pm 0.01	-0.27 \pm 0.02	195,24
15164448+0701180	UGC09799	143924	55647.338	136	2.0	10116.9 \pm 12.8	217.6 \pm 11.0	0.31 \pm 0.02	0.50 \pm 0.04	62,10
15174176-0042175	b19	250520	56010.377	90	1.0	32924.3 \pm 18.1	376.1 \pm 17.1	-	-	-
15192473+2053465	NGC5910	152346	55775.167	220	2.0	11863.6 \pm 13.5	277.8 \pm 7.7	0.36 \pm 0.08	0.00 \pm 0.18	18,5
15215656+0504139	NGC5921	351666	56445.157	181	1.0	1439.9 \pm 13.1	82.5 \pm 8.4	0.03 \pm 0.00	0.30 \pm 0.00	68,6
15232013-0409057	PGC054944	150303	55692.296	215	1.0	1941.7 \pm 15.8	27.5 \pm 29.3	-0.40 \pm 0.02	-0.11 \pm 0.16	43,6
15253931+2936129	PGC055060	162766	55959.450	30	2.0	16242.9 \pm 13.4	359.5 \pm 7.7	-	-	0,2
15325283+0028079	PGC055376	142909	55618.454	80	2.0	11548.6 \pm 14.0	278.2 \pm 7.3	0.23 \pm 0.62	-	3,0
15340245+5641081	NGC5965	351493	56433.358	400	1.0	3318.7 \pm 12.9	211.0 \pm 8.1	0.33 \pm 0.16	-	9,1
15358525-0936280	PGC3093250	252846	56101.182	255	1.0	7052.2 \pm 13.5	211.4 \pm 6.7	0.24 \pm 0.23	0.11 \pm 0.39	7,3
15362275+2230011	UGC09927	152417	55777.167	290	1.0	4252.4 \pm 12.1	133.8 \pm 5.5	0.38 \pm 0.21	-	3,0
15372289+2032593	UGC09937	152384	55776.170	195	2.0	4397.8 \pm 14.4	211.1 \pm 8.5	0.26 \pm 0.06	-	11,0
15383977+5921212	NGC5982	141713	55580.504	105	2.0	2881.9 \pm 14.2	260.2 \pm 7.7	0.53 \pm 0.39	-	2,0
15383977+5921212	NGC5982	142591	55611.433	105	2.0	2879.6 \pm 13.5	267.3 \pm 6.3	0.01 \pm 0.09	-0.38 \pm 0.12	5,5
15384478-0322477	PGC055679	143130	55623.476	150	2.0	7005.7 \pm 14.1	154.8 \pm 12.3	-0.16 \pm 0.00	0.37 \pm 0.01	185,28
15390769+4351549	UGC09959	352064	56459.331	305	1.0	5625.8 \pm 17.2	104.0 \pm 21.8	-0.34 \pm 0.01	-0.55 \pm 0.12	98,5
15393904+2146579	UGC09958	152347	55775.186	275	2.0	12257.2 \pm 15.0	299.0 \pm 10.0	-0.42 \pm 0.70	-	6,1
15461637+0224558	NGC5990	142258	55600.494	105	2.0	3763.8 \pm 14.4	159.1 \pm 11.6	-0.10 \pm 0.00	0.45 \pm 0.01	137,27
15502269+1856207	NGC6004	252913	56103.299	200	1.0	3766.4 \pm 11.5	97.7 \pm 9.5	-0.18 \pm 0.01	-0.18 \pm 0.12	97,5
15525603+2106017	NGC6008	352407	56480.256	250	1.0	4800.0 \pm 12.6	76.8 \pm 11.2	0.27 \pm 0.06	1.06 \pm 0.72	20,1
15554330+4752024	UGC10097	144506	55670.277	130	2.0	5866.7 \pm 14.8	325.1 \pm 6.7	0.29 \pm 0.03	0.65 \pm 0.15	24,3
15562359+1631246	PGC056437	352063	56459.313	220	1.0	4691.9 \pm 11.5	145.7 \pm 7.1	-	-	1,3
15570299+4810063	IC1153	163405	55979.418	165	2.0	5834.7 \pm 15.6	236.9 \pm 8.0	0.35 \pm 0.07	-	16,0

2MASS ID	Name	Frame	MJD	PA	slit ('')	V_{hel} (km s^{-1})	σ_c (km s^{-1})	[NII]/H α	[OIII]/H β	AoN
16171575-1143543	PGC057723	351848	56450.258	240	1.0	930.5±19.9	81.5±34.8	-0.47±0.00	-0.49±0.00	20,2
16191155+5759028	NGC6125	142699	55615.445	40	2.0	4649.4±13.1	263.4±5.8	-	-	0,0
16191155+5759028	NGC6128	252405	56084.359	400	1.0	4644.2±15.5	265.4±4.5	-	-	0,0
16200955+3747535	NGC6122	150189	55688.446	335	2.0	9841.4±13.3	217.0±9.3	0.35±0.18	-	8,0
16214862-0217003	NGC6118	351713	56447.300	200	1.0	1527.0±13.8	49.5±20.6	-0.41±0.00	-0.43±0.00	30,2
16251032+4053338	NGC6146	252293	56079.166	85	1.0	8654.2±16.3	310.8±6.4	0.17±0.05	-	21,1
16283827+3933049	NGC6166	060245	55421.197	210	2.0	9103.1±15.5	278.6±11.3	0.28±0.07	0.06±0.22	14,5
16283827+3933049	NGC6166	060246	55421.211	210	2.0	9101.3±17.4	282.7±14.0	0.31±0.06	-0.17±0.19	13,4
16375395+3604233	NGC6196	051353	55333.435	320	2.0	9161.2±14.3	318.2±6.1	-0.26±0.22	-	3,0
16375395+3604233	NGC6196	051354	55333.448	320	2.0	9160.1±15.2	309.6±7.2	-0.24±0.69	-	2,0
16375395+3604233	NGC6196	051438	55337.416	320	2.0	9180.8±13.7	322.7±5.9	-	-	0,0
16375395+3604233	NGC6196	051439	55337.431	320	2.0	9178.2±14.3	319.7±5.3	-0.09±0.33	-	3,0
16375395+3604233	NGC6196	051936	55362.356	320	2.0	9174.7±14.1	320.7±5.1	-0.19±0.48	-0.86±0.24	1,2
16375395+3604233	NGC6196	051937	55362.367	320	2.0	9171.8±15.3	324.5±5.8	-	-	0,2
16400325+1553004	PGC058719	351025	56419.265	50	1.0	10580.3±12.2	168.4±6.9	0.09±0.02	0.40±0.11	58,6
16430375+3649567	NGC6207	144336	55659.318	20	1.0	808.4±15.1	30.0±24.1	-0.44±0.00	-0.21±0.00	40,7
16430375+3649567	NGC6207	144337	55659.329	20	1.0	805.3±15.5	22.3±27.6	-0.43±0.00	-0.29±0.00	22,5
16430433+6134441	NGC6223	142700	55615.475	90	2.0	5719.6±14.3	293.0±6.0	0.47±0.19	-	5,0
16474706-0712456	PGC1022704	350069	56388.425	155	1.0	8348.1±13.0	169.9±7.2	0.38±0.13	-	11,0
16500502+4244234	NGC6239	351670	56445.393	295	1.0	890.3±20.8	59.1±32.9	-0.72±0.01	0.47±0.02	61,41
16522982+6030524	NGC6258	351782	56448.371	245	1.0	3047.8±13.4	142.3±5.3	0.37±0.34	-	8,0
16535220+3945369	UGC10599	141865	55585.525	25	2.0	9934.1±15.2	331.0±11.3	0.41±0.06	0.33±0.16	15,4
16535220+3945369	UGC10599	143494	55632.404	175	2.0	9888.0±13.6	384.3±11.2	0.25±0.05	0.08±0.11	24,6
16535220+3945369	UGC10599	351279	56428.240	181	1.0	9955.3±14.5	430.3±11.3	0.32±0.05	0.30±0.14	25,4
16535220+3945369	UGC10599	351339	56429.240	181	1.0	9922.3±16.4	364.2±9.7	0.39±0.11	0.63±0.54	16,2
16535220+3945369	UGC10599	352066	56459.370	361	1.0	9925.4±16.5	382.3±11.6	0.16±0.04	-0.07±0.10	27,6
16550959+2639463	IC4630	343029	56377.369	190	1.0	10141.1±15.9	218.3±9.6	0.30±0.06	-	22,1
16575809+2751157	NGC6269	252538	56089.380	255	1.0	10277.0±16.1	322.8±7.1	0.58±0.19	-	7,0
17032234+1214474	PGC059512	350869	56413.298	75	1.0	9014.2±14.2	170.5±5.3	0.62±0.08	-	10,0
17122865-0907269	PGC2817045	350336	56394.441	181	1.0	8582.3±17.2	218.5±14.1	-0.02±0.10	-	17,1
17125383-0718146	PGC1021213	260061	56146.142	215	1.0	7219.0±26.4	117.0±26.9	-0.18±0.33	-	10,1
17131806+4346563	NGC6323	251411	56038.300	1	1.0	7694.7±10.8	144.2±6.6	0.10±0.01	1.06±0.05	101,13
17141500+4341050	NGC6329	061675	55481.079	277	2.0	8122.8±12.6	295.7±11.1	0.22±0.42	-0.51±0.39	2,2
17175302+6146505	NGC6359	142771	55616.483	-40	2.0	2995.4±13.3	230.4±6.4	0.05±0.19	0.14±0.18	4,3
17180181+5014499	PGC060030	343094	56380.376	100	1.0	9873.0±15.5	273.3±8.2	-	-	0,5
17192134+4902256	UGC10814	252539	56089.398	335	1.0	7189.4±13.0	197.5±10.4	0.07±0.05	0.30±0.19	45,5
17223993+3052521	MRK0506	252561	56090.183	135	1.0	12674.9±38.3	200.0±33.8	-	-	AGN
17243782-0243062	PGC1084539	350954	56417.432	245	1.0	9788.0±28.5	334.1±28.3	-0.50±0.25	-	5,0
17322430+0703369	NGC6384	251055	56024.391	192	1.0	1609.8±20.1	154.6±20.0	0.08±0.32	-	4,0
17340802+0631053	PGC1302291	150220	55689.459	270	2.0	6659.2±16.0	51.8±42.6	-0.46±0.01	-0.43±0.05	65,8
17361111+0828558	PGC1347752	253280	56123.281	230	1.0	10768.8±12.5	224.5±8.5	0.35±0.15	0.78±0.50	8,2
17361220-0719287	PGC200524	260062	56146.160	119	2.0	7003.9±21.5	232.1±27.3	-0.29±0.10	-	12,1
17405482+3843560	ARK525	351193	56425.267	160	1.0	11859.2±15.0	220.7±8.9	-0.31±0.02	-0.27±0.05	108,9
17492651+7008396	NGC6503	252484	56087.351	301	1.0	-18.0±14.6	28.2±25.3	-0.13±0.02	0.41±0.18	47,4
17494097+5333541	PGC060936	151638	55737.362	330	2.0	-	-	-	-	-
17494650+7201162	NGC6508	150188	55688.420	405	2.0	7462.3±15.0	279.8±6.7	-0.07±0.11	-	7,1
17503509-0139063	PGC166871	143754	55640.498	210	2.0	7075.0±20.3	206.8±21.2	0.19±0.19	-	7,1
17503509-0139063	PGC166871	143925	55647.472	210	2.0	7081.0±13.8	239.2±13.7	0.05±0.15	-	10,0
17514880+2304190	NGC6482	051930	55362.180	68	2.0	3843.6±13.4	315.6±5.4	0.40±0.03	0.71±0.25	20,1
17514880+2304190	NGC6482	051931	55362.191	68	2.0	3835.5±14.9	318.6±5.6	0.37±0.03	0.37±0.10	22,3
17514880+2304190	NGC6482	051986	55363.397	248	2.0	3696.1±18.5	303.3±19.5	-	-	2,1
17514880+2304190	NGC6482	051987	55363.408	248	2.0	3722.9±20.3	292.8±19.0	-0.39±0.53	-	3,0
17514880+2304190	NGC6482	052210	55392.323	248	2.0	3708.6±18.4	309.9±16.8	-1.38±0.82	-	1,0
17514880+2304190	NGC6482	052211	55392.334	248	2.0	3736.0±24.9	271.7±19.7	-0.88±0.89	-	2,0
17524182+2950193	NGC6487	052337	55398.316	258	2.0	7511.0±15.9	285.4±9.6	-	-0.36±0.41	1,2
17524182+2950193	NGC6487	060250	55421.243	200	2.0	7510.5±13.7	286.1±5.5	-0.31±0.21	-0.22±0.26	3,4
17524182+2950193	NGC6487	060251	55421.254	200	2.0	7517.5±13.8	280.6±5.7	0.33±0.20	0.31±0.33	4,2
17545074+1819367	NGC6495	253281	56123.318	265	1.0	3128.2±13.1	225.0±5.3	-	-	0,0
17545181+3446343	UGC11041	151269	55724.192	70	2.0	4801.9±14.7	146.3±26.6	-0.35±0.01	-0.41±0.08	63,4
17554844+6236435	NGC6521	144291	55657.427	-10	2.0	8116.7±15.7	263.7±10.2	0.57±0.03	1.19±0.10	39,5
17555979+1820178	NGC6500	351626	56444.439	220	1.0	2950.7±11.5	219.8±4.1	-0.08±0.00	0.28±0.01	147,32
17561443+4759104	PGC2308263	250168	55999.454	5	1.0	15036.1±23.8	276.0±22.5	-	-	0,9
17565502+3238117	UGC11058	151647	55738.153	35	1.0	4691.2±13.5	54.5±20.4	-0.42±0.03	-0.52±0.25	36,3
17565663+2401022	PGC061152	343095	56380.396	45	1.0	5853.4±24.5	115.5±27.6	-0.04±0.02	0.14±0.11	111,6
17571064+2757411	UGC11060	151667	55738.380	305	2.0	4583.5±14.1	168.1±11.1	-0.29±0.02	-0.26±0.10	61,4
17571493+1210463	UGC11057	352041	56458.387	270	1.0	2810.8±16.2	79.8±21.7	-0.38±0.12	-	13,1
17571493+1210463	UGC11057	352067	56459.390	270	1.0	2811.6±14.8	60.7±22.9	-0.27±0.05	0.31±0.32	24,2
17591469+4553134	NGC6524	150994	55712.240	165	2.0	5689.6±13.9	154.9±13.2	-0.36±0.01	-0.33±0.04	95,10
18000551+2621597	UGC11082	142910	55618.478	175	2.0	4623.4±14.1	246.8±10.4	0.25±0.04	0.49±0.25	29,2
18015166+0658057	UGC11093	351784	56448.412	185	1.0	1932.8±34.2	93.2±57.3	-0.42±0.04	-	24,1
18032745-0017427	PGC061331	351721	56447.396	265	1.0	7252.6±16.5	347.4±12.6	-	-	0,1
18055923+1835139	NGC6548	150580	55701.277	160	2.0	2168.3±16.8	171.8±9.5	0.30±0.12	-	7,1
18065063+6949275	UGC11130	252331	56080.363	425	1.0	14846.5±21.1	247.0±25.3	-	-	0,9
18105749+3106584	NGC6575	150263	55690.301	55	2.0	6753.7±13.3	259.7±7.4	0.76±0.63	-0.10±0.40	1,2
18110729+1405352	NGC6570	152245	55769.279	300	1.0	2222.9±12.8	50.0±21.9	-0.38±0.02	-0.41±0.12	67,5
18115122+1458542	NGC6574	144339	55659.383	165	2.0	2223.9±13.1	139.5±12.9	-0.22±0.02	0.82±0.06	62,7
18123700+2532123	UGC11156	151777	55741.384	215	2.0	4586.2±12.7	165.7±7.7	1.29±0.81	-	1,1

Table continues on next page

2MASS ID	Name	Frame	MJD	PA	slit ('')	V_{hel} (km s^{-1})	σ_c (km s^{-1})	[NII]/H α	[OIII]/H β	AoN
18125527+6821484	NGC6621	252451	56085.355	-50	1.0	6023.4±16.8	150.3±19.6	-0.32±0.01	-0.34±0.07	124,8
18135090+1849312	NGC6587	051897	55361.405	200	2.0	3012.5±13.7	327.3±6.5	-0.90±0.31	-0.35±0.18	2,2
18135090+1849312	NGC6587	051898	55361.417	200	2.0	3014.1±13.8	324.2±5.9	-0.77±0.25	-0.35±0.22	2,2
18135090+1849312	NGC6587	051979	55363.197	200	2.0	3009.5±13.2	331.1±6.6	-0.89±0.41	-0.30±0.18	2,2
18135090+1849312	NGC6587	051980	55363.208	200	2.0	3003.4±14.1	325.7±5.4	-1.13±0.42	-0.59±0.16	1,2
18135090+1849312	NGC6587	052299	55397.315	200	2.0	3022.7±14.0	335.9±4.7	0.66±0.12	-	3,0
18135090+1849312	NGC6587	052300	55397.327	200	2.0	3020.7±13.6	337.1±5.3	-0.49±0.20	-0.84±0.19	3,2
18142795-0225052	PGC140814	150011	55684.402	145	2.0	1709.1±27.7	222.4±38.0	-0.21±0.11	0.19±0.61	23,1
18183348+1315541	NGC6615	152157	55761.319	255	2.0	2739.6±11.7	190.5±9.0	-0.69±0.39	-0.14±0.23	1,1
18185554+2339201	NGC6619	253226	56122.342	286	1.0	4916.7±12.4	206.0±4.5	0.51±0.10	-	11,1
18194285+2342346	NGC6623	153455	55812.195	270	2.0	4802.0±15.5	211.2±9.8	-	-	0,0
18264978+5108211	UGC11241	352069	56459.428	220	1.0	9792.0±13.3	118.4±8.0	0.22±0.06	0.50±0.00	11,1
18273712+1449085	NGC6635	061530	55478.105	237	2.0	5239.0±13.2	255.5±6.2	-0.92±0.66	-	1,0
18280147+1607327	UGC11242	352068	56459.411	270	1.0	10265.6±15.8	195.9±10.5	0.21±0.17	0.09±0.31	11,3
18282389+2244131	UGC11246	151232	55723.220	160	2.0	4072.8±12.8	156.9±14.7	-0.39±0.01	-0.40±0.04	128,9
18285975+0648277	PGC166900	351030	56419.346	170	1.0	2898.8±13.9	234.5±5.1	0.02±0.16	0.63±0.35	9,2
18294495+4501155	PGC2257255	352058	56459.210	155	1.0	-36.8±15.1	17.3±26.9	-	-	0,0
18335567+2253178	NGC6658	152135	55760.345	185	2.0	3735.4±15.2	209.5±8.9	-0.38±0.55	-	1,0
18343666+2254347	NGC6660	060895	55450.197	248	2.0	4209.3±13.1	221.5±7.4	0.25±0.04	0.88±0.29	14,1
18345024+7031259	NGC6690	252914	56103.322	340	1.0	449.9±19.7	60.5±49.6	-0.37±0.06	0.45±0.25	17,4
18350342+3241471	PGC062082	260001	56142.301	260	1.0	16658.1±47.0	229.8±54.7	-	-	AGN
18362058+5127594	UGC11298	052296	55397.118	68	2.0	10493.4±15.9	278.4±9.8	-	-	1,1
18362058+5127594	UGC11298	052350	55398.353	291	2.0	10462.8±15.2	296.1±9.2	-	-	0,1
18363966+1943454	PGC062122	252918	56103.406	200	1.0	4696.7±12.7	299.8±10.1	0.59±0.08	-	14,0
18401982+2411599	UGC11315	143308	56529.482	205	2.0	3939.8±14.1	225.0±7.8	0.07±0.03	0.61±0.13	35,4
18404012+3617226	NGC6688	144622	55674.353	40	2.0	5488.3±13.6	229.8±9.0	0.34±0.05	0.76±0.19	20,3
18440241+4533298	PGC062332	151831	55744.164	79	2.0	25818.2±12.4	281.6±12.3	-	-	-
18474418+2320500	UGC11353	150583	55701.319	155	2.0	4139.9±14.6	163.7±11.7	0.31±0.07	-	11,0
18490117+1919518	PGC1588608	153604	55825.161	210	2.0	4701.7±14.4	266.6±7.8	-	-	0,1
18530389+2750275	PGC100408	261671	56224.089	260	1.0	17986.6±29.7	123.5±57.2	-	-	AGN
18562403+5222394	NGC6732	052177	55391.344	261	2.0	7947.1±14.2	309.3±7.8	0.16±0.15	-	6,1
18562403+5222394	NGC6732	052178	55391.359	261	2.0	7960.3±12.9	302.8±9.1	-0.01±0.11	0.09±0.18	7,4
18562403+5222394	NGC6732	052212	55392.353	261	2.0	7937.8±13.5	305.0±7.1	0.06±0.14	0.43±0.26	6,2
18562403+5222394	NGC6732	052213	55392.368	261	2.0	7955.1±13.5	313.5±7.9	0.12±0.11	0.35±0.21	8,3
18573750+3800322	PGC062613	342845	56370.475	70	1.0	16136.7±17.4	357.2±12.7	-	-	0,2
18593477+1906217	PGC1580722	143495	55632.492	135	2.0	4766.0±18.1	271.2±12.4	-0.47±0.47	-	3,0
18593477+1906217	PGC1580722	143885	55646.459	140	2.0	4792.3±16.4	268.5±9.4	-	-	0,1
19050335+5542544	NGC6757	261365	56215.110	270	1.0	-	-	-	-	-
19134338+4549090	PGC062931	261606	56222.117	295	1.0	12365.9±16.1	323.3±8.4	0.06±0.53	-0.48±0.57	5,1
19235095+5559155	UGC11435	351669	56445.298	80	1.0	3623.7±33.0	43.2±42.3	-0.42±0.06	0.05±0.44	15,2
19310804+5406077	UGC11453	351623	56444.299	75	1.0	3803.7±13.8	93.5±13.4	-0.36±0.01	-0.54±0.05	165,10
19373299-0613046	PGC090334	351416	56431.440	190	1.0	3101.2±17.2	90.7±48.3	-	-	AGN
19395016-0332517	PGC204653	253279	56123.263	135	1.0	16153.5±18.2	222.1±10.9	-	-	0,3
19414211+5037571	UGC11465	351114	56423.360	160	1.0	7812.8±14.7	395.4±9.8	0.26±0.21	0.58±0.67	6,2
19424057-1019255	NGC6814	253441	56133.270	110	1.0	1533.6±13.6	101.1±16.8	-	-	AGN
19434067+5606339	NGC6824	144295	55657.474	45	2.0	3466.8±13.5	196.3±8.6	0.53±0.02	0.85±0.14	39,3
19485956+5018471	UGC11485	253520	56140.373	220	1.0	7574.8±16.3	195.7±11.0	-0.07±0.01	-0.08±0.06	161,9
19490928-1034253	PGC090341	150811	55707.422	165	2.0	7271.8±26.5	105.7±55.1	-	-	AGN
19523991+5727354	UGC11492	351990	56456.295	0	1.0	3523.5±13.4	72.7±14.5	-0.34±0.01	-0.21±0.05	112,12
19561287+4026021	PGC063832	144294	55657.456	140	2.0	4491.0±13.9	302.6±8.3	-	-	0,2
19564921+4024402	PGC063852	350953	56417.389	110	1.0	4641.5±13.4	272.6±6.8	1.00±0.51	-	3,0
19592833+4044022	PGC063932	253445	56133.389	340	1.0	16151.9±65.7	348.5±41.1	-	-	AGN
19592833+4044022	PGC063932	262189	56243.090	340	1.0	16335.0±23.3	130.2±33.5	-	-	AGN
20075080+5938105	PGC064144	253223	56122.227	20	1.0	11011.2±13.0	176.5±10.6	-0.21±0.01	0.08±0.03	173,23
20112927-0748485	PGC090353	151329	55726.392	150	2.0	5657.0±15.8	134.9±22.1	-0.20±0.01	-0.13±0.07	97,6
20183808-0009017	UGC11537	351783	56448.392	80	1.0	5327.9±13.6	128.1±10.1	0.32±0.18	-	9,1
20202850-1021209	PGC979256	253225	56122.320	135	1.0	8215.0±14.0	270.2±8.5	-	-	0,1
20223101+1009004	PGC064562	253277	56123.225	95	1.0	5356.0±12.8	203.2±5.4	0.32±0.07	-	15,1
20235734-0916531	PGC992999	253442	56133.289	245	1.0	8236.0±15.3	266.1±8.9	-0.78±0.25	-	3,0
20241125+3551304	2M2024	253360	56129.417	245	1.0	-33.6±15.3	33.1±21.9	-0.35±0.03	-	51,0
20274605-0304375	NGC6915	151147	55719.396	100	2.0	5597.5±14.0	179.1±7.7	0.31±0.03	1.12±0.35	23,1
20282884+2543241	NGC6921	150059	55685.410	140	2.0	4210.8±13.0	212.5±10.3	0.63±0.08	-	16,0
20325022+0955351	NGC6928	150012	55684.440	104	2.0	4635.9±14.4	182.6±10.5	0.45±0.03	-	23,0
20325594+5430316	UGC11592	151119	55718.334	55	2.0	1528.1±13.3	134.1±11.6	-0.25±0.34	-	2,0
20330610-0201390	NGC6926	253163	56121.365	175	1.0	5899.2±14.5	161.2±14.1	0.18±0.02	0.87±0.10	78,6
20330610-0201390	NGC6926	253405	56131.275	175	1.0	5914.5±21.5	212.2±28.6	0.12±0.03	0.88±0.16	53,3
20353105-0245536	PGC065021	150996	55712.414	245	2.0	5676.6±16.6	211.7±8.9	0.05±0.07	-	20,0
20371407+6606203	NGC6952	253282	56123.336	440	1.0	1365.9±14.3	115.2±6.4	0.42±0.01	0.96±0.04	102,6
20401346+5059165	PGC165861	150934	55710.367	100	2.0	2976.3±29.8	309.6±28.4	-0.71±0.19	-	8,0
20401346+5059165	PGC165861	150935	55710.378	100	2.0	3013.4±37.5	290.6±39.5	-0.58±0.21	-	6,1
20432938-1005316	PGC065257	261300	56214.086	270	1.0	10125.5±13.5	161.9±7.0	0.05±0.01	0.74±0.03	160,21
20432938-1005316	PGC065257	261363	56215.076	270	1.0	10126.8±13.4	167.3±7.8	0.07±0.01	0.75±0.03	134,17
20435368+1230429	NGC6956	262110	56240.115	155	1.0	4587.4±12.3	111.1±8.5	-0.31±0.01	-0.36±0.08	99,5
20440975-1043245	MRK0509	151330	55726.418	220	2.0	10041.7±0.0	10.3±47.5	-	-	AGN
20471908+0019150	NGC6962	052351	55398.368	208	2.0	4164.9±14.6	207.5±9.7	0.14±0.06	0.74±0.24	18,2
20494713+5206261	2M20494	261302	56214.195	230	2.0	3130.9±18.4	222.1±14.8	-1.00±0.26	-	3,0
20571538+2557534	UGC11651	351718	56447.335	181	1.0	1458.1±24.9	73.7±39.6	-0.41±0.23	-	6,0

Table continues on next page

2MASS ID	Name	Frame	MJD	PA	slit ('')	V_{hel} (km s^{-1})	σ_c (km s^{-1})	[NII]/H α	[OIII]/H β	AoN
20575949-0430026	PGC1057358	061720	55482.101	180	2.0	23775.9±15.1	270.9±13.2	-	-	0,1
21033361+2953504	NGC7013	252280	56078.361	181	1.0	705.1±13.5	106.8±6.4	0.16±0.04	0.90±0.35	40,1
21074732+1620090	NGC7025	052305	55397.442	239	2.0	4863.4±13.6	238.4±7.5	0.47±0.09	-	8,1
21074732+1620090	NGC7025	052353	55398.434	239	2.0	4882.5±13.7	238.9±7.6	0.33±0.08	0.47±0.16	10,2
21074732+1620090	NGC7025	052445	55408.411	239	2.0	4851.3±14.0	234.5±7.9	0.04±0.06	0.00±0.11	14,5
21074732+1620090	NGC7025	052446	55408.419	239	2.0	4867.0±14.1	229.2±11.3	0.29±0.15	-	6,0
21074732+1620090	NGC7025	052447	55408.427	239	2.0	4823.2±32.0	244.3±37.4	-	-	0,0
21090996-0940147	PGC089171	151732	55740.402	115	2.0	8090.0±22.3	160.8±43.6	-	-	AGN
21105420-0346348	PGC1067006	151124	55718.436	169	2.0	9245.1±13.4	186.4±11.3	-0.03±0.18	-	5,0
21183304+2626486	NGC7052	061574	55479.227	254	2.0	4626.6±14.5	313.9±6.2	0.14±0.03	0.24±0.15	31,4
21201566-0452356	IC1371	061721	55482.116	195	2.0	8791.8±16.9	269.4±12.0	0.09±0.09	-0.02±0.42	17,2
21204248+4423590	PGC066592	140051	55533.091	310	2.0	3988.2±14.4	198.0±9.0	0.37±0.06	-	13,1
21204618+4516221	PGC166712	253278	56123.242	90	1.0	181.4±62.4	158.0±90.1	-0.51±0.03	0.41±0.24	26,3
21210763+2305059	NGC7053	140050	55533.074	205	2.0	4659.4±14.5	208.5±9.0	0.24±0.05	0.50±0.17	19,3
21213904+4043499	PGC066627	252868	56101.301	75	1.0	3808.3±15.0	253.2±8.3	-	-	0,1
21253283+2519280	PGC3089540	151291	55725.347	120	2.0	4661.8±13.7	162.5±9.9	-	-	0,0
21353268+3523541	IC1392	052354	55398.456	265	2.0	4319.8±14.6	218.9±8.2	0.08±0.58	0.37±0.51	1,1
21362777-0953236	PGC189130	253444	56133.340	235	1.0	24578.6±12.2	355.3±19.8	-	-	-
21383340+3205060	PGC067084	252754	56098.323	145	1.0	7300.0±34.5	200.7±28.7	-	-	AGN
21383340+3205060	PGC067084	262111	56240.166	325	1.0	7314.0±25.4	224.4±22.1	-	-	AGN
21383461-0754261	PGC163280	151811	55742.420	182	2.0	15279.9±13.4	279.8±9.3	-	-	0,2
21423859+4330562	PGC165885	351168	56424.422	100	1.0	-	-	-	-	-
21424877-0652066	PGC189711	262080	56239.052	110	1.0	15651.7±13.1	282.1±6.8	-	-	0,2
21434945-0804261	PGC2800918	153412	55811.232	182	2.0	44882.0±17.0	275.6±9.6	-	-	0,0
21474092+4547394	PGC167519	351720	56447.371	160	1.0	5463.4±16.4	267.1±9.4	-0.02±0.24	-	5,0
21493100-0951450	PGC985487	152783	55796.269	180	2.0	23287.8±17.2	273.3±14.4	-	-	0,0
21560065-0131006	IC1411	151809	55742.388	200	2.0	-	-	-	-	-
21560065-0131006	IC1411	151810	55742.402	200	2.0	-	-	-	-	-
21560065-0131006	IC1411	152158	55761.336	179	2.0	7878.8±15.7	323.2±13.4	0.12±0.15	0.56±0.58	6,1
21570253+6626098	PGC2821703	352344	56474.379	305	1.0	-	-	-	-	-
22004125+1744172	NGC7177	252869	56101.341	90	1.0	1098.4±13.9	124.4±5.2	-0.15±0.01	0.13±0.05	68,11
22025805+4103322	NGC7197	140991	55557.053	285	2.0	4354.4±14.1	181.6±11.2	-0.12±0.07	0.55±0.44	13,2
22070282+5122417	2M22070	262241	56246.142	250	1.0	13299.0±26.1	338.9±24.8	-	-	0,0
22075236+3121333	NGC7217	253404	56131.256	85	1.0	914.4±13.9	145.8±4.8	0.50±0.01	0.61±0.07	42,4
22082737+4826268	UGC11920	153351	55810.135	45	1.0	1070.5±14.0	153.2±4.4	0.20±0.03	0.59±0.18	20,2
22123011+4519424	NGC7231	352065	56459.350	90	1.0	1052.0±22.8	60.5±39.0	-0.80±0.00	0.44±0.00	80,44
22153950+3717554	NGC7242	060036	55412.220	45	2.0	5787.2±12.2	259.5±8.0	-0.87±0.53	0.18±0.67	1,1
22153950+3717554	NGC7242	060037	55412.232	45	2.0	5785.5±16.2	261.5±9.5	-0.60±0.51	-	1,0
22165396+4030083	NGC7248	061483	55477.283	340	2.0	4286.3±13.7	269.1±5.3	-	-0.45±0.35	0,2
22182048+1337255	PGC068534	151688	55739.375	170	2.0	7329.2±17.2	48.0±45.5	-0.34±0.06	0.35±0.91	14,2
22182048+1337255	PGC068534	151807	55742.353	170	2.0	7289.2±17.1	93.1±30.3	-0.36±0.06	-0.13±0.30	15,3
22182048+1337255	PGC068534	151808	55742.368	170	2.0	7326.2±18.4	82.7±36.3	-0.40±0.06	-	14,1
22202270+4742212	UGC11991	161376	55893.139	255	1.0	5399.4±15.4	81.3±22.2	-0.34±0.10	-0.17±0.78	16,1
22222747+3612354	NGC7265	060758	55445.375	266	2.0	4981.2±14.4	246.2±6.7	0.21±0.11	-	10,0
22222747+3612354	NGC7265	060759	55445.389	266	2.0	4994.9±14.3	245.9±7.5	0.36±0.12	-	8,0
22231202+4003201	UGC12016	140054	55533.140	300	2.0	5247.8±14.2	300.8±6.2	-0.28±0.17	-	4,1
22241107+3607330	NGC7274	061582	55479.279	266	2.0	5946.5±12.5	288.2±7.3	-0.08±0.15	-	7,1
22265654+5130086	PGC068890	351722	56447.413	55	1.0	10909.6±16.2	274.2±10.2	0.19±0.18	-	4,0
22312062+3921298	UGC12064	253224	56122.300	-1	1.0	5004.6±13.4	249.0±9.4	0.30±0.06	0.67±0.36	27,2
22330629+0805508	UGC12074	352471	56484.336	145	1.0	2030.1±19.2	42.5±30.8	-0.51±0.01	-0.00±0.03	108,27
22340676+0534131	NGC7311	140285	55538.089	195	2.0	4473.5±13.2	201.9±7.8	0.50±0.07	-	8,0
22353169+3448128	NGC7315	151292	55725.370	20	2.0	6152.1±13.5	228.0±8.7	-	-	0,0
22354078+0129053	PGC087323	061841	55484.208	207	2.0	17018.4±16.6	319.3±9.2	-	-	0,2
22365619+3832527	NGC7330	153411	55811.150	70	2.0	5243.0±15.3	266.0±7.1	-0.34±0.35	-	2,0
22370410+3424573	NGC7331	151293	55725.393	68	1.0	815.9±12.0	131.0±4.6	0.23±0.03	-	21,0
22372452+2347540	NGC7332	351671	56445.415	155	1.0	1158.7±14.3	135.8±4.4	0.08±0.07	-	6,0
22401511-0225265	PGC069448	352506	56485.374	245	1.0	2900.4±12.1	17.6±27.1	-0.35±0.03	-0.23±0.15	44,5
22415367+3455106	UGC12157	151277	55724.390	95	2.0	6598.5±14.3	303.3±8.4	0.16±0.05	0.25±0.16	22,3
22434930+0842199	NGC7362	062541	55504.194	180	2.0	7447.6±13.9	274.5±7.8	-0.22±0.37	-0.04±0.43	2,3
22484014+5309449	PGC168062	151278	55724.409	155	2.0	13187.4±21.4	300.8±19.8	0.42±0.51	0.14±0.99	5,1
22484014+5309449	PGC168062	151279	55724.421	155	2.0	13207.8±21.9	320.8±17.2	-	-0.21±0.63	3,1
22500213+1141555	NGC7386	062169	55496.228	320	2.0	7154.3±14.4	301.6±6.8	-	-0.05±0.49	1,2
22503614-0132413	NGC7391	060754	55445.308	115	2.0	2985.8±14.2	257.5±6.3	0.58±0.20	-	5,1
22503614-0132413	NGC7391	060755	55445.323	115	2.0	2976.3±14.7	260.0±7.7	0.40±0.14	0.97±0.38	7,1
22510095+3122299	UGC12214	151541	55735.370	155	2.0	6525.1±13.8	251.6±5.9	0.02±0.17	-	3,0
22513158+2304499	IC5258	062214	55497.234	290	2.0	7646.5±14.1	187.2±9.1	-	-	0,0
22522259+0105332	NGC7396	060926	55451.201	149	2.0	4831.3±13.7	241.7±8.3	0.30±0.07	0.85±0.33	17,1
22535624-0634453	NGC7406	160368	55858.152	255	1.0	1531.1±13.3	49.5±19.4	-0.46±0.01	-0.15±0.04	121,17
22560284+3621411	NGC7426	060845	55448.162	93	2.0	5186.1±13.9	295.8±7.2	0.29±0.03	0.48±0.08	25,4
22560284+3621411	NGC7426	062215	55497.253	255	2.0	5190.9±14.2	298.9±7.4	0.31±0.03	0.67±0.12	30,4
22575750+2609000	NGC7436	061902	55485.287	180	2.0	7218.8±13.0	312.8±6.4	0.34±0.11	0.44±0.34	6,2
22580224-0346108	ARP314	160369	55858.171	195	1.0	3610.1±15.7	74.5±17.4	-0.26±0.00	-0.17±0.02	337,29
22581755+2546161	UGC12272	253406	56131.294	45	1.0	7180.9±13.1	191.5±10.2	0.67±0.10	-	5,0
22583186+1043545	PGC070147	351995	56456.423	150	1.0	11494.4±14.3	295.9±8.0	0.34±0.14	0.64±0.30	9,2
23005993+3008416	NGC7457	151776	55741.364	125	1.0	799.4±13.4	66.6±9.7	-0.96±0.89	-	3,0
23031567+0852252	NGC7469	253407	56131.322	120	1.0	4877.0±20.5	221.3±22.6	-	-	AGN
23031567+0852252	NGC7469	260502	56179.201	120	1.0	4842.1±29.1	256.2±43.4	-	-	AGN

Table continues on next page

2MASS ID	Name	Frame	MJD	PA	slit ('')	V_{hel} (km s^{-1})	σ_c (km s^{-1})	[NII]/H α	[OIII]/H β	AoN
23032450+2435497	PGC3089639	261439	56218.070	55	1.0	12174.5±14.3	218.6±7.7	0.22±0.15	-	15,1
23040267+2237272	MRK0315	351785	56448.429	60	1.0	11321.2±30.5	186.5±42.8	-	-	AGN
23060487+3406278	NGC7485	151294	55725.410	145	2.0	5732.1±18.2	257.1±7.0	0.03±0.02	0.32±0.08	40,5
23065893+2256113	IC5285	252916	56103.368	70	1.0	6056.5±12.9	206.2±5.9	0.35±0.07	-	20,1
23072021+3621450	ARK575	340826	56295.080	355	1.0	4993.1±15.4	258.7±6.4	0.25±0.11	0.97±0.51	11,2
23072021+3621450	ARK575	351723	56447.435	175	1.0	5007.1±12.8	270.1±6.2	0.38±0.13	0.57±0.31	8,2
23072021+3621450	PGC070520	140118	55534.169	355	2.0	5016.6±14.5	288.2±6.8	0.12±0.06	0.51±0.16	18,3
23072021+3621450	PGC070520	252452	56085.407	175	1.0	5007.5±14.1	264.3±8.4	0.19±0.10	0.49±0.20	10,2
23072515+3222303	NGC7490	153215	55806.421	250	2.0	6117.2±14.9	162.2±12.7	0.27±0.08	0.41±0.25	9,1
23104223+0734033	NGC7503	253283	56123.356	90	1.0	12880.9±14.6	290.4±6.4	0.96±0.45	-	4,0
23142943+2341053	NGC7539	062170	55496.254	310	2.0	5915.6±14.2	194.0±8.9	-	-	0,1
23151609+1857409	NGC7550	153307	55808.399	330	2.0	4960.5±14.5	246.2±7.8	0.32±0.04	0.42±0.09	26,4
23155750+0641149	NGC7562	140286	55538.112	265	2.0	3524.6±13.7	247.3±6.7	-	-	0,1
23171357+1842295	NGC7578B	060742	55445.198	117	2.0	11776.6±14.4	303.4±8.0	0.13±0.15	-	12,1
23173375+2901096	UGC12482	061903	55485.303	257	2.0	6849.2±13.9	321.6±8.3	-	-0.12±0.50	0,2
23175277+0722458	NGC7583	261073	56208.130	75	1.0	12257.3±13.0	352.2±8.4	0.11±0.42	-0.60±0.65	4,2
23185137+4203550	UGC12496	252917	56103.387	20	1.0	5119.3±12.8	160.6±6.8	-	-	0,0
23185663+0014376	NGC7603	060938	55451.335	208	2.0	8622.5±20.9	245.1±24.6	-	-	AGN
23192510+0554223	IC1481	352345	56474.396	80	1.0	5994.6±12.2	110.2±15.6	0.11±0.01	0.52±0.07	97,7
23194420+0834349	NGC7612	052088	55371.409	184	2.0	3137.3±13.7	176.0±10.9	-	-0.14±0.61	1,1
23194420+0834349	NGC7612	052089	55371.422	184	2.0	3148.8±14.3	176.6±9.2	-	-	0,1
23194420+0834349	NGC7612	052269	55396.341	184	2.0	3148.8±14.5	179.2±9.7	-	-	1,0
23194420+0834349	NGC7612	052270	55396.354	184	2.0	3165.4±13.9	179.5±10.1	0.10±0.30	-	2,0
23194420+0834349	NGC7612	052301	55397.345	184	2.0	3168.1±14.1	184.4±7.9	-	-0.50±0.27	0,2
23194420+0834349	NGC7612	052302	55397.357	184	2.0	3168.1±14.2	183.4±8.3	-	-	0,0
23194721+4251096	NGC7618	061473	55477.094	10	2.0	4962.1±15.1	323.4±8.9	0.47±0.22	0.14±0.37	5,2
23194721+4251096	NGC7618	061651	55480.308	276	2.0	4985.6±12.0	333.0±8.1	0.25±0.09	-	10,1
23194721+4251096	NGC7618	061788	55483.079	83	2.0	4979.3±14.8	301.6±8.7	0.37±0.11	0.55±0.30	7,2
23201452+0812226	NGC7619	060750	55445.221	133	2.0	3761.7±14.6	330.6±5.0	-	-	2,0
23204252+0813014	NGC7626	061842	55484.263	190	2.0	3380.4±13.7	283.1±6.2	0.58±0.08	-	7,0
23204252+0813014	NGC7626	061843	55484.277	190	2.0	3375.6±12.8	275.2±4.8	0.63±0.08	-	8,0
23220658+4050435	NGC7640	261478	56219.062	142	1.0	347.3±20.7	41.3±39.8	-0.46±0.08	0.01±0.29	11,4
23252175+2829425	UGC12591	060741	55445.179	103	2.0	6810.8±14.1	306.0±6.8	0.35±0.03	0.54±0.12	37,4
23254867+2701478	NGC7660	151639	55737.382	45	2.0	5637.5±13.3	263.8±7.2	-0.48±0.37	-	2,1
23255415+4232111	NGC7662	161412	55894.196	210	1.0	-	-	-	-	-
23271932+1228025	NGC7671	141197	55565.057	315	2.0	3790.3±14.3	269.1±5.7	0.41±0.08	-	10,1
23283508+3224565	NGC7680	061892	55485.083	98	2.0	5021.6±14.5	264.0±6.9	-	-	1,0
23322441+1550520	NGC7691	161583	55910.118	335	1.0	3970.7±15.6	28.9±28.7	-0.34±0.06	0.25±0.38	20,3
23334928+3003372	UGC12667	161377	55893.190	255	1.0	3728.0±14.5	49.2±25.7	-0.47±0.01	-0.54±0.08	86,7
23382938+2701526	NGC7720	060774	55446.182	200	2.0	8873.5±15.7	352.1±9.2	0.62±0.06	0.79±0.26	19,2
23382938+2701526	NGC7720	060775	55446.197	200	2.0	8877.5±14.3	343.2±7.7	0.57±0.05	0.44±0.17	24,4
23382938+2701526	NGC7720	151256	55723.431	60	2.0	8854.4±14.3	302.8±13.2	-0.72±0.82	-	2,0
23382938+2701526	UGC12716	062171	55496.279	254	2.0	8879.9±15.7	337.9±7.9	0.63±0.04	0.64±0.17	23,3
23400080+2708014	NGC7728	062172	55496.294	255	2.0	9235.0±16.0	323.8±10.2	0.36±0.09	-	11,0
23435437+2604320	NGC7741	253443	56133.320	105	1.0	732.8±16.6	52.1±28.8	-0.55±0.01	0.08±0.04	68,25
23435437+2604320	NGC7741	261364	56215.093	105	1.0	728.1±22.0	52.5±35.2	-0.54±0.01	0.21±0.06	51,15
23442113+0956025	NGC7743	261517	56220.101	95	1.0	1612.9±12.6	94.7±6.9	0.29±0.01	0.95±0.05	73,6
23481133-0225574	PGC196688	161348	55892.145	205	2.0	6644.9±12.8	191.9±8.1	-	-	1,0
23491399+1805394	PGC072514	153606	55825.369	240	2.0	24649.1±12.3	298.1±11.6	0.83±0.42	-	1,0
23505859+2708507	NGC7768	151295	55725.446	70	2.0	8007.0±14.9	267.1±7.7	0.15±0.24	-	3,1
23512488+2006425	NGC7771	140238	55537.167	255	2.0	4366.7±15.1	150.0±16.4	-0.37±0.00	-0.52±0.03	141,10
23512674+2035105	MRK0331	261480	56219.097	150	1.0	5312.3±12.1	124.7±11.9	-0.25±0.00	-0.35±0.02	276,11
23520987+3116356	NGC7773	160766	55866.273	230	1.0	8323.7±11.5	118.4±7.9	0.26±0.00	1.08±0.00	87,13
23551903+0554571	NGC7785	141011	55558.085	140	2.0	3811.9±14.1	247.8±7.4	0.24±0.12	-	7,0

Table 1 List of observations and derived parameters of the HETMGS survey galaxies. (1) 18 digit 2MASS XSC, or 12 digit 2MASSI identifier (2) HETMGS name, (3) LRS frame number (4) date of observation (5) PA of the slit N-E, (6) slit width (7,8) stellar Heliocentric velocity and dispersion of the central 3.5'' (8,9,10) Log ratio of [NII]/H α and [OIII]/H β and their Amplitude-over-Noise (AoN), respectively.